RESISTOR NETWORKS AND FINITE ELEMENT MODELS

A thesis submitted to the University of Manchester
for the degree of Doctor of Philosophy
in the Faculty of Engineering and Physical Sciences

2011

Abdulaziz Al-Humaidi
School of Mathematics

Contents

Word count: 18684

List of Tables

List of Figures

The University of Manchester

Abdulaziz Al-Humaidi
Doctor of Philosophy
Resistor Networks And Finite Element Models
June 25, 2011

There are two commonly discrete approximations for the inverse conductivity problem. Finite element models are heavily used in electrical impedance tomography research as they are easily adapted to bodies of irregular shapes. The other approximation is to use electrical resistor networks for which several uniqueness results and reconstruction algorithms are known for the inverse problem. In this thesis the link between finite element models and resistor networks is established. For the planar case we show how resistor networks associated with a triangular mesh have an isotropic embedding and we give conditions for the uniqueness of the embedding. Moreover, a layered finite element model parameterized by the values of conductivity on the interior nodes is constructed. Construction of the finite element mesh leads to a study of the triangulation survey problem. A constructive algorithm is given to determine the position of the nodes in the triangulation with a knowledge of one edge and the angles of the finite element mesh. Also we show that we need to satisfy the sine rule as a consistency condition for every closed basic cycle that enclosing interior nodes and this is a complete set of independent constraints.

Declaration

No portion of the work referred to in this thesis has been submitted in support of an application for another degree or qualification of this or any other university or other institute of learning.

Copyright Statement

Acknowledgements

All thanks and praise go to God for all His blessings. I am thankful to God for providing me with the knowledge, consent, patience and without whose mercy and clemency nothing would have been possible. I would like to thank the University of Manchester and in particular I would like to extend my special thanks to my supervisor Prof. Bill Lionheart for his friendship and his concern regarding my health during my illness last year, and for his encouragement and creative ideas without which this research would not have been possible. It has been a great pleasure to take my PhD under his supervision. My appreciation also goes to the Royal Commission in Jubail and the Saudi Cultural Bureau in London for their financial support. I also want to express especial gratitude to my father (God bless his soul) and my mother, and to my wife for her patience and support throughout the past few years. My thanks also go to my wife's Father, her mother, my sisters and brothers for their support.(I would also like to thank more people deserve the thanks specially) Hussain, Ashraf, Zainab, Ahmed, Jafer and Mohammed Alwi. Finally, I would like to thank my daughter Zahra and my sons Mohammed, Reda and Moaed for helping me enjoy every single second of my life.

Abbreviations, Symbols and Notations

EIT	Electrical impedance tomography	P.24
FEM	Finite element method	P.57
FDM	Finite difference method	P.57
FVM	Finite volume method	P.57
BEM	Boundary element method	P.57
PVIN	Parameterized by values at interior nodes	P.103
Λ_γ	Dirichlet to Neumann (D-N) map	P.18
Ω	Domain with boundary	P.18
$\partial\Omega$	The boundary of the domain Ω	P.19
γ	The conductivity	P.25
σ	The conductivity	P.34
$G(V, E)$	Graph	P.36
V	Set of all vertices of graph G	P.36
E	Set of all edges of graph G	P.36
$\overline{G}$	Directed graph	P.36
$\overline{E}$	Arc (oriented edge)	P.36
V_0	Set of all interior nodes	P.37
V_b	Set of all boundary nodes	P.37
n_{V_0}	Number of interior nodes	P.80
n_{V_b}	Number of boundary nodes	P.80

n_V	Number of vertices	P.80
n_θ	Number of angles	P.80
n_{eq}	Number of equations	P.80
n_t	Number of triangles	P.80
n_e	Number of edges	P.80
N(p)	Neighbours of node p	P.37
$C^0(\overline{G})$	0-Cochain	P.41
$C^1(\overline{G})$	1-Cochain	P.41
d	Co-differential operator	P.41
∂	boundary operator	P.41
D	A unit disc in the plane	P37
M	Medial graph	P.48
$\epsilon(G)$	The number of edges in circular planar network of resistors	P.53
K	Non oriented abstract simplicial complex	P.55
$\overline{K}$	An oriented abstract simplicial complex	P.55
Q_γ	Anticipated power	P.26
Z	The set of all cycles of one dimensional chains	P.83
$+$	The label of pivot element of sum of angles equal to π equations	P.98
$\times$	The label of pivot element of sum of angles equal to 2π equations	P.98
$\circ$	The label of pivot element of sine equations consistency condition	P.98
Δ	The label of pivot element of cotangent equations	P.98

Chapter 1

Introduction

1.1 Aims and objectives

Inverse boundary problems deal with the determination of internal properties of a medium from measurements at its boundary. These problems arise in a variety of important physical situations such as geophysics and medical imaging. The physical situation is modelled by using a partial differential equation within the medium. The boundary measurements are represented by a map on the boundary. The inverse boundary value problem is the recovery of the coefficients of the partial differential equation in the interior of the medium knowing the boundary map. A typical example of an inverse boundary problem is the inverse conductivity problem proposed by Calderón [13]. In this inverse problem one aims to recover the electrical conductivity within a medium from the boundary voltage to current map known as the Dirichlet to Neumann map Λ_γ. Another version of the same problem is determining the conductivity inside the medium from the knowledge of the Neumann to Dirichlet map. In a mathematical context, the conductivity problem is formulated as follows: Let $\Omega \subseteq \mathbb{R}^n$ be a bounded domain with a smooth boundary, $\gamma \in L^\infty(\Omega)$ be the conductivity of Ω where γ is strictly positive and the potential $u \in \Omega$ with voltage f on the boundary $\partial\Omega$ satisfies

$$L_\gamma = \nabla \cdot (\gamma(x)\nabla u) = 0 \text{ in } \Omega. \tag{1.1}$$

$$u \mid_{\partial\Omega} = f$$

$$\Lambda_\gamma(f) = \nu.\gamma u \mid_{\partial\Omega}$$

where u is the solution of (1.1) and ν is the unit outer normal to $\partial\Omega$. So the inverse problem is to recover γ knowing Λ_γ. More specifically we are interested in:

- Identifiability: the map $\gamma \to \Lambda_\gamma$ is injective.
- Stability: the map $\gamma \to \Lambda_\gamma$ and its inverse, if it exists, are continuous.
- Characterization: the range of the map $\gamma \to \Lambda_\gamma$.
- Reconstruction: finding a procedure to recover γ from Λ_γ.

In practice, discrete approximations to the conductivity problem are used. These approximations rely on a finite number of voltage and current measurements at the boundary. Discrete approximations to the conductivity problem include finite element models and resistor networks. Finite element models are widely used in electrical impedance tomography (EIT) [11]. Research in this area uses a technology designed to determine spatially varying conductivity inside a body from surface measurements. Electric currents are injected by means of electrodes attached on the surface. The information obtained from the surface are measured voltages which correspond to a variety of applied current patterns. This collected data is used to reconstruct the image of the conductivity distribution within the body. There are biomedical and geophysical applications for this method [28]. In biomedical imaging one may monitor the influx or efflux of a conducting fluid such as blood flow in the brain or the heart in a body under investigation. Similarly, in geophysics [42], through measurements on the surface of a field one may monitor the fluid through rocks and soils by reconstruction of the conductivity image. Finite element approximations provide useful spatial information about the body under study. Moreover, there are several reconstruction algorithms from current to voltage map in the boundary refer to [55] for early work and [2] for a recent survey. However, this approximation has a lack of or indeed has no uniqueness results available. Another approximation of the conductivity inverse problem is provided by electrical resistor networks. Nakayama et al. studied the change of the conductivity on electrical resistor networks corresponding to the change in the measured voltage [40]. Similar work by Murai and Kagawa [37] appeared in 1985. Also, Yorkey [56] showed that (FEM) approximates the conductivity distribution with a suitable resistor network. Moreover, Yorkey, Webster and Tompkins [55] explained how the Jacobian matrix can be computed using a discrete formulation. In this research area, rectangular networks [17] and circular networks [15] have been studied extensively by E. Curtis and J. Morrow. Several uniqueness results were proved and reconstruction algorithms for γ from Λ_γ were obtained. Furthermore, some results analogous to continuous case such as maximum principals and discrete Green's functions were shown [16].

The process of harmonic continuation in a domain was introduced. This idea enabled E. Curtis and J. Morrow to prove that a harmonic function can be locally constant without being constant in the whole domain. This property in the discrete version is in contrast with the continuum case where the harmonic function is constant in the whole domain if it is constant in part of the domain. This abstract theory of electrical resistor networks lacks a practical application as no spatial information about the body can be obtained. Thus, there is a need to fill such gap as resistor network approximation is not useful without a practical application. On the other hand, for finite element approximations uniqueness of solution for the inverse problem is not guaranteed. This motivated us to consider the link between the two approximations.

Questions that naturally arise:

1. Which resistor network corresponds to a finite element model?

2. Do all assignments of conductance to a resistor mesh with the same topology as a finite element mesh correspond to a choice of vertex positions and conductivities?

3. What are the conditions needed to obtain a unique embedding of a resistor network associated with a finite element model?

4. Can a finite element mesh equivalent to a resistor networks be constructed?

5. Is there a canonical form for triangular resistor networks?

Note that the finite element models with piece-wise linear basis functions and piece-wise constant conductivity produce a system matrix equivalent to the Ohm-Kirchhoff matrix for a resistor network. For the planar case we show how resistor networks associated with a certain class of an isotropic (FEM) have an isotropic embedding and we give conditions for the uniqueness of the embedding. Moreover, we construct a layered finite element model parameterized by the values of conductivity on the interior nodes. Construction of the finite element mesh leads to a study of the survey problem. A constructive algorithm to determine the position of the nodes in the triangulation with a knowledge of one edge and the angles of the finite element mesh is obtained. Also we show that we need to satisfy the sine rule as a consistency condition for every closed basic cycle enclosing interior node. Finally, an isomorphism between the space of basic cycles in the triangulated mesh and the space of logarithm of sines is proved.

1.2 Thesis organization

In the context of this thesis, the first chapter starts with a brief introduction to the inverse conductivity problem. In this introduction, the two most popular discrete methods in literature used to determine the conductivity of medium are discussed and compared. Chapter 2 introduces a brief review of uniqueness results of electrical impedance tomography (EIT) in the continuum context. The formulation of Calderón's Inverse Problem of conductivity is introduced. The developments of uniqueness results in both isotropic and anisotropic conductivities are summarized. Chapter 3 presents the resistor networks as a discrete analogue of the continuous case of conductivity problem. We review previously known results on inverse problems of resistor networks. The concept of harmonic continuation introduced by E. Curtis and J. Morrow is discussed as it is an important technique to recover the conductivity on edges in rectangular and circular planar resistor networks. One of our contributions in this thesis is the derivation of a discrete analogue of continuum conductivity in differential forms. Another contribution is the development of the concept of simplicial complex which is useful in the discussion of necessary and sufficient consistency condition. Also, we explain the important concepts of medial graph as it plays a role to characterize the circular planar resistor networks. We applied the medial graph in layered triangulated circular resistor networks and justified that they are over determined. Chapter 4 discuses the finite element models as another version of discrete conductivity problem. This method is used to reconstruct the image of the conductivity distribution inside a body by boundary measurements. We also present the correspondence of Ohm-Kirchhoff matrix and (FEM) system matrix as the topic of this thesis is to study the link between the finite element models and resistor networks. Chapter 5 deals with the classical problem of a triangulation survey considered by early cartographers including Tycho Brahe and Snellius. Also, we go over the work done in geometric design where the sine rule is introduced as a consistency condition. Moreover, we illustrate the sine rule in basic cycles around each interior vertex in triangulated mesh. Our contribution in this chapter is to show the necessary and sufficient consistency condition to be satisfied corresponding to the number of interior nodes in the triangulation mesh. Another contribution in this chapter, we obtained a constructive algorithm to determine the position of the nodes in the triangulation knowing one edge and the angles of the finite element mesh. Chapter 6 is the main contribution chapter of this thesis. We study the problem of finding a piece-wise linear invertible change of coordinates that makes the conductivity isotropic for a given planar (FEM) with anisotropic conductivity. In the continuum setting we have an abstract conductive manifold and embedding in Euclidean space. In discrete setting a resistor network with the same topology as (FEM) and an embedding (position of vertices) with a conductivity on each element is identical to Ohm-Kirchhoff system matrix. Finding such an embedding is a discrete equivalent of isothermal coordinates. In order to use optimisation techniques to find an isotropic embedding, it is natural to constrain the variables to obtain a local unique solution. To do this, we assumed the position of one boundary edge and we constrain $n_{v_b} - 1$ angles at the boundary. Then we assigned one conductivity variable per interior vertex and defined conductivity in the triangular face to be the average of these variables at each vertex in the triangle. Numerical experiments show that a unique isotropic embedding can be found with these constraints over a wide range of anisotropic conductivities.

Chapter 2

Electrical Impedance Tomography

2.1 Introduction

This chapter reviews uniqueness results for Electrical Impedance Tomography (EIT) in the continuum context. EIT is an imaging method that determines the conductivity of the body under investigation from electrical measurements at the boundary. This technology is designed to reconstruct the image of the conductivity distributions inside the body Ω by measurements of the currents and voltages in the external of the body $\partial\Omega$. During the last three decades much research has been conducted in different aspects of EIT. Here we will focus on the uniqueness results. Readers interested in medical applications may refer to books by Holder [28, 29]. Geophysical applications and reconstruction techniques can be found in the notes written by Loke [36] or paper [42].

2.2 Sobolev spaces

As usual we take the weak solution of the $\nabla \cdot \gamma \nabla u = 0$ to be in the Sobolev space $H^1(\Omega)$. Here $H^1(\Omega)$ is the set of distribution u in $L^2(\Omega)$ with $\nabla u \in L^2(\Omega)$. The trace theorem tells us there is an extension of the restriction operator $u \to u|_{\partial\Omega}$ which is bounded from $H^1(\Omega)$ to $H^{\frac{1}{2}}(\partial\Omega)$, where $H^s(\partial\Omega)$ is the subset of distribution f in $L^2(\partial\Omega)$ with $(1-\Delta)^s f \in L^2(\partial\Omega)$ where Δ is the surface Laplacian on $\partial\Omega$, for example $\Delta = \frac{\partial^2}{\partial\theta^2}$ on the disc. The D-N map Λ_γ is bounded from $H^{\frac{1}{2}}(\partial\Omega)$ to $H^{-\frac{1}{2}}(\partial\Omega)$. For a detailed description of Sobolev Spaces refer to [24].

2.3 Calderón's inverse problem

A body is represented by a domain $\Omega \subseteq \mathbb{R}^n$ with conductivity $\gamma : \Omega \to \mathbb{R}_+$. An electrical potential $u(x)$ produces current given by the equation

$$j(x) = -\gamma(x)\nabla u, \tag{2.1}$$

The continuum equivalent of Ohm's law. Also with no interior current sources, we have the following equivalent to Kirchhoff's law in Ω

$$\nabla \cdot (\gamma(x)\nabla u) = 0. \tag{2.2}$$

Now we formulate Calderón's Inverse Problem as follows. Given $f \in H^{\frac{1}{2}}(\partial\Omega)$, $u \in H^1(\Omega)$ solves the Dirichlet problem

$$L_\gamma u = \nabla \cdot (\gamma(x)\nabla u) = 0, \tag{2.3}$$

$$u \mid_{\partial\Omega} = f.$$

We then define

$$\Lambda_\gamma(f) = \nu.\gamma\nabla u \mid_{\partial\Omega}, \tag{2.4}$$

where ν is the unit outer normal vector and Λ_γ is the Dirichlet-to-Neumann map or voltage to current map [13]. Calderón posed the question :"Decide whether γ is uniquely determined by Λ_γ, if so, calculate γ in terms of Λ_γ". Calderón dealt with a domain in $\mathbb{R}^n$, $n \geq 2$, with Lipschitz boundary $\partial\Omega$. He assumed that γ is a bounded measurable function with a positive lower bound. The quadratic form associated with Λ_γ is defined by

$$Q_\gamma(f) = \langle f, \Lambda_\gamma f \rangle = \int_\Omega \gamma \, |\nabla u|^2 \, dx. \tag{2.5}$$

$Q_\gamma(f)$ is the power required to obtain electrical potential u when a direct current is applied. The bilinear form associated with $Q_\gamma(f)$ is obtained by the polarisation identity:

$$\begin{aligned}
B_\gamma(f,g) &= \frac{1}{2}\left[Q_\gamma(f+g) - Q_\gamma(f) - Q_\gamma(g)\right] \\
&= \frac{1}{2}\left[\int_\Omega \gamma \, |\nabla(u+v)|^2 - \gamma \, |\nabla(u)|^2 - \gamma \, |\nabla(v)|^2\right] dx \\
&= \int_\Omega \gamma \nabla u \cdot \nabla v \, dx
\end{aligned}$$

where $L_\gamma(v) = 0$ in Ω and $v \mid_{\partial\Omega} = g \in H^{\frac{1}{2}}(\Omega)$. Knowing $\Lambda_\gamma(f)$ is equivalent to knowing $Q_\gamma(f)$ or $B_\gamma(f,g)$. Calderón focused on the forward map $\phi : \gamma \to Q_\gamma$ and was able to prove that it is bounded and analytic in the space from $L^\infty(\Omega)$ to bilinear forms on $H^{\frac{1}{2}}$ where functions γ are real with a positive lower bound. He linearized the problem and verified the injectivity of the Fréchet derivative of ϕ at $\gamma = constant$. Calderón noticed that if the linear operator at $d\phi \mid_{\gamma=constant}$ had a closed range then ϕ is injective in a sufficiently small neighbourhood of $\gamma = constant$. But the range $d\phi$ is not closed so he was unable to show the injectivity of ϕ. Finally, he used harmonic functions to approximate the conductivity γ if $\gamma = 1 + \delta$ for sufficiently small δ in $L^\infty(\Omega)$. His method was based on the construction of the low frequency oscillating solutions [13].

2.4 Determination of the conductivity of isotropic medium

In 1984 Kohn and Vogelius [31] showed that the knowledge of Q_γ or Λ_γ determines the boundary values and the derivatives at the boundary values of smooth isotropic conductivity γ followed by an extension of their result to a piece-wise real analytic [32]. They also studied the special case of a layered structure. They proved that the conductivity can be identified by boundary measurements if it is three times differentiable. In 1987 Sylvester and Uhlmann studied complex geometrical optics solutions (CGO) of the Schrödinger equation with potential q [49, 50]. They proved the uniqueness of solution for the inverse Schrödinger equation for a bounded and compactly supported potential. As a consequence of this result they were able to prove uniqueness of solution for the inverse conductivity problem for three dimensions by reducing it to the inverse problem of the Schrödinger equation. They showed that the conductivity can be determined uniquely if the boundary is C^∞. Note that there is an important relationship between the conductivity and Schrödinger equation given by

$$\gamma^{-\frac{1}{2}} L_\gamma(\gamma^{-\frac{1}{2}}) = \nabla^2 - q. \tag{2.6}$$

where $\gamma \in C^2(\overline{\Omega})$ is strictly positive [50, 52]. Global uniqueness in two dimensions remained open until 1995 when Nachman had the first result towards global uniqueness by considering the conductivities with two derivatives [39]. The challenge in two dimensions is that the problem is not over-determined. This means all the information in Λ_γ must be used to recover γ. However, for $n \geq 3$ the large complex frequency information is sufficient to maintain the global uniqueness. Sylvester and Uhlmann proved a local uniqueness for two dimensions [49]. They considered conductivities near $\gamma_0 = constant$ in $W^{3,\infty}(\Omega)$. Global uniqueness has been justified for pairs of conductivities in a dense open subset of $W^{3,\infty}_{pos}(\Omega) \times W^{3,\infty}_{pos}(\Omega)$ by Sun and Uhlmann [45]. Global uniqueness holds for the special cases of conductivities γ and γ^α which are harmonic for some α in $\mathbb{R}$ [50, 46] or γ radially symmetric in a disc with radius R [48]. Now we state Nachman's result for the isotropic conductivity in bounded domain in $\mathbb{R}^2$,

Theorem 2.4.1. Let Ω be a bounded Lipschitz domain in $\mathbb{R}^2$. Let γ_1 and γ_2 be in $W^{2,p}(\Omega)$ for some $p > 1$, and have positive lower bounds: if $\Lambda_{\gamma_1} = \Lambda_{\gamma_2}$ then $\gamma_1 = \gamma_2$.

Astala and Päivärinta finally proved Calderón's conjecture in two dimensions. They considered the case of isotropic conductivity where $\Omega \subset \mathbb{R}^2$ is bounded, a simply connected domain and $\gamma_i \in L^\infty(\Omega)$, $i = 1, 2$ with an assumption of a positive number c such that $c^{-1} \leq \gamma_i \leq c$. Under this assumption Λ_γ determines γ uniquely [7].

2.5 Non-uniqueness for an anisotropic conductivity

In practice many materials are anisotropic conductors. This means that measured conductivity depends upon the direction as it passes through the material. Mathematically this anisotropic conductivity is represented by a positive definite symmetric matrix function $\gamma = [\gamma^{ij}]_{i,j=1}^n$.

Therefore, the conductivity problem should be adjusted as follows: Let $\Omega \subset \mathbb{R}^n$ be a domain with smooth boundary $\partial\Omega$.

$$L_\gamma(u) = \nabla \cdot \gamma \nabla u = \sum_{i,j=1}^{n} \frac{\partial}{\partial x^i}(\gamma^{ij} \frac{\partial}{\partial x^j} u) = 0 \text{ in } \Omega, \tag{2.7}$$

$$u|_{\partial\Omega} = f,$$

where $f \in H^{\frac{1}{2}}(\partial\Omega)$.

The Dirichlet-to-Neumann map will be written as:

$$\Lambda_\gamma f = \sum_{i,j=1}^{n} (\gamma_{ij} \frac{\partial u}{\partial x^j}) \nu_i | \partial\Omega, \tag{2.8}$$

where $\nu = (\nu_i)_{i=1}^n$ is the unit outer normal to Ω. The weak formulation of the Dirichlet-to-Neumann map associated with the conductivity problem is

$$\Lambda_\gamma : H^{\frac{1}{2}}(\partial\Omega) \to H^{-\frac{1}{2}}(\partial\Omega)$$

given by

$$\langle \Lambda_\gamma f, \eta \rangle = \int_\Omega \sigma(x) \nabla u(x) \cdot \nabla \phi(x) dx, \tag{2.9}$$

for any f,$\eta \in H^{\frac{1}{2}}(\partial\Omega)$, u,$\phi \in H^1(\Omega)$, $\phi|_{\partial\Omega} = \eta$ and u are the weak solution of (2.7). In the previous section it is clearly understood that the uniqueness of the isotopic conductivity inverse problem is completely solved. However, the anisotropic conductivity in general cannot be determined by the Dirichlet-to-Neumann map Λ_γ.i.e. the solution is non-unique. This was observed by Tartar [2] while a detailed derivation is missing in the literature, therefore, a proof is given below.

Proposition 2.5.1. If $\Psi : \overline{\Omega} \to \overline{\Omega}$ is a C^1 diffeomorphism such that $\Psi(x) = x$, for each $x \in \partial\Omega$, then γ and $\hat{\gamma} = \frac{(D\Psi)\gamma(D\gamma)^T}{\det(D\Psi)} \circ \Psi^{-1}$ have the same Dirichlet-to-Neumann map.

Proof. Let $y = \Psi(x)$ and make change of variable in the Dirichlet integral

$$\int_\Omega \gamma_{ij}(x) \frac{\partial u}{\partial x^i} \frac{\partial u}{\partial x^j} dx = \int_\Omega \hat{\gamma}_{ij}(y) \frac{\partial \hat{u}}{\partial y^i} \frac{\partial \hat{u}}{\partial y^j} dy, \tag{2.10}$$

where $\hat{\gamma}(y) = \frac{(D\Psi)\gamma(D\gamma)^T}{\det(D\Psi)} \circ \Psi^{-1}(y)$ and $\hat{u}(y) = u \circ \Psi^{-1}(y)$, note that the solution u of the Dirichlet problem

$$\nabla \cdot \gamma \nabla u = 0 \text{ in } \Omega,$$

$$u|_{\partial\Omega} = f,$$

minimizes the left hand side integral of (2.10), therefore $\hat{u}$ minimizes the right hand side of the same. This means $\hat{u}$ is a solution of

$$\nabla \cdot \hat{\gamma} \nabla \hat{u} = 0 \text{ in } \Omega,$$

$$\hat{u}|_{\partial\Omega} = \hat{f} = u \circ \Psi^{-1}.$$

Let v be a solution of

$$\nabla \cdot \gamma \nabla v = 0 \text{ in } \Omega,$$

$$v|_{\partial\Omega} = g,$$

and let $\hat{v}$ be obtained by v by the change of variable, therefore $\hat{v}$ solves

$$\nabla \cdot \hat{\gamma} \nabla \hat{v} = 0 \text{ in } \Omega,$$

$$\hat{v}|\partial\Omega = \hat{g} = g \circ \Psi^{-1}.$$

By the change of variables in the Dirichlet integrals we have

$$\int_\Omega \gamma_{ij}(x) \frac{\partial u}{\partial x^i} \frac{\partial v}{\partial x^j} dx = \int_\Omega \hat{\gamma}_{ij}(y) \frac{\partial \hat{u}}{\partial y^i} \frac{\partial \hat{v}}{\partial y^j} dy,$$

that can be written as

$$\int_\Omega \gamma \nabla u \cdot \nabla v dx = \int_\Omega \hat{\gamma} \nabla \hat{u} \cdot \nabla \hat{v} dy.$$

This is equivalent to

$$\int_\Omega \nabla \cdot (v\gamma\nabla u) dx - \int_\Omega v \nabla \cdot (\gamma \nabla u) dx = \int_\Omega \nabla \cdot (\hat{v}\hat{\gamma}\nabla u) dy - \int_\Omega \hat{v} \nabla \cdot (\hat{\gamma} \nabla \hat{u}) dy.$$

Apply the divergence theorem

$$\int_{\partial\Omega} v\gamma\nabla u \cdot \nu ds = \int_{\partial\Omega} \hat{v}\hat{\gamma}\nabla\hat{u} \cdot \nu ds,$$

since $\hat{v} = v \circ \Psi^{-1} = v = g$ and $\hat{u} = u \circ \Psi^{-1} = u = f$ at the boundary $\partial\Omega$, then

$$\int_{\partial\Omega} g\Lambda_{\gamma}(f)ds = \int_{\partial\Omega} g\Lambda_{\hat{\gamma}}(f)ds.$$

Then $\Lambda_{\gamma} = \Lambda_{\hat{\gamma}}$. $\square$

Definition 2.5.1. Given a diffeomorphism Φ we define the push forward $\Phi_{*}\gamma = \frac{(D\Phi)\gamma(D\gamma)^{T}}{\det(D\Phi)} \circ \Phi^{-1}$

2.6 Uniqueness up to-diffeomorphism in two dimensions

Research on anisotropic conductivity in two dimensions is focused on uniqueness up to-diffeomorphism. Sylvester showed in [47] that the anisotropic conductivity can be reduced to isotropic in two dimensions using isothermal coordinates. This argument together with Nachman's previous result Theorem (2.4.1) [39] enabled him to prove the following theorem

Theorem 2.6.1. Let Ω be a bounded domain in $\mathbb{R}^2$ with a C^3 boundary, and let γ_1, γ_2 be anisotropic C^3 conductivities in $\overline{\Omega}$. If $\Lambda_{\gamma_1} = \Lambda_{\gamma_2}$, then there exists a C^3 diffeomorphism Φ of Ω such that $\gamma_2 = \Phi_{*}\gamma_1$ and $\Phi \mid_{\partial\Omega} = I$

Astala and Päivärinta examined [6] anisotropic conductivity as well. They were able to show the uniqueness of the anisotropic conductivity up to diffeomorphism. Moreover they studied the inverse problem in the half-space and in the exterior domain. As we have seen from Proposition (2.5.1)

$$\Lambda_{\Phi_{*}\gamma} = \Lambda_{\gamma}.$$

Therefore, the change of variable indicates that there is a large class of conductivities that result in the same electrical measurements at the boundary. Astala and

Päivärinta studied the opposite of this statement for two dimensions: if we have two conductivities that have the same Dirichlet-to-Neumann map, then either of the conductivities is a push forward of the other.
They considered the class of matrix functions $\gamma = [\gamma^{ij}]$ such that

$$[\gamma^{ij}] \in L^{\infty}(\Omega; \mathbb{R}^{2\times 2}), \tag{2.11}$$

$$[\gamma^{ij}]^t = [\gamma^{ij}],$$

The main theorem of Astala and Päivärinta on anisotropic conductivity states:

Theorem 2.6.2. Let Ω be a simply connected bounded domain in $\mathbb{R}^2$ and $\gamma \in L^{\infty}(\Omega; \mathbb{R}^{2\times 2})$. Suppose that the assumptions 2.11 are valid . Then the Dirichlet-to-Neumann map Λ_γ determines the equivalence class
$E_\gamma = \{\gamma_1 \in \sum(\Omega) | \gamma_1 = F_*\gamma, F : \Omega \to \Omega$ is $W^{1,2}$ -diffeomorphism and $F|_{\partial\Omega} = I\}$,
where $\sum(\Omega) = \{\gamma \in L^{\infty}(\Omega; \mathbb{R}^{2\times 2}) \mid C_0 < \infty\}$.

$$\{C_0^{-1} I \leq [\gamma^{ij}] \leq C_0 I\},$$

where $C_0 > 0$

As a consequence of Theorem (2.6.2) Astala and Päivärinta were able to solve the uniqueness problem of the inverse problem in the half-space. This inverse problem has great importance in geophysical prospecting, seismological imaging and non-destructive testing. At least, in the case where a two dimensional approximation is valid, as there is a diffeomorphism that maps the half space to the unit disc, the previous result is applicable.

2.7 Uniqueness of predetermined anisotropic conductivity

Another way to recover the anisotropic conductivity is to assume that it is of a predetermined type. In 1984 Kohn and Vogelius studied the case where the entries of the conductivity matrix are known except one eigenvalue [31]. In 1990, Alessandrini treated the case in which the conductivity γ has the form $\gamma = A(a(x))$. Where $A(a(x))$ is a matrix function and $a(x)$ is piece-wise real-analytic perturbation. He used the monotonic assumption

$$D_t A(t) \geq CI,$$

where $C > 0$ is a constant [3]. In 1997, Lionheart showed that a piece-wise analytic conductivity is determined up to a multiplicative scalar field [34]. Alessandrini and Gaburro improved the result in 2001. They considered a conductivity of the type

$$\gamma(x) = A(x, a(x)),$$

where $A(x,t)$ is given and satisfies the monotonicity condition with respect to the parameter t

$$D_t A(x,t) \geq CI,$$

where $C > 0$ is constant [4]. Recently Gaburro and Lionheart extended the result to manifolds [25]. Finally, Alessandrini and Gaburro considered the case where the local Dirichlet-to-Neumann map is prescribed on an open portion of the boundary [5].

2.8 Geometric formulation

Anisotropic electrical conductivity problems can be considered in differential geometric context. This approach is well-known for those familiar with the work by

Lee and Uhlmann [33], Silvester [47], Astala and Päivärinta [7] and Lionheart [34]. Instead of dealing with electric field and current density as a vector field in Cartesian coordinates we treat them to be differential forms. The vector space of forms consists of functions, zero forms, and one-forms, two-forms, etc, up to n-forms. In two dimensions we have zero forms, functions, and one-forms which can be written as $\alpha = \sum_{i=1}^{n} a_i dx^i$ where a_i are functions and the coordinates are x^i. In differential forms Ohm's law is given by

$$i(x) = \sigma(x) du(x). \tag{2.12}$$

It is clear from Ohm's law in two dimensions the voltage $u(x)$ is a zero form, the current density is one-form. The total current passing through the surface is the integration of $i(x)$ over the surface. The conductivity σ is a mapping from one-form du to one-form $i(x)$. Then $\sigma(x)$ is positive definite and symmetric which means in differential forms:

$$\sigma\alpha \wedge \beta = \sigma\beta \wedge \alpha, \tag{2.13}$$

$$\sigma\alpha \wedge \alpha = \phi(x) dx^1 \wedge dx^2, \tag{2.14}$$

where $\alpha(x) \neq 0$ and $\phi(x) > 0$. If there is no source of internal current the current density is a closed form i.e

$$-d(\sigma du) = 0. \tag{2.15}$$

A discrete analogy of the continuum conductivity in forms will be discussed later in this thesis Section (3.4).

Chapter 3

Electrical Resistor Networks

3.1 Introduction

In this chapter we review previously known results on inverse problems for resistor networks. Electrical resistor networks are a discrete analogue of the continuous case of inverse conductivity problem introduced by E. Curtis and J. Morrow. As well as being of interest as a discrete analogue of the continuum problem, resistor networks are also used to test EIT measurement systems [26]. First the definitions of graph, resistor networks and an example is given. Second, some fundamental electrical principles are discussed including the maximum principle for the discrete resistor networks. Then, matrix theory related to resistor networks represented by planer graph is explained. Next, harmonic continuation process in resistor networks is introduced since it is an important procedure for determining the conductivity from boundary measurements in resistor networks. Medial graph for circular planar resistor network is constructed as it plays a role in characterizing the circular planar resistor networks. Some useful definitions and results about well-connected graphs are also presented. Finally, we discuss the resistor networks with the same topology as finite element mesh.

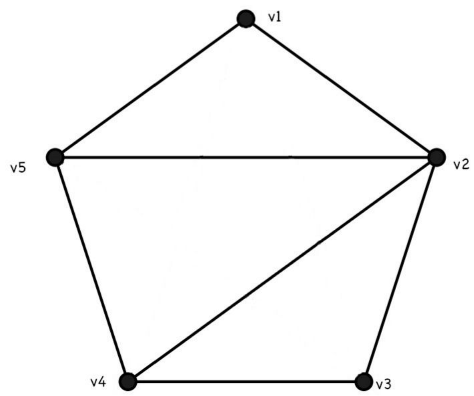

Figure 3.1: Graph of five nodes.

3.2 Resistor networks

A graph G is an ordered pair (V, E) where V is the set of all nodes (vertices) and E is the set of unordered pairs $\{u, v\}$ [8, 9]. The elements of the set E are called edges. Figure (3.1) is an example of a graph with five nodes and seven edges.
The set of nodes are: $V = \{v_1, v_2, v_3, v_4, v_5\}$ while the set of edges are:
$E = \{\{v_1, v_2\}, \{v_1, v_5\}, \{v_2, v_3\}, \{v_2, v_4\}, \{v_2, v_5\}, \{v_3, v_4\}, \{v_4, v_5\}\}$.

The graph is simple if it has no loops and no two edges that share the same pair of nodes. From the graph $G = (V, E)$ we define a digraph $\overline{G} = (V, \overline{E})$ by choosing an orientation. Therefore, digraph is an ordered pair $(V, \overline{E})$ where V is a finite set of nodes and $\overline{E} \subset V \times V$ is the set of ordered pairs (u, v) i.e. $\overline{E}$ is a binary relation on V. The elements of V are called vertices or nodes and the elements of $\overline{E}$ are arcs. An oriented graph is a digraph where the relation $\overline{E}$ is antisymmetric. Before we define an immersion, note that V is an abstract finite set, essentially just labels.

Definition 3.2.1. A graph G is immersed in the plane if there is a map (immersion) $f : G \to \mathbb{R}^2$ such that:

1. The vertices of G are mapped to distinct points in $\mathbb{R}^2$.

2. The edges of the graph are mapped to simple curves joining the nodes.

Definition 3.2.2. An embedding of a graph in the plane is an immersion such that two edges may intersect only at the end points.

Definition 3.2.3. Any graph embedded in a two dimensional plane is called a planar graph.

A network of resistors (V, E, γ) is defined by a simple graph (V, E) and a function $\gamma : E \to \mathbb{R}^+$ which represents the conductance.
This is a model for a collection of resistors with resistance $\frac{1}{\gamma(e)}$. Here, V represents the set of nodes while E represents the set of conductors. Now, we will construct two specific types of resistor networks: circular networks and rectangular networks.
Each resistor network G has interior nodes denoted by V_0 and boundary nodes denoted by V_b. The boundary nodes of a network of resistors varies from one network to another. Therefore, we will define the boundary nodes for every considered network. The interior nodes in any network of resistors are simply $V \setminus V_b$. Each node in the network of resistors has neighbours i.e. when there is an edge that connects the pair. The set of all neighbours of the node p will be denoted by $N(p)$. The edge that connects an interior node to a boundary node is called a boundary edge.
A circular resistor network is a planar graph embedded in a disc D in the plane such that the boundary nodes V_b lie on the outer circle and the rest of the nodes are inside the disc [14]. E. Curtis and J. Morrow studied special types of embedded circular networks that are constructed as follows : Let $G = (V, E) = C(m, n)$ where m is the number of circles and n the number of rays. The nodes are the points $p_{(i,j)}$ in the plane centred at the origin $p_0 = (0, 0)$ where $p_{(i,j)}$ has the coordinates expressed in polar coordinates by $p_{(i,j)} = (i, \frac{\pi j}{n})$. The nodes are labelled cyclically and the boundary nodes are given by $p_j = (m + 1, j)$ where $1 \leq j \leq n$. Note that the central node has n neighbouring nodes while the other interior nodes have only four neighbours and the boundary nodes have exactly one neighbour.
An example of circular network of resistors is shown in Figure (3.2).

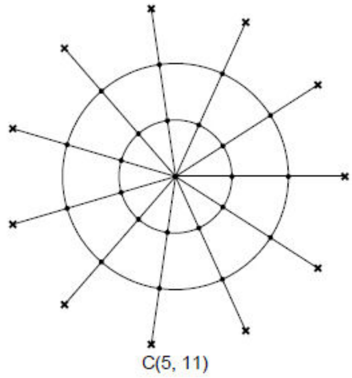

Figure 3.2: Circular network of resistors.

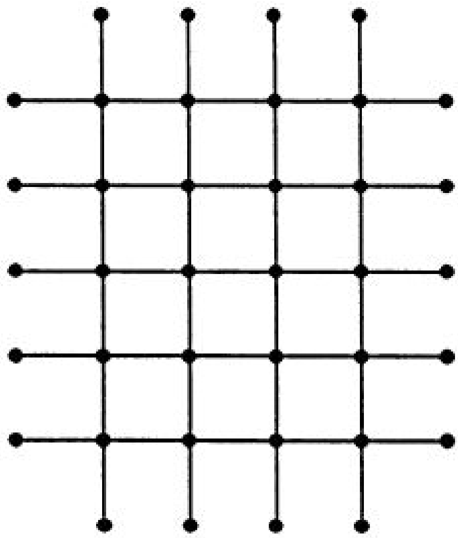

Figure 3.3: Rectangular network of resistors.

Now we will construct a rectangular embedded network of resistors. The nodes of the network of resistors lie at the lattice points given by $p_{i,j} = (i, j)$ where $0 \leq i \leq m+1$ and $0 \leq j \leq n+1$ with the four corner points $(0, 0)$, $(m+1, 0)$, $(m+1, n+1)$, $(0, n+1)$ omitted. The interior points in the rectangular networks have four neighbouring nodes while the boundary nodes have only one neighbour [18]. Figure (3.3) is an example of rectangular network resistors. In this thesis we deal with another type of circular networks. Our resistor network has the same topology as a finite element triangular mesh that is simply a mesh with triangular faces.

An example of our circular resistor network is shown in Figure (3.4).

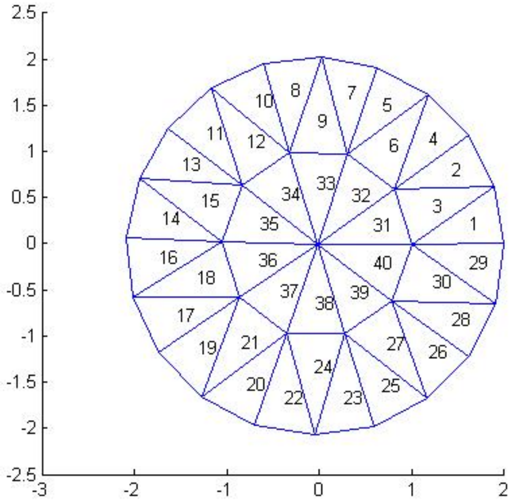

Figure 3.4: Triangulated network of resistors.

3.3 Electrical principles

Let $\Gamma = (V, V_b, E, \gamma)$ be a network of resistors with conductivity function γ where $\gamma : E \to \mathbb{R}^+$ and $\gamma(pq)$ is the conductance through the arc (p, q) and $V_b \subset V$ is the set of all boundary nodes of Γ. If $u : V \to \mathbb{R}$ is a function defined in the nodes of the network Γ then the current passing through the conductance $\gamma(pq)$ is defined by Ohm's law:

$$I(p, q) = \gamma(pq)[u(p) - u(q)]. \tag{3.1}$$

If p is an interior node with neighbours $q \in N(p)$ then according to Kirchhoff's law the currents that enter the node p are equal to the algebraic sum of the currents leaving the node p. That is:

$$(L_\gamma u)(p) = \sum_{q \in N(p)} \gamma(pq)[u(p) - u(q)]. \tag{3.2}$$

Note that the algebraic sum of the currents over the whole network is zero. That is

$$\sum_{p \in V} L_\gamma(p) = 0. \tag{3.3}$$

u is said to be γ-*harmonic* if $L_\gamma(p) = 0$ at every interior node $p \in V_0$.

Thus Eq. (3.2) becomes

$$\sum_{q \in N(p)} \gamma(pq)[u(p) - u(q)] = 0. \tag{3.4}$$

and the sum of the currents over the boundary nodes will be zero. That is:

$$\sum_{p \in V_b} L_\gamma(p) = 0. \tag{3.5}$$

If u is γ-*harmonic* then Eq.(3.4) can be written by

$$\left(\sum_{q \in N(p)} \gamma(pq) \right) u(p) = \sum_{q \in N(p)} \gamma(pq)u(q), \tag{3.6}$$

or

$$u(p) = \frac{\sum_{q \in N(p)} \gamma(pq)u(q)}{\sum_{q \in N(p)} \gamma(pq)}. \tag{3.7}$$

Since, assuming that the conductances $\gamma(pq)$ are positive real numbers, Eq.(3.7) imply that the value of $u(p)$ is a weighted average of the values at the neighbouring nodes. Now if the value of u at some neighbouring nodes is less than $u(p)$ then the value of u must be more than the value of $u(p)$ at some other neighboring nodes [16]. This proves the following lemma:

Lemma 3.3.1. Suppose u is a γ-*harmonic* function on Γ, and let p be an interior node. Then either $u(p) = u(q)$ for all nodes $q \in N(p)$ or there is at least one node $q \in N(p)$ for which $u(p) > u(q)$ and there is at least one node $r \in N(p)$ for which $u(p) < u(r)$.

The importance of the previous lemma is that it leads to any γ-*harmonic* function attaining its extremum at the boundary in the network of resistors.

Theorem 3.3.1. Let u be a γ-*harmonic* function on V then the maximum and minimum values of u occur on the boundary.

Proof. Suppose on the contrary that the maximum value occurs at $p_0 \in V_0$, such that $u(p_0) > u(q)$ for every $q \in V_b$. Let $\{p_0, ..., p_n\}$ be a sequence of nodes in V such that $p_j p_{j+1}$ is an edge in E and $p_n \in V_b$. Then let j be the first index for which $u(p_j) < u(p_0)$. This means that $u(p_{j-1}) = u(p_0) \geq u(q)$ for all $q \in N(p_{j-1})$ and $u(p_{j-1}) > u(p_j)$. This contradicts Lemma (3.3.1) same arguments for the minimum. □

As a consequence of the maximum principle for the network of resistors any γ-*harmonic* function that is zero at every node in the boundary, is identically zero at all nodes [18].

3.4 Discrete geometric formulation

In this section we derive a discrete analogue of continuum conductivity in differential forms discussed earlier in Section (2.8). This is a discrete version of exterior derivative.

Definition 3.4.1. Let $\phi : V \to \mathbb{R}$ be a 0-cochain $C^0(\overline{G})$ and $\psi : E \to \mathbb{R}_+$ be 1-cochain $C^1(\overline{G})$

The co-differential $d : C^0(\overline{G}) \to C^1(\overline{G})$ is :

$$d\phi(ij) = \phi(j) - \phi(i). \tag{3.8}$$

The boundary operator $\partial : C_1(\overline{G}) \to C_0(\overline{G})$ is:

$$(\partial j)(i) = \sum_{j:(i,j)\in E} J(e). \tag{3.9}$$

γ is a diagonal linear map $C^1(\overline{G}) \to C_1(\overline{G})$

we define L_γ to agree with Eq. (3.2) as

$$L_\gamma = \partial\gamma d. \tag{3.10}$$

3.5 Response and Kirchhoff matrix

If a voltage function f is applied at the boundary of a resistor network then a current will pass through the conductances γ_{ij} of the network. If the network has n nodes then the voltage to current function will be represented by $n \times n$ matrix called a response matrix. The response matrix has three properties:

1. Λ is symmetric:
$$\Lambda_{ij} = \Lambda_{ji}.$$

2. The sum of entries in each row is equal to zero

3. For $i \neq j$, $\Lambda_{ij} \leq 0$

Let $\Gamma = (\Omega, \gamma)$ is a network of resistors consisting of n nodes $\{v_1, v_2, ..., v_n\}$ and γ_{ij} are the conductances on the edges of the network. Note that if there is no edge between v_i and v_j then $\gamma_{ij} = 0$ and if there is an edge between v_i and v_j then $\gamma_{ij} > 0$. The Kirchhoff matrix is defined as follows:

1. If $i \neq j$ then $k_{i,j} = -\gamma_{ij}$.

2. If $i = j$ then $k_{i,j} = \sum_{i \neq j} \gamma_{ij}$.

If u is a voltage whose components are $(u_j) = (u(v_j))$ then $\phi(v_i) = \sum_j K_{i,j} u_j$ is the current passing through the node v_i in the network [18, 14].

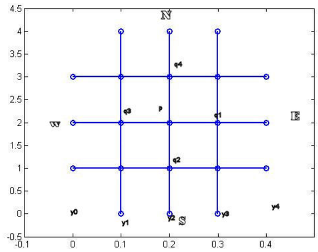

Figure 3.5: Square network of resistors.

3.6 Harmonic continuation

Kirchhoff's law is useful to construct a γ-*harmonic* function with a pre-assigned boundary condition at some nodes in the network and the current is also known for some of the nodes. Let u be a γ-*harmonic* function and consider a rectangular network similar to the one shown in Figure (3.5). Recall Kirchhoff's law written in the form

$$\left(\sum_{q\in N(p)} \gamma(pq)\right) u(p) = \sum_{q\in N(p)} \gamma(pq)u(q). \tag{3.11}$$

Note that the above equation is a five point formula. That is, when the values of $u(q_2), u(q_3), u(q_4), u(p)$ are known $u(q_1)$ can be determined provided that the conductances are known. Moreover, if the current passing through q_3p is known, together with the values of $u(q_2), u(q_3), u(q_4)$, then $u(p)$ and $u(q_1)$ can be calculated by using Ohm's law and Kirchhoff's law. A similar idea can be used if we replace $u(q_2), u(q_3), u(q_4)$ by the South (S), West (W) and North (N) respectively. If the values of the γ-*harmonic* function are known in the (W), (S) and (N) and a current is applied in the west (W) then we can construct the γ-*harmonic* function in the interior of the network and in the East (E). This process is called harmonic continuation.

Example 3.6.1. Let the conductors in Figure (3.5) have the value 1, and assume the γ-*harmonic* function u has the boundary values 0 for all nodes in South, West and north faces and the current imposed in the West face is given by $\phi(0, j) = (-1)^j$ for $1 \leq j \leq 3$. The γ-*harmonic* function with these boundary values can be constructed as follows: first we use Omh's law in the horizontal conductors joining Y_0 and Y_1 to find the values of the γ-*harmonic* values in Y_1

$$u(0,1) - u(1,1) = \phi(1) = -1 \Rightarrow u(1,1) = 1$$
$$u(0,2) - u(1,2) = \phi(2) = 1 \Rightarrow u(1,2) = -1$$
$$u(0,3) - u(1,3) = \phi(3) = -1 \Rightarrow u(1,3) = 1$$

Since we assume all the conductors have the same value 1 Kirchhoff's law will be

$$4u(p) = \sum_{q \in N(p)} u(q).$$

Now we use Kirchhoff's law in the nodes of Y_1 to obtain the values of the γ-*harmonic* function in Y_2

$$4u(1,1) = u(1,0) + u(0,1) + u(1,2) + u(2,1) \Rightarrow u(2,1) = 5$$
$$4u(1,2) = u(1,1) + u(0,2) + u(1,3) + u(2,2) \Rightarrow u(2,2) = -6$$
$$4u(1,3) = u(1,2) + u(0,3) + u(1,4) + u(2,3) \Rightarrow u(2,3) = 5$$

Similarly, apply Kirchhoff's law on the nodes of Y_2 to get the values in Y_3

$$4u(2,1) = u(2,0) + u(1,1) + u(2,2) + u(3,1) \Rightarrow u(3,1) = 25$$
$$4u(2,2) = u(2,1) + u(1,2) + u(2,3) + u(3,2) \Rightarrow u(3,2) = -33$$
$$4u(2,3) = u(2,2) + u(1,3) + u(2,4) + u(3,3) \Rightarrow u(3,3) = 25$$

By applying the harmonic continuation process one may extend a γ-*harmonic* function on a larger set. Consider the network of resistors in Figure (3.6). Let C_i represent the nodes lying on the vertical line $x = i$. The vertical lines in Ω_0 are numbered from left to right as $C_0, ..., C_n$. Take the set $S \subset \Omega_0$ which consist of the columns $C_0, ..., C_k$.

Lemma 3.6.1. Let u be a γ-*harmonic* function defined in the set S then u can be

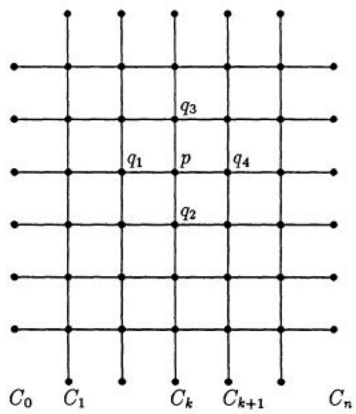

Figure 3.6: Harmonic continuation extension.

extended to be γ-*harmonic* function on the set $S\bigcup\{C_{k+1}\}$. The definition of u is uniquely determined on the interior nodes of C_{k+1} and can be given arbitrary values at the end of column C_{k+1}.

Proof. The assumed harmonicity of u at any of the nodes in columns $\{C_0, ..., C_{k-1}\}$ will not be affected by the definition of u on the nodes of column C_{k+1}.
Apply Kirchhoff's law in the node p in column C_k and you get

$$\left(\sum_{q\in N(p)} \gamma(pq)\right) u(p) = \sum_{q\in N(p)} \gamma(pq)u(q).$$

$u(q_4)$ is determined by the values of $u(q_1), u(q_2), u(q_3), u(p)$. Similarly, all the interior nodes of C_{k+1} will be calculated. The value of u at the end nodes will be assigned arbitrarily. $\square$

In the continuous case, if a harmonic function is constant in an open domain then it will be identically constant in the whole domain. The next lemma will show this is not the case in the discrete harmonic functions. The γ-*harmonic* function can be locally constant.

Lemma 3.6.2. Let $(\Omega_0, \Omega_1, \gamma)$ be a network of resistors. Suppose a function u is defined to be constant on the nodes of columns $C_1, ..., C_k$. Then u can be continued as γ-*harmonic* function where u is constant on or below the diagonal indicated by

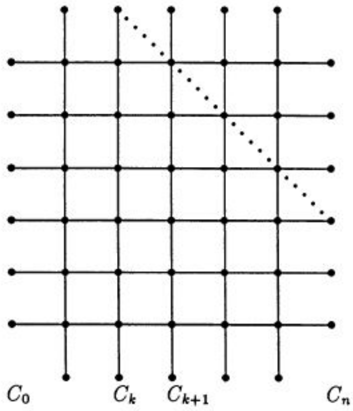

Figure 3.7: γ-*harmonic* continuation.

the dotted line in Figure (3.7). The values of u at the boundary nodes at the tops of columns $\{C_{k+1}, ..., C_n\}$ are arbitrary [16].

Proof. Immediate from previous lemma. $\square$

3.7 Uniqueness for rectangular resistor network

In [16] E. Curtis and J. Morrow studied the rectangular network of resistors. They introduced the γ-*harmonic* and the process of harmonic continuation explained in the previous section. Using this process they proved global uniqueness and continuity of Λ_γ. Moreover, they obtained a reconstruction procedure to recover γ from the Neumann to Dirichlet map Λ_γ on the boundary. They also characterized the Dirichlet to Neumann map for square networks of resistors and they provided a reconstruction algorithm to determine the conductivity γ from Dirichlet to Neumann map on the boundary [17].

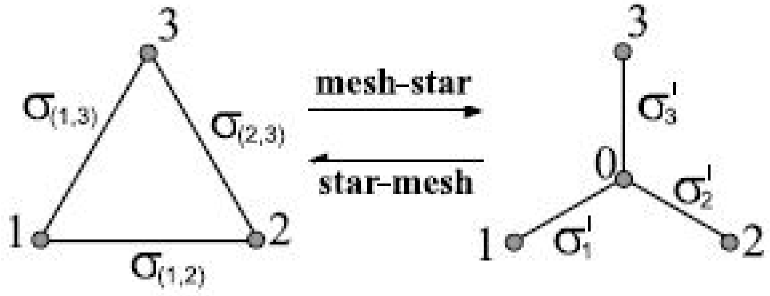

Figure 3.8: $Y-\Delta$ transformation.

3.8 Uniqueness of circular resistor network

E. Curtis, D. Ingerman and J. Morrow dealt with circular graphs and circular planar resistor networks in [14]. They introduced the concept of k-connection between sequences of boundary nodes through a circular planar graph that is if $P = (p_1, ..., p_k)$ and $Q = (q_1, ..., q_k)$ are two sequences of boundary nodes then there is a set of disjoint paths $p_i \leftrightarrow q_i$. They even calculated the possible number of pairs of sequences connected through the circular planar graph. Also they defined the critical circular planar graphs and showed that any two critical circular planar graphs are Y-Δ equivalent if, and only if, they have the same connections. The Y-Δ transformation is a well-known electrical transformation which does not affect the response of the network. This transformation is shown in Figure (3.8). Readers interested in detailed discussion of Y-Δ transformation may refer to [18, 20]. Using the concept of medial graph that will be discussed in detail in the next section, they proved that two circular graphs are Y-Δ if, and only if, their medial graphs are equivalent. Moreover, they gave a reconstruction algorithm of the conductivity on a circular planar network of resistors from a voltage to current map measurements on the boundary. Finally, they described the set of network response matrices that happen for circular planar networks. In another work, E. Curtis, E. Mooers and J. Morrow [15] characterized the boundary measurements data that resulted from circular networks. Also, an algorithm for determining the values of the conductors from Dirichlet to Neumann map on the boundary was given for special types of circular planar resistor networks.

Moreover, they obtained some numerical reconstruction results of the values of the conductors from boundary measurements.

3.9 Medial graphs

Medial graphs, described by Colin de Verdière [20] are an important tool in understanding resistor networks. Consider networks of resistors with circular planar graphs G that are embedded in a disc D in the plane such that the boundary nodes lie on a circle C that bounds D and the rest of the nodes are inside the circle. As in [14, 15] the boundary nodes $V_b = \{v_1, ..., v_n\}$ are arranged in clockwise circular order around C. The medial graph is constructed as follows:

1. For each v_i lying on the circle C place one point v_{i_-} before v_i and v_{i_+} after v_i
2. Put a 4-valent vertex on each edge with two medial graph edges on each side of the original edge in the mid point m_e
3. The vertices of the medial graph M are the points v_{i_-}, v_{i_+} and m_e.
4. Moving in an anti-clockwise direction along the circle C join the vertex v_{i_-} to the mid point of the edge incident to v_i then moving in clockwise direction along the circle C join the vertex v_{i_+} to the mid point of the edge incident v_i.
5. If e and f are edges in G having a common vertex and incident to the same face in G then the line $m_e m_f$ joining the mid points m_e and m_f is an edge of M. Figure (3.9) illustrates a medial graph of a circular planar resistor network with a topology similar to finite element mesh.

The vertices of the medial graph m_e inside D are 4-valent while the vertices of the medial graph that lie along C are one-valent. Any 4-valent vertex v of M an edge uv has a direct extension vw. A path $u_0 u_1, ..., u_k$ in M is called a geodesic fragment

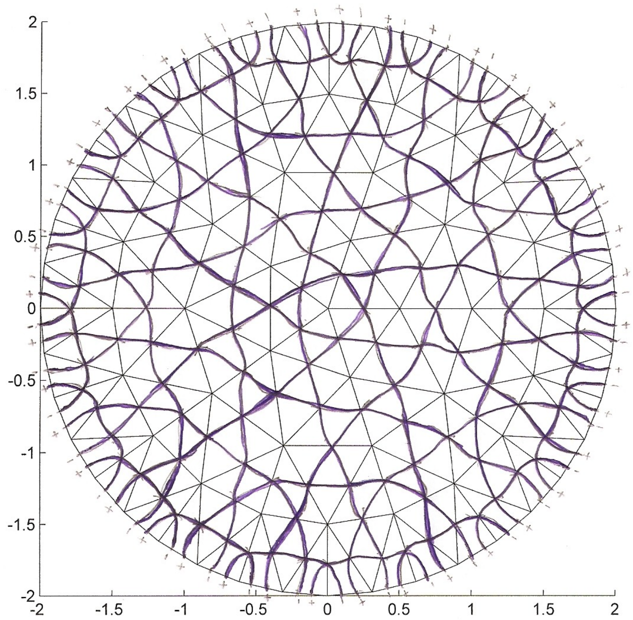

Figure 3.9: Medial graph from a triangular mesh.

if each edge $u_{i-1}u_i$ has a direct extension u_iu_{i+1}. A geodesic is a geodesic fragment which satisfies one of the following conditions:

1. u_0 and u_k are points on the circle C.

2. $u_k = u_0$ and $u_{k-1}u_k$ has a direct extension u_0u_1.

A chord is an arc which starts and ends on the boundary circle C and has no self intersection.

Colin de Verdière [20] made the following definition of taut ("tendu" in French).

Definition 3.9.1. A medial graph M is a taut if it has no cycles and if any two chords have at most one intersection point.

Taut graphs are useful in light of the following:

Proposition 3.9.1. Two graphs are equivalent taut if and only if their chords have the same end points. One can be obtained from the other by Y-Δ transformation.

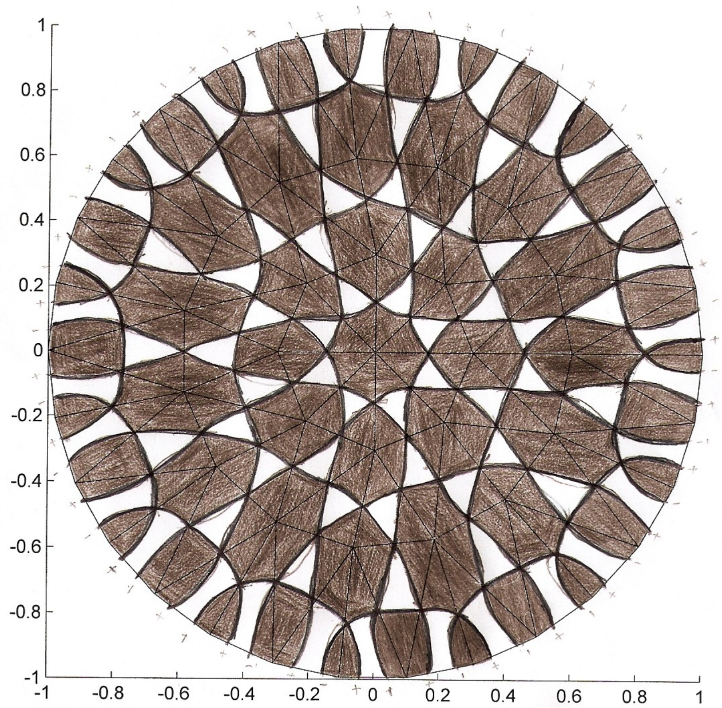

Figure 3.10: Medial graph of three layered triangulated network.

A circular planar graph with triangular faces is called triangular mesh. For the special case of a layered triangular mesh with no more then two inward pointing triangles for one outward pointing triangle we prove the following:

Proposition 3.9.2. A layered triangulated mesh is a taut graph.

Proof. In a medial graph of layered triangulated mesh the arc of that crosses another arc on an edge of non-spoke triangle will not meet this arc again because their direct extensions are in opposite directions. Also an arc which crosses another arc on a spoke triangle will not meet the same arc again as one arc has a direct extension moving upwards to next layer, while the other with direct extension is moving downwards in the opposite direction. Hence, in any case the arcs cross each other at most once. □

Figure (3.10), Figure(3.11), Figure (3.12) and Figure (3.13) are taut graph of triangulated circular planar networks.

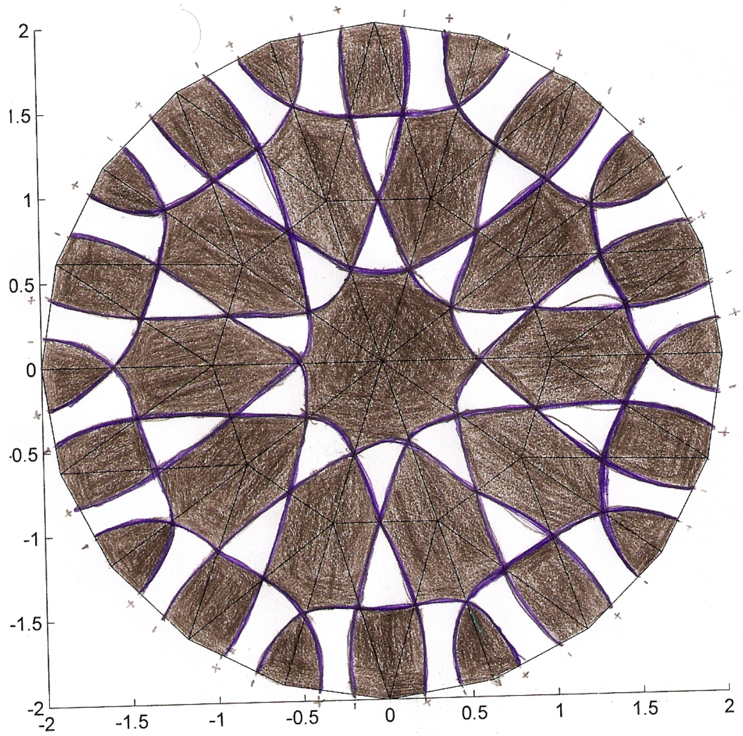

Figure 3.11: Medial graph of two layered triangulated network.

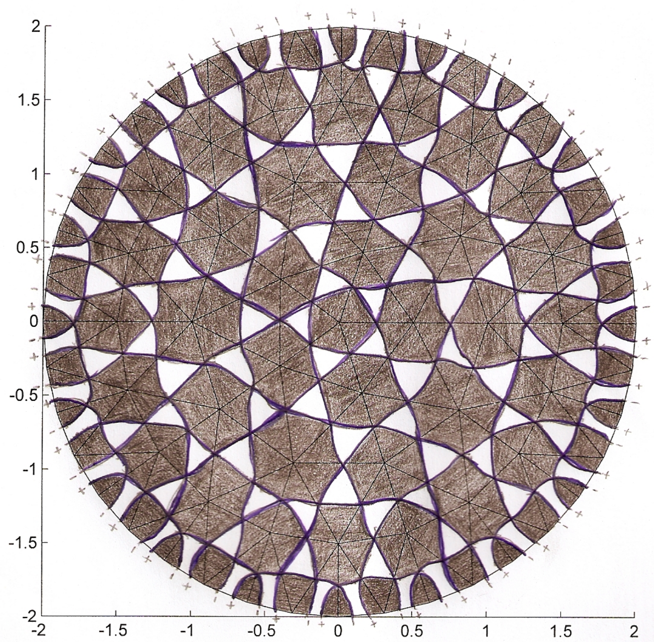

Figure 3.12: Medial graph of four layered triangulated network.

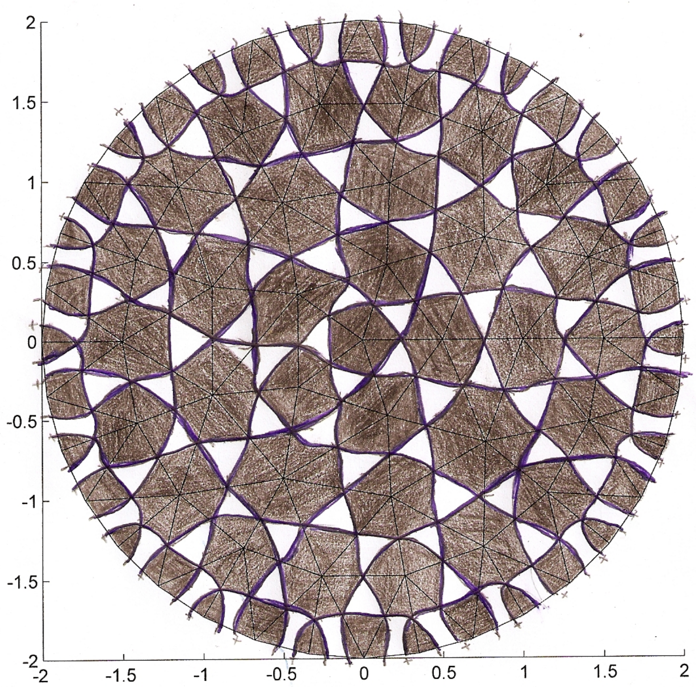

Figure 3.13: Medial graph of a four layered triangulated network.

3.10 Well-connected circular planar resistor network

Consider networks of resistors with circular planar graph G that is embedded in a disc D in the plane such that the boundary nodes lie on circle C that bounds D and the rest of the nodes inside the circle. As in [14, 15] the boundary nodes $V_b = \{v_1, ..., v_n\}$ are arranged in clockwise or anticlockwise circular order around C. Let a pair of sequences $(P; Q)$ to be subset of V_b such that $P = \{p_1, ..., p_k\}$ and $Q = \{q_1, ..., q_k\}$ belong to disjoint arcs. The pair is circular if the nodes $\{p_1, ..., p_k, q_k, ..., q_1\}$ are in circular order in V_b. A circular pair $(P; Q)$ is called connected through G if there are k disjoint paths $\{\alpha_1, ..., \alpha_k\}$ in G such that for each i we have a path α_i starting with p_i ending with q_i passing through non boundary nodes other then p_i and q_i. Let $\pi(G)$ be the set of all connected circular pairs, then the graph is said to be well-connected if all circular pairs are in $\pi(G)$. Consider a graph G' obtained from G by removing one edge by deleting or contracting. The network G is said to be critical if removal of an edge breaks some connection in $\pi(G)$. Colin de Verdière in [20] characterized the minimal planar resistor networks using the medial graph as a tool. He proved the following theorem which gives the necessary condition for planar resistor network to be well-connected i.e γ can be determined from Λ_γ. Let $\epsilon(G)$ be the number of edges in the planar resistor network and n_{v_b} be the number of boundary nodes.

Theorem 3.10.1. The well-connected planar resistor network from a connected component of ζ must satisfy the property $\epsilon(G) = \frac{n_{v_b}(n_{v_b}-1)}{2}$. If $\epsilon(G) < \frac{n_{v_b}(n_{v_b}-1)}{2}$ then the planar resistor network is not well-connected.

If a planar resistor network is not well-connected then we have over determined network of resistors because the number of data is more than the number of unknowns. We are interested in planar resistor networks that have the same topology as triangulated mesh. Triangular meshes suitable as FEM meshes for the conductivity equation generally have smaller triangles near the boundary, where current densities are high. Such meshes generally correspond to resistor networks that are over determined. As an example we show that this is the case assuming the sides of the triangles are no smaller than $\frac{2\pi}{n_{v_b}}$ and the angles are bounded away from $\frac{\pi}{2}$. Figure (3.14) shows an example of circular planar resistor network associated with triangulated mesh. The number of triangles $n_t < \frac{\pi}{A}$ where A is the minimum area of the triangles and $A > \alpha l^2$ for some $0 < \alpha < 1$. So we have

$$n_t < \frac{\pi}{\alpha l^2} = \frac{n_{v_b}^2}{4\alpha\pi} \Rightarrow 4\alpha\pi n_t < n_{v_b}^2.$$

Also we know

$$n_t = \frac{2n_e - n_{v_b}}{3}.$$

Hence

$$4\alpha\pi(\frac{2n_e - n_{v_b}}{3}) < n_{v_b}^2 \Rightarrow \frac{2}{3}\alpha\pi(2n_e - n_{v_b}) < \frac{1}{2}n_{v_b}^2,$$

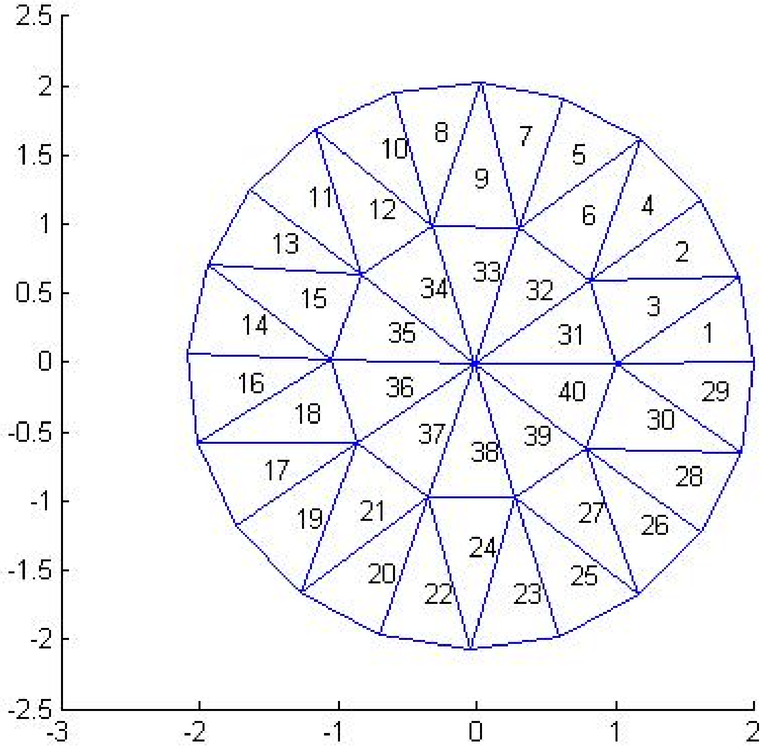

Figure 3.14: Triangulated mesh.

Therefore we have

$$\frac{4\alpha\pi}{3}n_e < \frac{1}{2}n_{v_b}(n_{v_b} + \frac{4}{3}\alpha\pi) < \frac{1}{2}n_{v_b}(n_{v_b} - 1).$$

This means

$$n_e < (\frac{3}{4\alpha\pi})\frac{1}{2}n_{v_b}(n_{v_b} - 1).$$

Choose $\alpha = \frac{3}{2\pi}$

$$n_e < \frac{1}{2}n_{v_b}(n_{v_b} - 1).$$

So we conclude that a circular planar resistor networks associated with a layered finite element mesh is over determined.

3.11 Simplicial complex

In this section we will develop abstract complexes that are useful in the discussion of necessary and sufficient consistency condition that will follow later in Section (5.10). Moreover, an embedded conductive simplicial complex gives rise to a system matrix equivalent to the Ohm-Kirchhoff matrix. This correspondence will be discussed in Subsection (4.2.4).

Definition 3.11.1. Consider a non oriented abstract simplicial complex $K = (V, E, T)$ in two dimensions where V is set of vertices, E is the set of edges and T is the set of faces. The graph $G = (V, E)$ is called one-skeleton

Definition 3.11.2. Consider an oriented abstract simplicial complex $\overline{K} = (V, \overline{E}, T)$ in two dimensions where V is the set of vertices, $\overline{E}$ is the set of arcs with arbitrary direction and T is the set of faces. The digraph $(V, \overline{E})$ is directed one-skeleton.

Definition 3.11.3. Consider a conductive abstract simplicial complex (K, γ) where γ is a quadratic form defined on arcs. Let the map $\omega : \overline{E} \to \mathbb{R}^+$ be a one-cochain which represents the current in each arc then

$$\gamma(\omega) = \sum_{e \in \overline{E}} \gamma(e)\omega(e). \tag{3.12}$$

Let the voltage u be the 0-cochain, then the power anticipated in the conductive abstract simplicial complex is given by

$$Q_\gamma(u) = \sum_{(v_1,v_2) \in \overline{E}} \gamma_{(v_1,v_2)}(u(v_2) - u(v_1))^2. \tag{3.13}$$

Define the Dirichlet problem:

minimise

$$Q_\gamma(u), \tag{3.14}$$

subject to

$$u|_{V_b} = f,$$

for which the minimum is the Ohm's-Kirchhoff's solution.

Definition 3.11.4. A conductive simplicial complex has embedding if there is a map $\phi : K \to \mathbb{R}^2$ that maps V to points, E to line segments and T to triangles.

An embedded conductive simplicial complex is equivalent to a FEM as we shall see in the next chapter.

Chapter 4

Finite Element Models

4.1 Introduction

Most methods for image reconstruction of the conductivity distribution inside a body by boundary measurements need a solution of the forward problem for assumed conductivity to compare the predicated voltages with the measured data. Also the interior electric field $E = -\nabla u$ is required to calculate the Jacobian. Analytical methods can solve the forward problem only in a limited, simple geometry, and homogeneous or simple conductivity distributions. In dimension two irregular bodies can be handled to some extent using conformal mapping techniques although this can be difficult. This makes analytical methods useful to determine approximation of the potential from an initial guess of the conductivity. After the approximation of the conductivity it is essential to use numerical techniques. Numerical methods for general geometry and inhomogeneous conductivity need the discretization of both the body and the conductivity. There are various numerical methods used in EIT for forward solution such as the Finite Element Method (FEM) [51], the Finite Difference Method (FDM) [41], the Finite Volume Method (FVM) [22] and the Boundary Element method (BEM) [19]. The Finite Element Method decomposes the domain into irregular elements (triangular or quadrilaterals) for dimension two and polyhedra (tetrahedra, prisms or hexahedra) for dimension three. Basis functions interpolate between specified nodal values to approximate the potential. On each element the potential is represented by a polynomial and the resulting approximation space is piece-wise polynomial. There are two advantages of the Finite Element Method: irregular bodies can be accurately approximated by irregular elements and the size of the elements may vary to have a better approximation to the electrical field. The Finite Difference Method and the Finite Volume Method are very similar to FEM. The potential is approximated by its values at the nodes of a regular rectangular elements. These methods have the advantage that their regular grids are easily generated. Also, their implementation is fairly easy and the result is easy to display. Another advantage is that more efficient solvers can be used to accurately represent curved boundaries or smooth interior structures. The Boundary Element Method discretizes the surface of the body and an analytic Green's function is used within enclosed homogeneous volumes. In forward modeling of EIT boundary element method is used with piece-wise constant homogeneous conductivity on a smooth boundary. This method has an advantage of dealing with unbounded domains. Those working on EIT reconstruction typically prefer to use FEM due to the close integration of the Jacobian calculation and the FEM forward problem [11]. Moreover, the Complete Electrode Model (CEM) is a non-standard type of boundary condition not included in commercial FEM software implementation. So implementation of FEM specific to EIT are used in [54]

4.2 Finite element formulation

4.2.1 Approximation space

The starting point in constructing the approximation space of the domain Ω is to divide the domain into a finite number of irregular elements called simplices. Usually the simplex in two dimensions is a triangle and in three dimensions is tetrahedron.

Each element involves a number of nodes that include the vertices of the element and possibly a point in the interior or boundary point. The division of the domain into elements must be consistent. That is, if a node belongs to two faces it must be a node in both elements, also no coincident faces are parallel. The union of the elements is called the finite element mesh. In the case of a simplicial mesh in two dimensions consisting from a set of triangular elements $\{T_k\}$, the union $\bigcup_k T_k$ is an approximation to the domain Ω.

4.2.2 Approximation of the potential

We also need to approximate the potential function u. On each triangular element consider a nodal basis functions $\phi_i(x)$ to be a piece-wise linear function such that $\phi(x_i) = 1$ and $\phi(x_j) = 0$, $j \neq i$. Then the approximation of the potential will be:

$$u(x) = \sum_i u_i \phi_i(x). \tag{4.1}$$

4.2.3 The system matrix

The finite element equivalent to the operator Λ_γ defined earlier, is called the system matrix. Assign a positive definite matrix σ^k to each simplex T_k. The finite element system matrix $K \in \mathbb{R}^{n_v \times n_v}$ where n_v is the number of nodes in a simplicial mesh is defined by

$$K_{ij} = \sum_{k:\{x_i,x_j\}\subset T_k} \nabla\phi_i \cdot \sigma^k \nabla\phi_j |T_k|, \tag{4.2}$$

where $|T_k|$ is the area of the triangular element. Note that $\nabla\phi_i$ is constant on T_k. Now, we will derive the cotangent formula referring to Figure (4.1).

$$L_1 =\mid x_3 - x_2 \mid,$$

$$\nabla N_1 = \frac{(x_2 - x_3)^\perp}{(x_1 - x_2)\cdot(x_2 - x_3)^\perp},$$

$$\nabla N_2 = \frac{(x_3 - x_1)^{\perp}}{(x_2 - x_3) \cdot (x_3 - x_1)^{\perp}},$$

$$\begin{aligned}
\nabla N_1 \cdot \nabla N_2 &= \frac{(x_2 - x_3)^{\perp} \cdot (x_3 - x_1)^{\perp}}{(x_1 - x_2) \cdot (x_2 - x_3)^{\perp} \cdot (x_2 - x_3) \cdot (x_3 - x_1)^{\perp}} \\
&= \frac{(x_2 - x_3) \cdot (x_3 - x_1)}{(x_1 - x_2) \cdot (x_2 - x_3)^{\perp} \cdot (x_2 - x_3) \cdot (x_3 - x_1)^{\perp}} \\
&= \frac{L_1 L_2 \cos\theta_3}{L_3 L_1 \sin\theta_2 L_1 L_2 \sin\theta_3} \\
&= \frac{\cot\theta_3}{L_1 L_3 \sin\theta_2} \\
&= \frac{\cot\theta_3}{2|T_k|},
\end{aligned}$$

so we have local system matrix:

$$\begin{aligned}
k_{12} &= \sigma \nabla N_1 \cdot \nabla N_2 \cdot |T_k| \\
&= \frac{\sigma}{2} \cot\theta_3.
\end{aligned}$$

Note $k_{ij} = k_{ji}$, $k_{ij} = 0$ for any nodes i, j not sharing an edge and $k_{ii} = -\sum_{i \neq j} k_{ij}$. Now consider a boundary current density

$$J = \sigma \nabla u \cdot \nu, \tag{4.3}$$

where ν is an outer normal.

Define the current vector $I \in \mathbb{R}^{n_v}$ by

$$I_i = \int_{\partial\Omega} J \phi_i dx. \tag{4.4}$$

The finite element system will be

$$Ku = I. \tag{4.5}$$

An extra condition is needed to have uniqueness because the voltage is only determined up to an additive constant. For a chosen vertex i_g we can force $u_{ig} = 0$ by

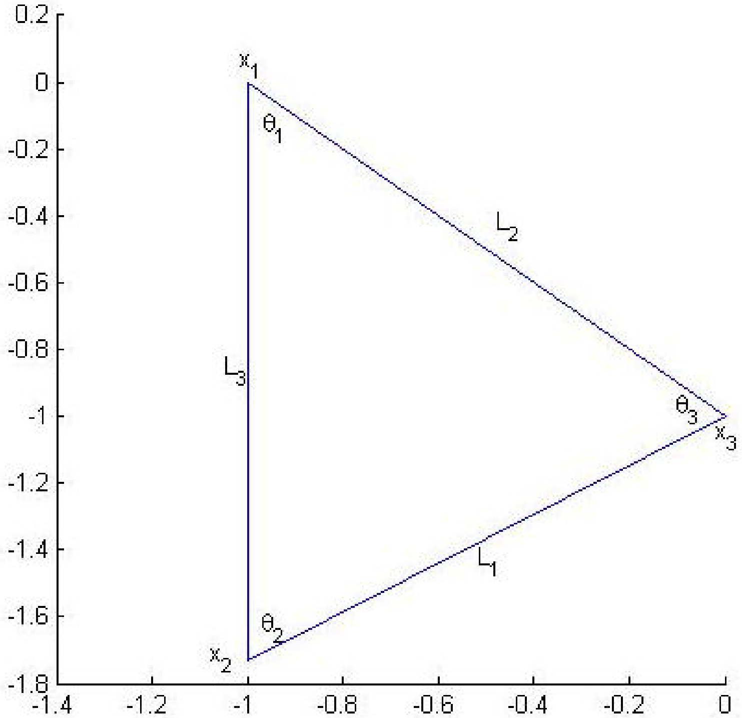

Figure 4.1: Cotangent formula.

deleting the i_g row and column from the system [35].

4.2.4 Correspondence of Ohm-Kirchhoff matrix and FEM system matrix

Consider an embedded simplicial complex $\Omega(V, E, T)$ associated with FEM triangular mesh, where V is the set of vertices, E is the set of all edges and T is the set of all triangles. Let the angle in the triangle (i, j, k) and opposite to the edge (i, j) be denoted by $\alpha_{(i,j)}^{(i,j,k)}$. Define $J : \mathbb{R}^E \to \mathbb{R}$, $\phi : \mathbb{R}^V \to \mathbb{R}$ and $\gamma : \mathbb{R}^E \to \mathbb{R}_+$. Then, Ohm's law is given by:

$$J(i, j) = \gamma_{(i,j)}(\phi(j) - \phi(i)), \tag{4.6}$$

where $(i, j) \in E$. For each interior node $i \in V_0$ we have Kirchhoff's law

$$\sum_{i \in e \in E} J(e) = 0. \tag{4.7}$$

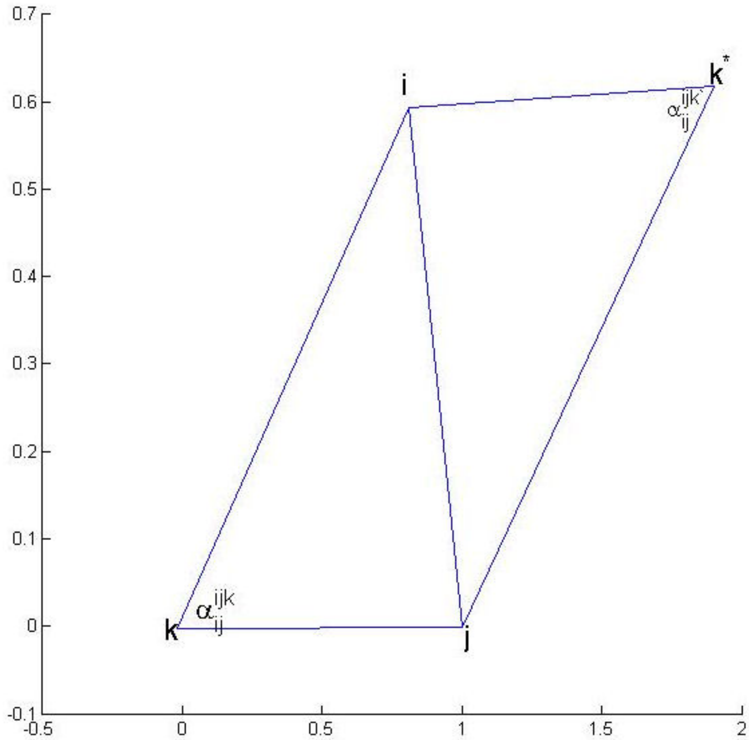

Figure 4.2: Assembled triangles in a mesh.

Finite element models with piece-wise linear basis functions and a piece-wise constant conductivity produce a system matrix equivalent to the Ohm-Kirchhoff matrix for resistor networks. The construction of a resistor network that is equivalent to the finite element model is summarized as follows:

1. Consider a triangle with angles numbered such that $\alpha_{(i,j)}^{(i,j,k)}$ is the opposite to the edge (i, j)
2. The conductance on each side (i, j) is given by $\sigma_{(i,j,k)} \cot \alpha_{(i,j)}^{(i,j,k)}$.
3. If the triangles are assembled into a mesh the conductances are added in parallel for the coincide edges from adjacent triangles and the conductance on edges is given by

$$k_{ij} = \frac{1}{2}(\sigma_{(i,j,k)} \cot \alpha_{(i,j)}^{(i,j,k)} + \sigma_{(i,j,k^*)} \cot \alpha_{(i,j)}^{(i,j,k^*)}). \tag{4.8}$$

Figure (4.2) shows two assembled triangles in resistor networks.

4.2.5 Prior knowledge of conductivity

Some finite elements models in EIT assume the conductivity to be piece-wise constant on elements. However, it is more accurate to approximate the conductivity distribution of a body as a piece-wise constant by assuming that each organ is homogeneous. It is impossible to have the boundary of the organ lying on the boundary of the elements, unless we have prior knowledge of the shape and position of the organ. Since this information is not available, it is required to add the position of the elements as a free variable to be fitted to the observed measurements.

4.3 Mesh generation

Mesh generation is an important research area that has several challenges. The predicted measured voltage as a function of conductivity needs a fine enough mesh to approximate the potential with sufficient accuracy. This should include the shape of the surface of the body under investigation, and the geometry of the electrodes. The regular meshes on rectangular surfaces are fairly easy to generate. However, for circular domains meshing has few difficulties. Since the electrical field varies with the used current pattern, the mesh should be suitable for all current patterns.

The mesh generator requires structural information to approximate the geometry of the domain to be meshed and the external boundary shape. Also, the internal structures and the contact area of the electrodes should be known. Several generator programs are available and a simple one is rmesh [53]. The rmesh program generates a triangular mesh for a circular domain. The number of nodes n_i in the circle with radius r_i and a decreasing order sequence of radii will be the input of the program. The number of nodes must satisfy the condition $k(n_i - n_{i+1}) = n_i$ for some integer k. The number of triangles will be decreased in a successive annuli. The maximum radius of the elements affects the accuracy of the finite elements approximation.

It is important to be able to refine an existing finite element. This will help to verify the experimental stability of the approximation of both forward modeling and inverse problem solution. Moreover, representing the conductivity on a coarser mesh than the potential, will require a finer mesh. A mesh refinement program divides each triangular element into four smaller triangles similar to the ordinal one. This guarantees that the radii of the elements will decrease uniformly with the increasing number of elements. Finally, we point out that the standard results for FEM [44] require that the ratio of the circumscribing circle of the triangular element to the inscribing circle is bounded away from zero as the size of the triangle tends to zero. That is, for an isotropic medium without a prior knowledge of the field strengths, triangles close to equilateral are the best while those with high aspect ratio are the worst.

Chapter 5

Survey Problem

5.1 Introduction

Studying the planar case of resistor networks associated with an isotropic conductivity turns out to be a construction of triangulation with a knowledge of angles and position of two nodes as we will show in this chapter. This requires us to look in the literature for similar work. We find that it had been considered by several people. Triangulation is an old problem initiated by the Dutch geographer G. Frisius. Next, the famous Danish astronomer T. Brache $(1546-1601)$ who set the basis of the map of the kingdom of Denmark, borrowed his triangulation idea from Frisius's scientific work. Then, Snellius used the triangulation to invent the famous meridian chain. We summarize the triangulation work done by these authors for more details we refer to [27]. Then we go on to the work that has been done in Computer Geometric Design. We then illustrate the sine rule consistency condition. Moreover, we will show the necessary and sufficient consistency condition that needs to be satisfied. Finally, a constructive algorithm is needed, to determine the position of the nodes in the triangulation where we know one edge and the angles of the finite element mesh.

5.2 Description of Frisius's triangulation

G. Frisius who lived between 1508 and 1555 defined the magnetic bearings and invented the principles of triangulation. The measurements of the bearings of the whole province, including the surrounding town and villages, needs an instrument. The instrument consists of a circle that is divided into four quadrants. Each quadrant is decomposed to 90°. The centre of the circle is attached to one end of a sight rule and the other end of the sight rule is attached, with a sighting device moving along the circumference. This very basic goniometer was set up at a station called tower A in the area that needed to be measured. The plane of the circle has to be horizontal and the line that connects the centre to the zero of the graduation, must point towards the magnetic North using a compass. The instrument now has an orientation and the compass is then replaced by the sighting device to read the magnetic bearings on the horizontal circle of the instrument. The bearing to a tower B or to another place in the area was plotted by a protractor. It could be said that knowing bearings without distances between towers was not useful. However, they may travel to another tower called B, and make similar measurements to surrounding locations. On the map with the bearings in A, a choice of a point B on the line AB will be made at an arbitrary distance. The line to the magnetic north is plotted in B, parallel to that in tower A, and the bearings in B are drawn in a similar way to those in A. The intersection point of the radii in both A and B will represent the tower C at the assumed scale. As they moved from tower to tower, in each tower two bearings were drawn. A third bearing is necessary to fix the intersection point if the point to be drawn lies on the connecting line of the points from which the bearings are measured. An example given by Frisius describing his method is shown in Figure (5.1). On the tower of Antwerp the following measurements were obtained by Frisius: Gent 80° North West, Lier 30° South East, Mechelen approximately 8° South West, Leuven 4° South East, Brussels 25° South West, Middelburg 30° North West and Bergen op Zoom 20° North West. Then theoretically he moved to Brussels and made the

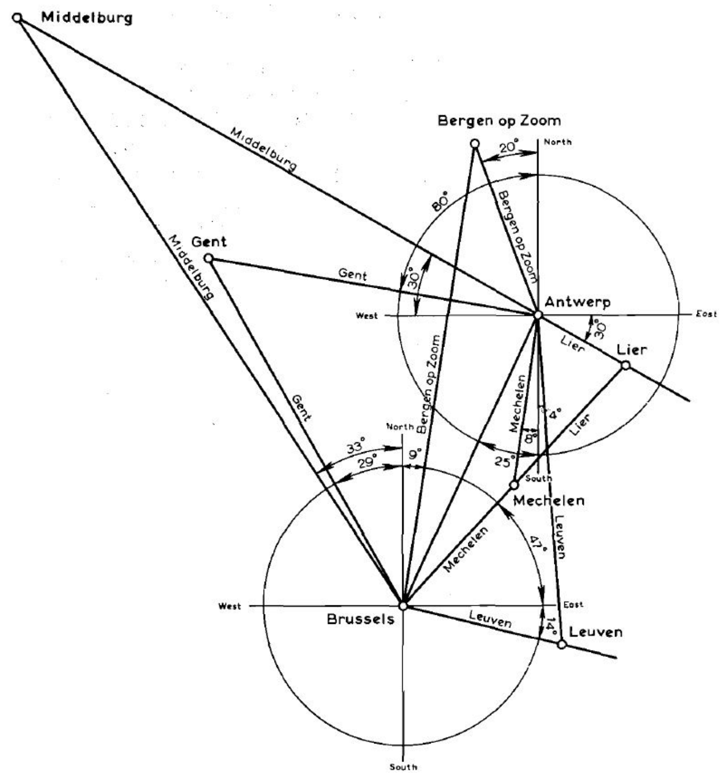

Figure 5.1: Frisius measurements.

following measurements: Leuven almost 14° South East, Mechelen and Lier are on one line 47° North East, Gent 29° is North West, Middelburg 33° is North West and Bergen op Zoom 9° is North East. It is important to point out the triangulations of Brahe, Gemma and Snellius are:

1. Non planar networks.

2. Networks are immersed rather than embedded.

5.3 Brahe's triangulation network

The second triangulation is made by T. Brahe. Figure (5.2) is the geometrical network measured by T. Brahe which served as the base of the map of Denmark. Some angles in the network were derived from his observations. The centre of the network is Uraniborg from where no angle was measured, instead astronomical azimuths were used [27]. The astronomical azimuths and the distances from Uraniborg are shown

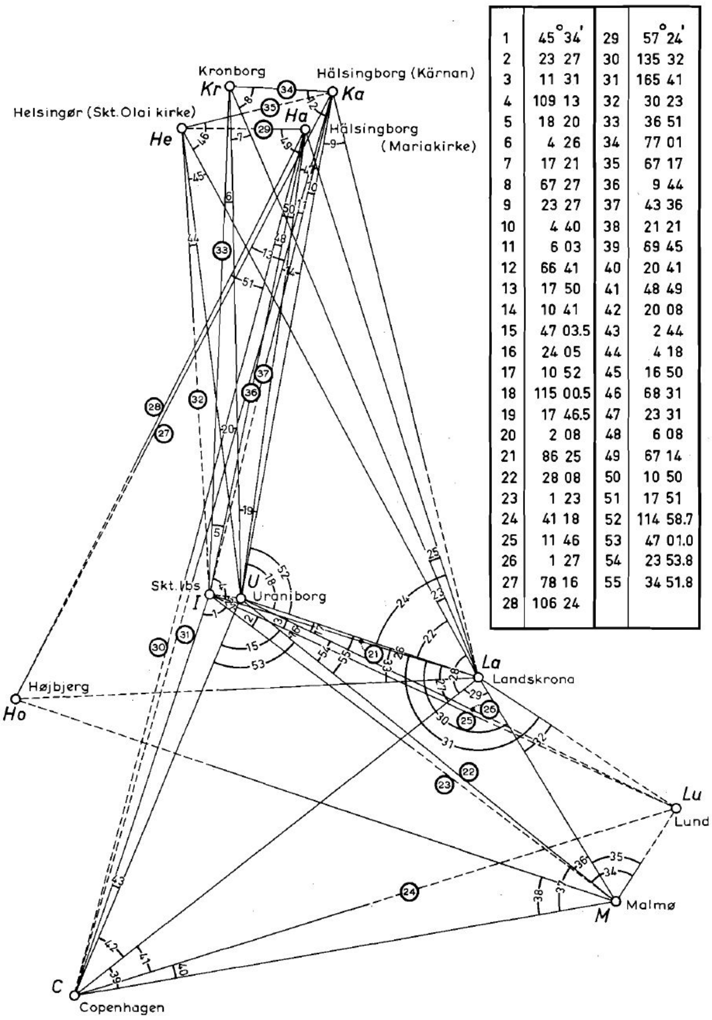

1	45° 34'	29	57° 24'
2	23 27	30	135 32
3	11 31	31	165 41
4	109 13	32	30 23
5	18 20	33	36 51
6	4 26	34	77 01
7	17 21	35	67 17
8	67 27	36	9 44
9	23 27	37	43 36
10	4 40	38	21 21
11	6 03	39	69 45
12	66 41	40	20 41
13	17 50	41	48 49
14	10 41	42	20 08
15	47 03.5	43	2 44
16	24 05	44	4 18
17	10 52	45	16 50
18	115 00.5	46	68 31
19	17 46.5	47	23 31
20	2 08	48	6 08
21	86 25	49	67 14
22	28 08	50	10 50
23	1 23	51	17 51
24	41 18	52	114 58.7
25	11 46	53	47 01.0
26	1 27	54	23 53.8
27	78 16	55	34 51.8
28	106 24		

Figure 5.2: T. Brahe's geometrical network.

in Table (5.1).

Angular points	Distance in (km)	Series a	Series b	Differences	angles
Copenhagen	26.6		$197°18.5'$		
Malmo	38.6		$150°15'$	$47°03.5'$	15
Lund	38.5		$126°10'$	$24°05'$	16
Landskrona	9.3		$115°18'$	$10°52'$	17
Helsingborg Krnan	15.6		$0°17.5'$	$115°00.5'$	18
Kronborg	15.3		$342°31'$	$17°46.5'$	19
Helsingr Skt .Olai kirke	15.1		$340°23'$	$2°08'$	20
Skt.Ibs gamle	1.3	$283°25'$		$86°25'$	21

Table 5.1: Azimuths in Uraniborg to other angular points.

5.4 Snellius triangulation network

5.4.1 Motivations of Snellius

Snellius measured a meridian chain between Alkmaar and Bergen op Zoom that are separated from each other by 130 km. These measurements lead to the determination of the earth's circumference. He was the first to determine the arc of the meridian by triangulation. His network of triangulation between Alkamaar and Bergen op Zoom enabled him to determine the distance between these locations. He was also the first geodesist to compute the length of a side of a network using only real measurements. He transferred the measured length of a specific base and measured angles by computation to a side of the triangulation. Snellus realized that the unit of length (a Rhineland rood) must be defined accurately. He paid more attention to this area of study than any one else previously. The Snellius triangulation is shown in Figure (5.3)

5.4.2 Snellius' triangulation network

The construction of the Snellius network consists of several stages. In the first stage he considered the measured length of the base line tc and the measurement of angles to calculate the side of the network (Leiden-The Hague) see Figure (5.4). He considered part of the network which contains the triangles surrounding the base line tc in

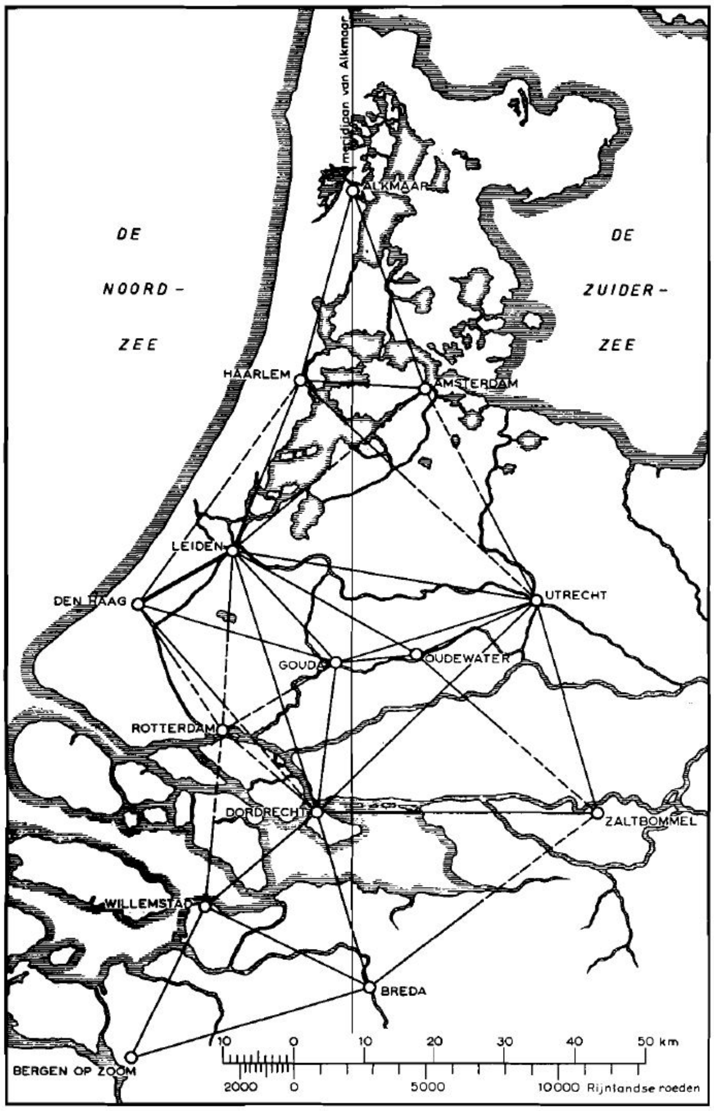

Figure 5.3: Snellius triangulation (Note: It is not planar - see the Oudewater-Zaltbmmel).

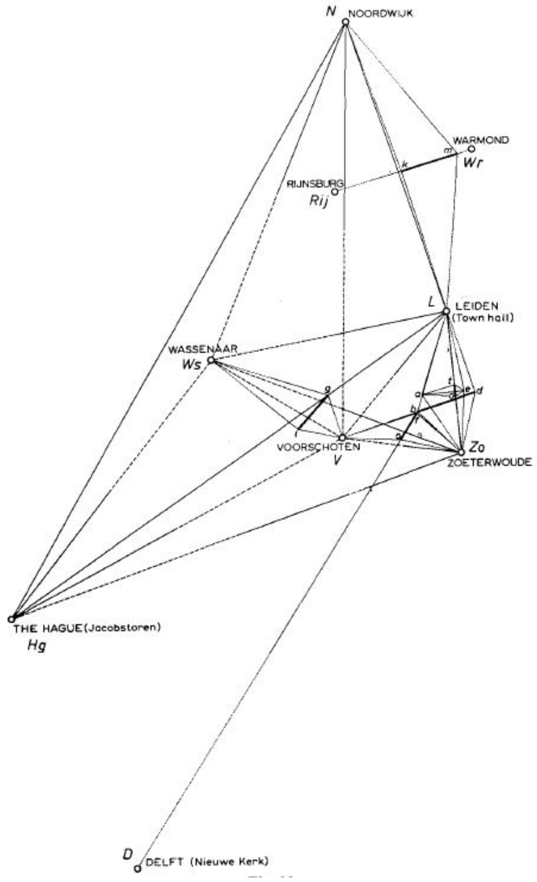

Figure 5.4: Leiden-The Hage side.

Figure (5.5). Using the measured length of the base line tc and the measured angles in the triangle tce, the other sides of the triangle were computed. Similarly, all the sides of the triangles summarized in Table (5.2) were computed. In the second stage he considered the base ig and calculated all the sides of the triangles in Table (5.3) using similar methods done in the previous stage. In both stages he obtained almost the same result for the side of the network LHg. In the first stage he got $LHg = 4103.21 rood$ while in the second stage he got $LHg = 4103.36 rood$, which are both excellent results. He repeated his method several times in different towers and obtained the triangulation which is shown in Figure (5.6).

All the calculations are summarized in Table (5.4), Table (5.5) and Table (5.6).

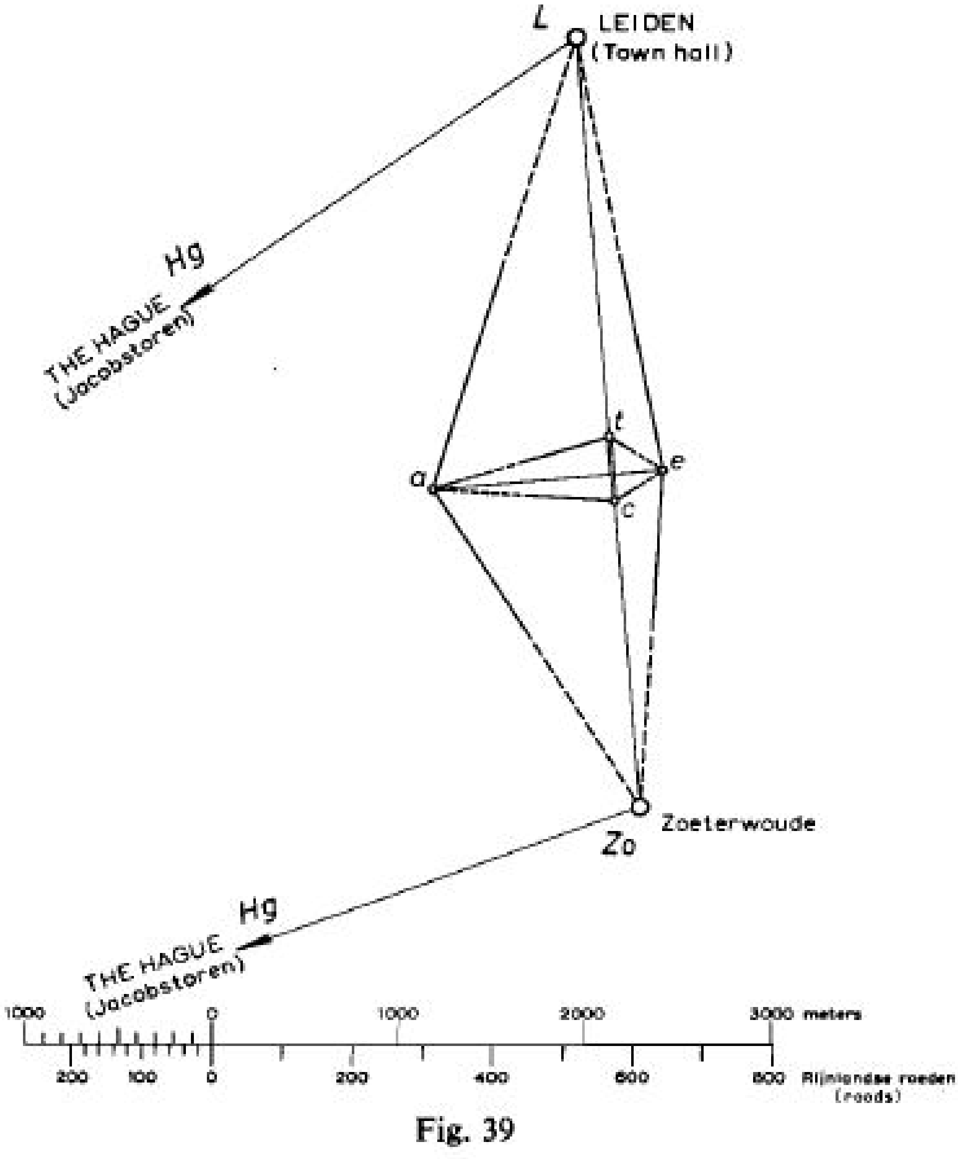

Figure 5.5: The base line tc.

No.	Triangle	angles	Opposite sides (roods)
1	t	$54°00'$	79.66
	c	$63°52'$	88.40
	e		87.05
2	t	$78°30'$	257.34
	c	$82°8.5'$	260.15
	a		87.05
3	a		88.40
	t	$132°30'$	326.45
	e		260.15
4	a		79.66
	c	$146°0.5'$	326.45
	e		257.34
5	a	$67°44'$	624.45
	e	$83°20'$	670.20
	L		326.45
6	a	$61°38'$	478.60
	e	$81°29'$	537.91
	Zo		326.45
7	L		537.91
	a	$128°52'$	1093.55
	Zo		670.20
8	L		478.60
	e	$164°49'$	1093.55
	Zo		624.45
9	L	$60°32'$	
	Zo	$104°32'$	4107.87
	Hg		1093.55

Table 5.2: Measurement of the base and its extension to side (Leiden-The Hague).

No.	Triangle	angles	Opposite sides (roods)
1	i	$92°10'$	938.71
	g	$66°05'$	874.65
	Ws		348.10
2	i	$60°11'$	347.06
	g	$59°20'$	
	V		348.10
3	Ws		347.06
	g	$125°25'$	1174.40
	V		938.71
4	L	$23°36'$	
	Hg	$17°09'$	1855.69
	Ws		4107.98

Table 5.3: Measurement of the base line ig.

No.	Triangle	angles	Opposite sides (roods)
1	L	$97°13.67'$	7604.4
	H	$50°22.00'$	5903.4
	G	$32°24.33'$	4107.92
2	L	$25°45.39'$	5880.3
	G	$128°22.67'$	10608.1
	D	$25°51.94'$	5903.4
3	L	$71°28.27'$	10085.1
	Hg	$85°48.60'$	10608.1
	D	$22°43.13'$	4107.92
4	Hg	$90°19.50'$	6984.5
	L	$53°38.98'$	5625.4
	R	$36°01.52'$	4107.92
5	L	$43°34.68'$	4888.0
	G	$80°03.69'$	
	R	$56°21.63'$	5903.4
6	L	$37°41.20'$	7817.6
	G	$114°49.17'$	11606.5
	R	$27°29.63'$	5903.4
7	L	$63°26.59'$	11711.1
	G	$62°26.22'$	11606.5
	U	$54°07.19'$	10608.1
8	L	$20°22.83'$	4980.1
	D	$125°44.67'$	11606.5
	U	$33°52.50'$	7970.7
9	L	$17°18.37'$	2921.3
	O	$36°57.14'$	5903.4
	G	$125°44.49'$	7970.7
10	Hg	$20°45.12'$	7047.3
	L	$147°19.71'$	10736.8
	Hl	$11°55.17'$	4107.92
11	Am	$75°23.93'$	11606.5
	L	$50°38.68'$	9274.0
	U	$53°57.39'$	9697.9

Table 5.4: Computation of the length of side (Alkmaar-Bergen op Zoom).

No.	Triangle	angles	Opposite sides (roods)
12	L	$77°45.42'$	12234.6
	Hl	$67°59.12'$	11606.5
	U	$34°15.46'$	7047.3
13	L	$27°06.74'$	4695.3
	Hl	$109°43.69'$	9697.9
	Am	$43°09.57'$	7047.3
14	Hl	$77°58.72'$	8145.3
	Am	$67°42.14'$	7705.2
	Al	$34°19.14'$	4695.3
15	O	$65°27.36'$	8535.3
	U	$82°29.31'$	9302.6
	Z	$32°03.33'$	4980.1
16	D	$44°18.87'$	8535.3
	U	$62°14.62'$	10811.9
	Z	$73°26.51'$	11711.1
17	D	$72°18.42'$	10944.8
	Z	$37°27.02'$	6985.7
	B	$70°14.56'$	10811.9
18	D	$54°14.00'$	4888.0
	G	$48°18.98'$	4499.0
	R	$77°27.02'$	5903.4
19	D	$86°21.72'$	6822.5
	W	$41°09.36'$	4499.0
	R	$52°28.92'$	5422.3
20	D	$66°12.72'$	6902.5
	W	$67°49.87'$	6985.7
	B	$45°57.41'$	5422.3
21	W	$89°23.66'$	9402.6
	B	$43°22.67'$	6458.1
	Bz	$47°13.67'$	6902.5

Table 5.5: Computation of the length of side (Alkmaar-Bergen op Zoom).

No.	Triangle	angles	Opposite sides (roods)
22	Am	$110°51.71'$	14719.3
	L	$31°08.27'$	8145.3
	Al	$38°00.02'$	9697.9
23	L	$4°01.52'$	7705.2
	Hl	$172°17.59'$	14719.3
	Al	$3°40.89'$	7047.3
24	L	$81°46.95'$	17393.4
	U	$56°53.04'$	14719.3
	Al	$41°20.01'$	11606.5
25	L	$26°24.82'$	8535.3
	U	$116°21.80'$	17191.4
	Z	$37°13.38'$	11606.5
26	Al	$39°06.71'$	17191.4
	L	$108°11.78'$	25889.0
	Z	$32°41.51'$	14719.3
27	Al	$2°13.31'$	8535.3
	U	$173°14.83'$	25889.0
	Z	$4°31.86'$	17393.4
28	D	$53°49.12'$	9402.6
	B	$89°20.08'$	11648.4
	Bz	$36°50.80'$	6985.7
29	B	$159°34.64'$	20027.0
	Z	$9°25.75'$	9402.6
	Bz	$10°59.61'$	10944.8
30	Bz	$47°59.15'$	25889.0
	Z	$96°55.92'$	34590.1
	Al	$35°04.93'$	20027.0

Table 5.6: Computation of the length of side (Alkmaar-Bergen op Zoom).

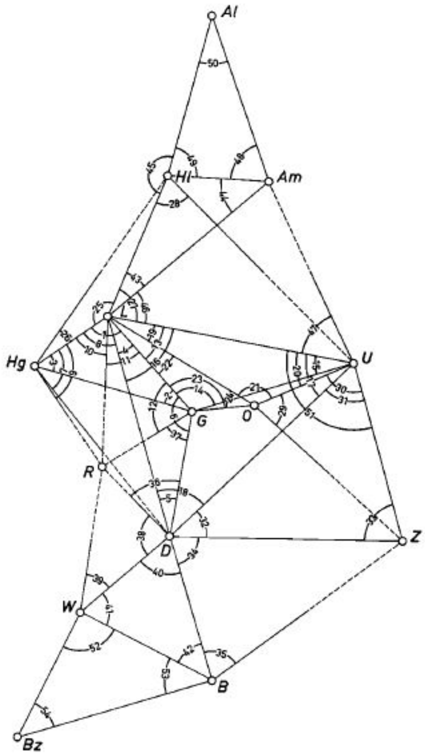

Figure 5.6: Angles of Snellius triangulation.

5.4.3 Snellius' solution to the resection problem

Snellius performed his astronomical measurements in Leden on the Town Hall tower instead of on the roof of his house, see Figure (5.7) [27]. To determine the latitude of L and the azimuth LHg we need to compute the distance OL. The mutual position of the spires P, L and Ho were known. Two more independent data were needed to find OL in quadrangle $PLHoO$. He measured the two angles $POL = 32°57'$ and $POHo = 64°40'$ and using this information he solved the resection problem. Note n and m are the centres of the circumscribed circles of the triangles $OPHo$ and OPL The line connecting the centres passes through the mid-point of the line OP is perpendicular to OP. Since all sides of triangle $PLHo$ are known, we have the following:

$$Pn = \frac{PHO}{2\sin(POHo)}, \tag{5.1}$$

$$Pm = \frac{PL}{2\sin(POL)}. \tag{5.2}$$

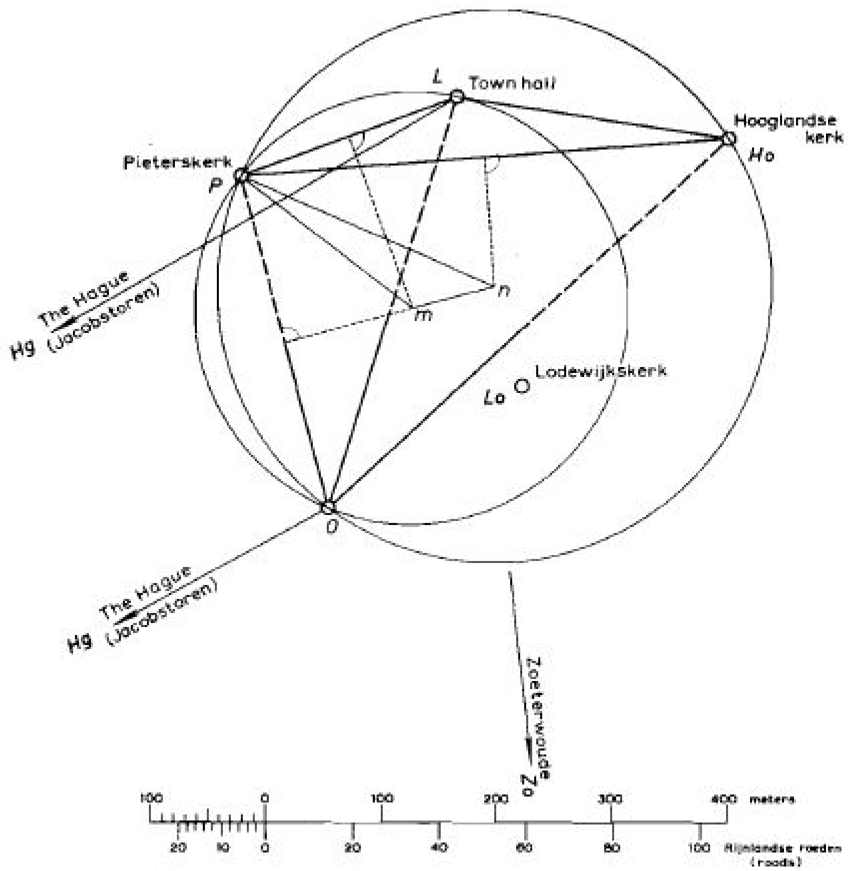

Fig. 54

Figure 5.7: Resection problem.

Since $LPm = 90° - POL = 32°57' = 57°03'$ and $HoPn = 90° - POHo = 25°20'$

$$\begin{aligned} npm &= Lpm - HoPn - LPHo \\ &= (90° - POL) - (90° - POHo) - LPHo \\ &= POHo - POL - LPHo. \end{aligned}$$

Note that the angle $LPHo$ can be calculated from the sides of the triangle $PLHo$. Also the angles m and n can be found from:

$$\sin n = \frac{PO}{2Pn}, \tag{5.3}$$

$$\sin m = \frac{PO}{2Pm}. \tag{5.4}$$

So we have:

$$OP = 2Pn \sin n = 2Pm \sin m. \tag{5.5}$$

Finally, OL follows from the sine rule in triangle OPL and OHo and can be computed from the sine rule in the triangle $OPHo$.

5.5 Parameterizations of triangulated surfaces

Planar triangulation meshing is considered in computer geometric designs in a problem called flattening or triangular surface parametrization. M. Floater [23] considered the flattening problem as a mapping of three-dimensional node positions to the plane. Based on graph theory the nodes $x_i \in \mathbb{R}^3$ of a surface S are mapped to points $\omega_i = (u_i, v_i) \in D$ where $D \subset \mathbb{R}^2$ is convex. His parameterizations set each ω_i to be a convex combination of its neighbours. The flattened surface was computed by solving a linear system. A major disadvantage of this parametrization is the requirement of the boundary of the two dimensions mesh to be predefined and convex. On the other hand [43] Sheffer and Sturler defined the flattening problem as a constrained optimisation problem in terms of angles only. They computed a projection that minimised the distortion of the surface metric structures (length, angles, etc). Their method requires solving a non linear system of equations. The algorithm used constraints for a valid two dimensional triangulation. They were aware of the consistency condition of the sine rule that needs to be satisfied on a cycle enclosing an interior node. However, it was not clear that they knew how many linearly independent sine rule equations we have in the entire triangulation mesh. In the coming sections we will discuss this issue in details.

5.6 Number of equations and variables

In this section we need to determine the degrees of freedom of the survey problem. Since we have two vertices for each edge, we will show that the degrees of freedom is less than twice the number of vertices by four, as we will fix the position of two vertices. Assuming one sine rule per interior vertex we will show that $n_\theta - n_{eq} = 2n_v - 4$ where n_θ is the number of angle in the triangulation, n_{eq} is the number of equations and n_v is the number of vertices in the triangulation. This is previously needed to be known that these equations are independent and a complete set. Let n_t be the number of triangles in the triangulation, n_v is the number of vertices, n_{v_0} is the number of interior vertices, n_e is the number of edges in the triangulation and n_{v_b} is the number of boundary vertices. There are three well-known relations available for any triangulation.

$$n_v = n_{v_0} + n_{v_b}, \tag{5.6}$$

$$n_v - n_e + n_t = 1, \tag{5.7}$$

$$3n_t = 2n_e - n_{v_b}. \tag{5.8}$$

The number of angles in the triangulation is obviously $3n_t$, we also assume one sine rule per interior node so we have n_{v_0}. Moreover, we have n_t equations from the fact that the sum of angles is π in each triangle and n_{v_0} equations from the fact that the sum of angles is 2π on each interior vertex.

$$
\begin{aligned}
\text{degrees of freedom} &= n_\theta - n_{eq} \\
&= 3n_t - (2n_{v_0} + n_t) \\
&= 2n_t - 2n_{v_0} \\
&= 2n_t - 2(n_v - n_{v_b}) \\
&= 2n_t - 2n_v + 2n_{v_b} \\
&= 2n_t - 2n_v + 2(2n_e - 3n_t) \\
&= 2n_t - 2n_v + 4n_e - 6n_t \\
&= -2n_v + 4n_e - 4n_t \\
&= -2n_v + 4(n_v - 1) \\
&= 4n_v - 2n_v - 4 \\
&= 2n_v - 4.
\end{aligned}
$$

Thus we have the correct number of degrees of freedom since knowing an edge means we have $2n_v - 4$ number of variables.

5.7 The space of cycles

A plane graph is a one dimensional complex consisting of zero-dimensional simplices (nodes) and one-dimensional simplices (branches) [38]. A cycle that encloses exactly one interior node forms a basis cycle.

For example, in Figure (5.8) $\{e_1, e_2, e_3, e_4, e_5\}$ and $\{e_6, e_7, e_8, e_9, e_{10}, e_{11}\}$ are basis cycles while the $\{e_1, e_2, e_7, e_8, e_9, e_{10}, e_5\}$ is not a basis cycle because it encloses two interior nodes. The number of basis cycle is denoted by k.

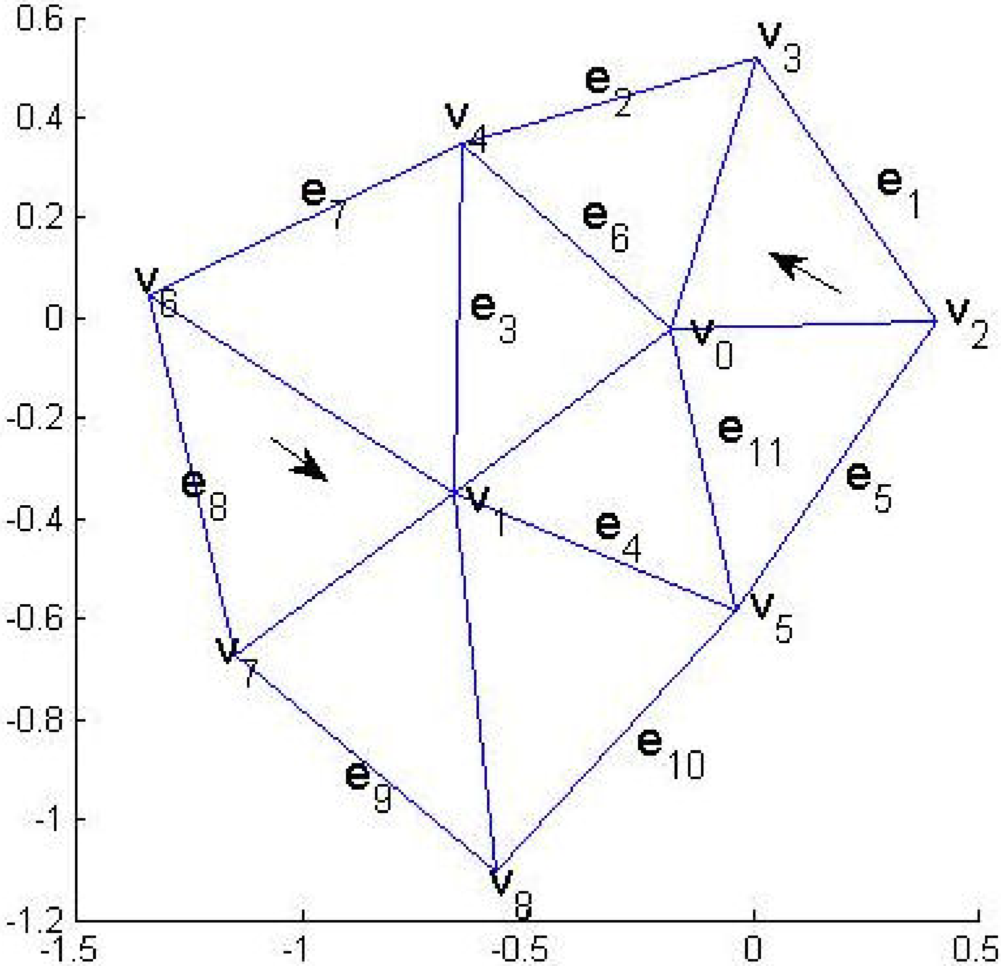

Figure 5.8: Oriented cycles.

Definition 5.7.1. A one-dimensional chain is the function which takes values equal in absolute value but opposite in sign at the opposite orientations of one dimensional simplices.

Let us represent the chains as $Z = \sum_{e \in E} z_e e$. Let Z_1 and Z_2 be two chains defined on the adjacent basis cycles. If all the one-dimensional simplices are oriented as in Figure (5.8), then any cycle containing two interior nodes can be written as a sum of the two basis cycles i.e the cycle containing the interior nodes of Z_1 and Z_2 can be written as $Z_1 + Z_2$. In general the chain Z defined on an arbitrary closed cycle can be written as a linear combination of chains defined on the basis cycles:

$$Z = \{\alpha_1 Z_1 + \alpha_2 Z_2 + ... + \alpha_k Z_k\}. \tag{5.9}$$

Note that the system of basis cycles $\{Z_1, Z_2, ..., Z_k\}$ is linearly independent and any cycle of a one-dimensional chain is a linear combination of basis cycles. The set of cycles of one-dimensional chain Z is a formal vector space generated by E.

5.8 Sine rule consistency condition

This section illustrates the sine rule consistency condition. We will use the terminology of wheel and spoke edges in the construction procedure. We define a wheel as a set of triangles enclosing a vertex and an edge joining the enclosed vertex to the base of triangle which is called a spoke edge. The sine rule consistency condition that needs to be satisfied by the triangles enclosing a vertex is explained as follows: Refer to Figure (5.9), using the sine rule in the first face on the spoke edges:

$$\frac{L_1}{L_2} = \frac{\sin\theta_1}{\sin\beta_1}. \tag{5.10}$$

Also by applying the sine rule in the second face, we get:

$$\frac{L_2}{L_3} = \frac{\sin\theta_2}{\sin\beta_2}. \tag{5.11}$$

Eq.(5.10) and Eq.(5.12) can be combined by:

$$\frac{L_1}{L_3} = \frac{L_1}{L_2} \cdot \frac{L_2}{L_3} = \frac{\sin\theta_1}{\sin\beta_1} \cdot \frac{\sin\theta_2}{\sin\beta_2}. \tag{5.12}$$

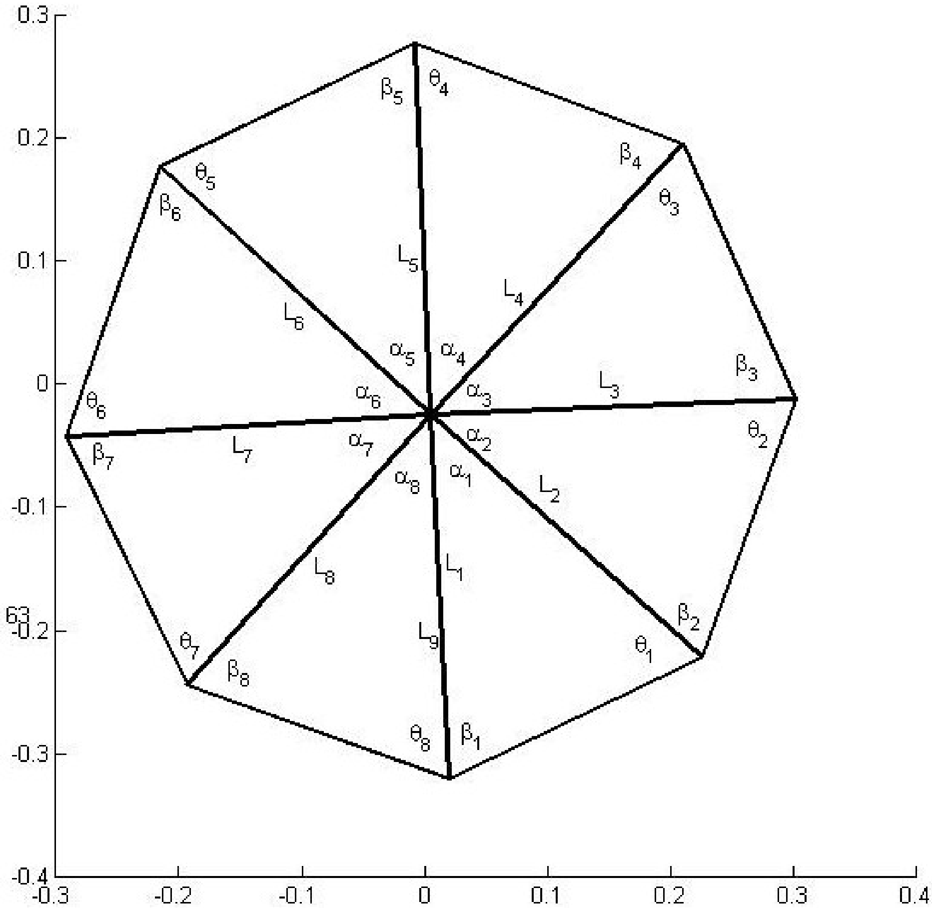

Figure 5.9: Illustration of sine rule.

Continuing in the same way in all faces we end up with the following sine rule:

$$
\begin{aligned}
\frac{L_1}{L_9} &= \frac{L_1}{L_2}\cdot\frac{L_2}{L_3}\cdot\frac{L_3}{L_4}\cdot\frac{L_4}{L_5}\cdot\frac{L_5}{L_6}\cdot\frac{L_6}{L_7}\cdot\frac{L_7}{L_8}\cdot\frac{L_8}{L_9}\\
&= \frac{\sin\theta_1}{\sin\beta_1}\cdot\frac{\sin\theta_2}{\sin\beta_2}\cdot\frac{\sin\theta_3}{\sin\beta_3}\cdot\frac{\sin\theta_4}{\sin\beta_4}\cdot\frac{\sin\theta_5}{\sin\beta_5}\cdot\frac{\sin\theta_6}{\sin\beta_6}\cdot\frac{\sin\theta_7}{\sin\beta_7}\cdot\frac{\sin\theta_8}{\sin\beta_8}\\
&= 1.
\end{aligned}
$$

The sine rule can be written in the following form:

$$\sum_{i=1}^{n}[\ln\sin\theta_i - \ln\sin\beta_i] = 0 \tag{5.13}$$

where n is the number of triangles in the wheel

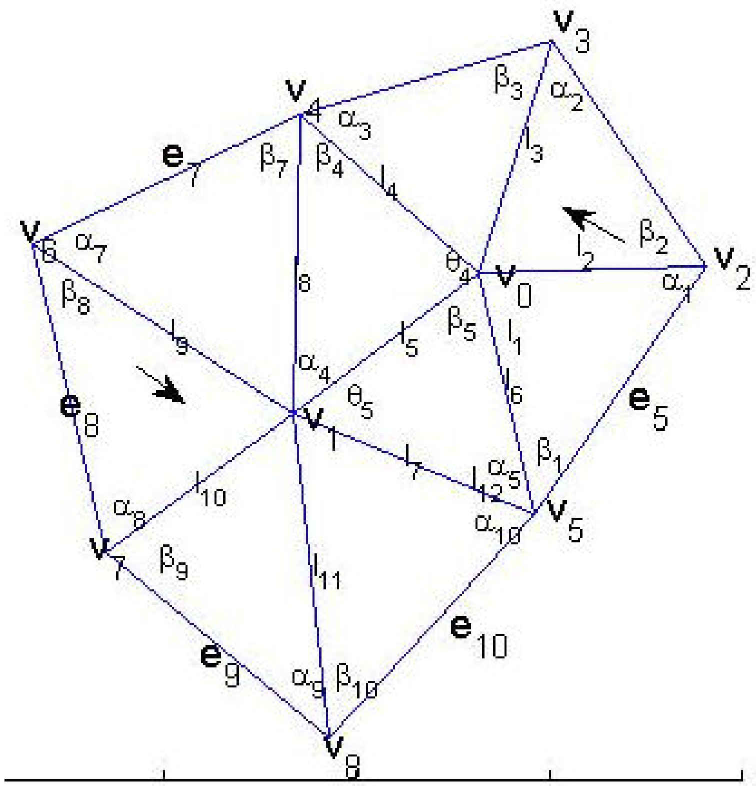

Figure 5.10: Sum of sine rules.

5.9 Sine rule of a cycle enclosing two vertices

Consider the sine rule in the cycle enclosing the interior node V_0 in Figure (5.10)

$$\frac{\sin\alpha_1}{\sin\beta_1}\cdot\frac{\sin\alpha_2}{\sin\beta_2}\cdot\frac{\sin\alpha_3}{\sin\beta_3}\cdot\frac{\sin\alpha_4}{\sin\beta_4}\cdot\frac{\sin\alpha_5}{\sin\theta_5}=1,$$

this can be written as :

$$G_1=\log\left[\frac{\sin\alpha_1}{\sin\beta_1}\cdot\frac{\sin\alpha_2}{\sin\beta_2}\cdot\frac{\sin\alpha_3}{\sin\beta_3}\cdot\frac{\sin\alpha_4}{\sin\beta_4}\cdot\frac{\sin\alpha_5}{\sin\theta_5}\right]=0. \tag{5.14}$$

Also consider the sine rule in the cycle enclosing the interior node V_1 in Figure (5.10)

$$\frac{\sin\beta_5}{\sin\alpha_5}\cdot\frac{\sin\beta_4}{\sin\theta_4}\cdot\frac{\sin\alpha_7}{\sin\beta_7}\cdot\frac{\sin\alpha_8}{\sin\beta_8}\cdot\frac{\sin\alpha_9}{\sin\beta_9}\cdot\frac{\sin\alpha_{10}}{\sin\beta_{10}}=1,$$

which can be written in the form:

$$G_2 = \log\left[\frac{\sin\beta_5}{\sin\alpha_5}\cdot\frac{\sin\beta_4}{\sin\theta_4}\cdot\frac{\sin\alpha_7}{\sin\beta_7}\cdot\frac{\sin\alpha_8}{\sin\beta_8}\cdot\frac{\sin\alpha_9}{\sin\beta_9}\cdot\frac{\sin\alpha_{10}}{\sin\beta_{10}}\right] = 0. \tag{5.15}$$

Now we consider the sine rule in the cycle enclosing both interior nodes :

$$\frac{\sin\alpha_1}{\sin\beta_1}\cdot\frac{\sin\alpha_2}{\sin\beta_2}\cdot\frac{\sin\alpha_3}{\sin\beta_3}\cdot\frac{\sin\alpha_4}{\sin\theta_4}\cdot\frac{\sin\alpha_7}{\sin\beta_7}\cdot\frac{\sin\alpha_8}{\sin\beta_8}\cdot\frac{\sin\alpha_9}{\sin\beta_9}\cdot\frac{\sin\alpha_{10}}{\sin\beta_{10}}\cdot\frac{\sin\beta_5}{\sin\theta_5} = 1,$$

that is equivalent to

$$\frac{\sin\alpha_1}{\sin\beta_1}\cdot\frac{\sin\alpha_2}{\sin\beta_2}\cdot\frac{\sin\alpha_3}{\sin\beta_3}\cdot\frac{\sin\alpha_4}{\sin\beta_4}\cdot\frac{\sin\alpha_5}{\sin\theta_5}\cdot\frac{\sin\beta_5}{\sin\alpha_5}\cdot\frac{\sin\beta_4}{\sin\theta_4}\cdot\frac{\sin\alpha_7}{\sin\beta_7}\cdot\frac{\sin\alpha_8}{\sin\beta_8}\cdot\frac{\sin\alpha_9}{\sin\beta_9}\cdot\frac{\sin\alpha_{10}}{\sin\beta_{10}} = 1.$$

If we take the logarithm of both sides then this can be written as:

$$G_1 + G_2 = 0. \tag{5.16}$$

5.10 The necessary and sufficient consistency condition

In the previous section we saw that we needed to satisfy a sine rule consistency condition for any closed cycle enclosing a vertex. A typical dual graph of triangular mesh has several closed cycles. A question arises naturally: how many independent consistency conditions need to be satisfied in the dual graph of a triangular mesh? It turns out that there is an elegant way to determine the necessary and sufficient consistency constraints that need to be satisfied. Let $K = (V, E, T)$ be a connected homogeneous abstract simplicial complex of two dimensions, f is a piece-wise linear immersion of K in $\mathbb{R}^2$ and $G = (V', E')$ be the dual graph of K, that is $\{t, t'\} \in E'$ if and only if $t \cap t' \in E$. Of course there is a natural correspondence between E' and E: for any $\{t, t'\} \in E'$, $t \cap t'$ is the edge shared by the two faces. Let $\overline{G} = (V', \overline{E})$

be a digraph obtained from G by assigning an arbitrary orientation of the edges. Let $W \subset V \times T$ be $(v,t) \in W$ if and only if $v \in t$, the relation, vertex incident on a face. For any $t \in T$ the radius of the circumcircle $r(t) = \frac{|f(e)|}{2\sin\theta_v^t}$ for any v with $(v,t) \in W$ and $e \in E$ the edge opposite v, $e = t \setminus v$ and $\mid f(e) \mid$ is the length of the edge. Define $\rho : T \to \mathbb{R}$ as:

$$\rho(t) = \ln(2r(t)). \tag{5.17}$$

We consider $\rho(t)$ to be 0-cochain on $\overline{G}$. For any $\overline{e} \in \overline{E}$, $\overline{e} = (t, t^{'})$, define:

$$\sigma(\overline{e}) = \rho(t^{'}) - \rho(t), \tag{5.18}$$

which can be extended uniquely to a 1-cochain with $d\rho$ where d is the co-boundary differential operator. Let $c \in C_1(\overline{G})$ be a chain then by definition of d we have (the discrete version of Stokes' theorem)

$$\langle c, d\rho \rangle = \langle \partial c, \rho \rangle, \tag{5.19}$$

where $\langle ., . \rangle$ is the dual pairing between chains and co-chains. We see that for any cycle $c \in Z_1(\overline{G})$ we have:

$$\langle c, d\rho \rangle = 0. \tag{5.20}$$

This is exactly the consistency condition derived from applying the sine rule around that cycle. It is clear then that given a basis of cycles $\{c_k | k = 1, ..., \dim Z_1(\overline{G})\}$ a complete and independent set of sine rule constraints is given by $\langle c, d\rho \rangle = 0$. In particular the set of basic cycles of $\overline{G}$ form a basis, and the set of basis cycles of $\overline{G}$ is in one to one correspondence with the interior vertices of K. Note that the interior vertices are simply the vertices in V that are in an edge in E that is a member of two faces of T.

5.11 Isomorphism

Theorem 5.11.1. The vector space of basic cycles Z is isomorphic to the vector space of sine rule consistency condition.

Proof. For every oriented cycle there is only one sine rule. This means the map from the space of cycles Z to the vector space of sine rules is one to one. Conversely, for every sine rule there is only one oriented cycle, that is the map from the vector space of sine rules to the vector space of cycles Z. Therefore, we have a bijective map between the two vector spaces, so they are isomorphic to each other. □

Since the space of cycles is spanned by the basis cycles, the space of sine rules is spanned by the image of the basis cycles. So, we can conclude that one sine rule per interior node is needed in a triangulated mesh.

5.12 Construction of triangulated mesh

This section introduces a method to construct a triangulated mesh given the angles and the position of two vertices.

Theorem 5.12.1. If the coordinates of two vertices of an edge and the angles of triangulation are given, then the triangulation can be constructed.

Proof. By knowing the coordinates of vertices of an edge and the angles, the coordinate of the third vertex is determined as follows:
referring to Figure (5.11), since we know the angles α and β then $\gamma = \pi - \alpha - \beta$.
The length of the given edge is calculated by:

$$d = V_1 - V_2,$$

$$L_3 = \|d\|.$$

Since we know the angles and the length of one side L_3 we apply the sine rule to determine the length of the two other sides of the triangle. A perpendicular unit vector to d is given by:

$$p = \frac{(d_2, -d_1)}{L_3}.$$

Then the coordinates of the third vertex are given by:

$$V_3 = V_2 + s \cdot \frac{d}{L_3} + h \cdot p,$$

where $h = L_1 \sin \alpha$ is scalar quantity, p is a unit vector perpendicular to $(V_1 - V_2)$ and $s = L_1 \cos \alpha$ is a scalar quantity. Now we need a way to move from one triangle to another. To do so, we choose any spanning tree of the dual graph rooted at this triangle. Moving along the edges of the spanning tree we pass a known edge in the triangle of the previously calculated triangle. We have also the angles, so the coordinates of any vertex are determined by the procedure explained in the previous step. By induction, let us assume that the position of the vertices in k triangle are computed. Then there is a connected path on the spanning tree to the root through the k triangles. So we have a known edge and the angles, consequently the position of the vertices are determined. This position is independent of the choice of triangle containing the vertex. $\square$

5.13 Numerical results

We used the MATLAB graph theory tool box adopted by Sergii Iglin [30] to construct a spanning tree, then traverse this tree calculating vertex positions using Theorem (5.12.1). An example is given in Figures (5.12) and (5.13). The function grMinSpanningtree uses greedy algorithm followed by my own treesort routine. We show an example of finding an embedding where angles are calculated from edge conductances as in the next chapter.

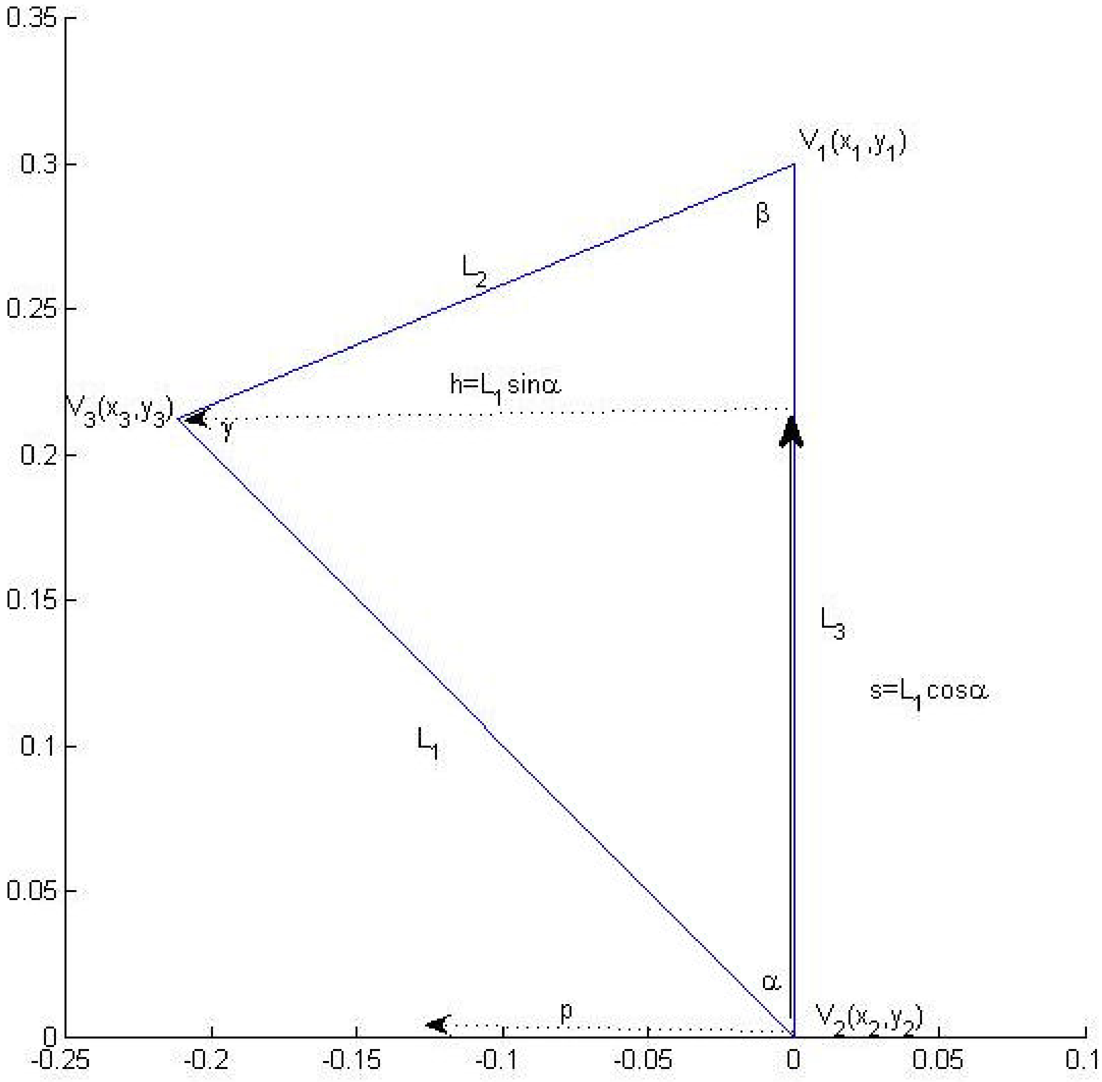

Figure 5.11: Determination of third vertex in a triangle.

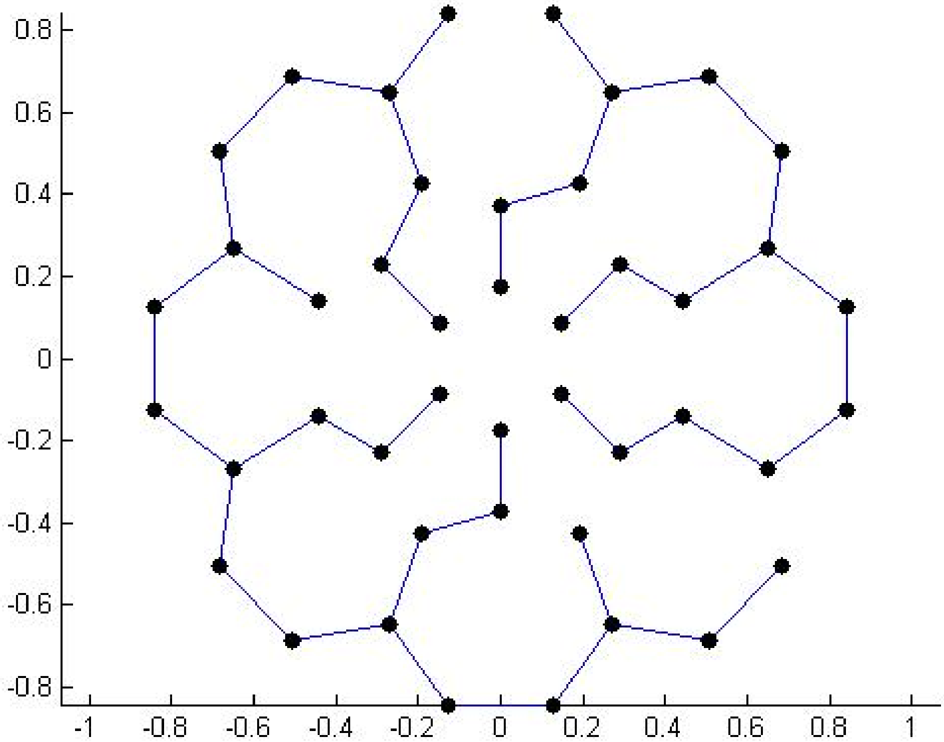

Figure 5.12: Spanning tree.

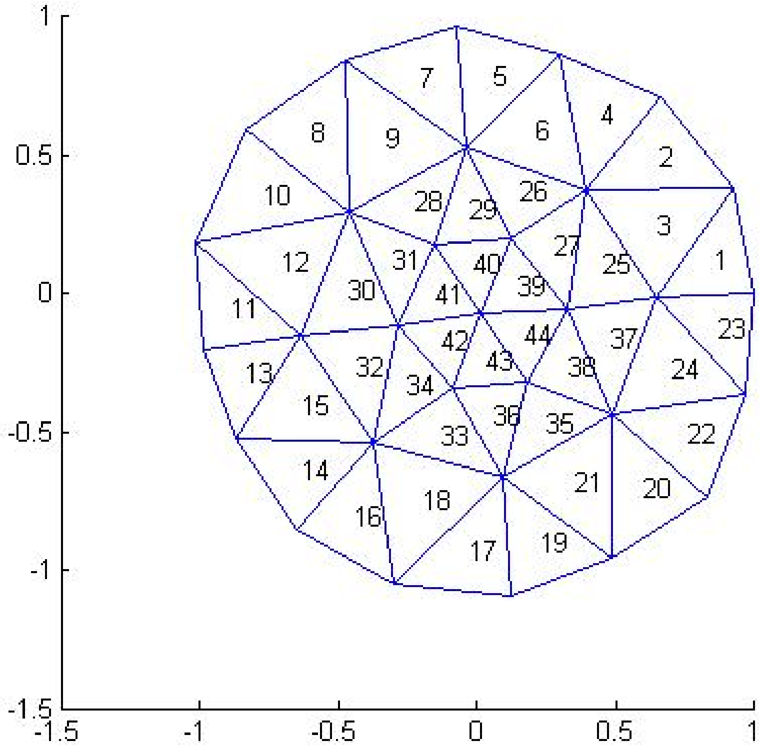

Figure 5.13: Triangulation.

Chapter 6

Isotropic Embedding of Planar Resistor Network

6.1 Introduction

This chapter deals with an isotropic embedding of planar resistor networks associated with anisotropic FEM. Our result relies on the inverse function theorem so will only apply to an open neighborhood conductivities close to one that is known to have an isotropic embedding. We give sufficient conditions for the existence of the uniqueness of the embedding. This is a discrete analogy of isothermal coordinates. We begin by discussing the requirements needed to obtain an isotropic embedding of planar resistor networks and explain the system of equations produced by these requirements. Moreover, we propose a parametrization of the conductivity through an assignment of conductivity to each interior node to get a correctly determined system. Then we move to justify that we have the correct number of equations and variables. Next we discuss the Jacobian of the obtained system of equations. This system of equations applies to a general planar resistor network associated with a finite element model. Although we believe this system of equations to be linearly independent we do not have a complete proof for a general resistor network with the same topology of a finite element model. Therefore, we consider the system of equations in a layered triangulated mesh where two inward pointing triangles are between any two upward pointing triangles. For this special case we were able to prove that the Jacobian of the system has full rank using a colouring approach where we assign to each equation a label representing a pivot element. Using this method we show that the Jacobian of the system can be written as a Gaussian elimination form without losing any pivot which implies the Jacobian has full rank. Finally, we test our result using the MATLAB optimisation toolbox function fsolve and our own implementation of Newton's method.

6.2 Description of the system of equations

An isotropic embedding of planar resistor network associated with an isotropic FEM has to satisfy geometric and consistency conditions together with cotangent equations, which relate the conductances on the edges with the conductivity of the triangular faces. As we previously mentioned in Section (5.6) we have a 2π condition around each interior vertex, a π condition for each triangle and the sine rule consistency condition around each basic cycle of the dual graph. In addition, we need to satisfy the cotangent equation (4.8) stated before in Section (4.2). The number of independent angles from the survey problem is known to be $2n_v - 4$ as we showed before in Section (5.6). Compared to the survey problem, we have an additional cotangent equation for each interior edge, but we also have potentially added n_t new isotropic conductivity variables. To find a solution for the angles with specified edge conductance we would expect to have $n_t - n_e$ degrees of freedom. This suggests that there is typically a non-unique solution to the isotropic embedding problem. For the system to be correctly determined we propose that a conductivity is assigned to each interior vertex, and the conductivity on each triangle is taken to be the average value of all the interior vertices in the triangle. We also impose an additional $n_{v_b} - 1$ constraints to the exterior angles to produce a formally correctly determined system. Once existence and uniqueness of solution, with these additional constraints, has been proved, the set of unconstrained solutions can easily be identified. Numerically it is simpler to solve a correctly determined system as we can use Newton's method.

6.3 Number of equations and variables

In Section (5.6) we showed that we have $2n_v - 4$ independent angles in the survey triangulation. Now we have added n_{v_0} equations as we have one cotangent equation for each interior edge and $n_{v_b} - 1$ equations from the exterior angles condition. Since we know

$$n_v - n_e + n_t = 1 \Rightarrow 3n_v - 3n_e + 3n_t = 3. \tag{6.1}$$

Also we have, from counting edges,

$$3n_t = 2n_e - n_{v_b}. \tag{6.2}$$

So we have

$$3n_v - 3n_e + 2n_e - n_{v_b} = 3$$

$$\Rightarrow n_e = 3n_v - n_{v_b} - 3$$

$$\Rightarrow n_{e_0} + n_{e_b} = 3n_v - n_{v_b} - 3.$$

The number of boundary edges and vertices are the same, so

$$n_{e_0} + n_{v_b} = 3n_v - n_{v_b} - 3$$

$$\Rightarrow n_{e_0} = 3n_v - 2n_{v_b} - 3$$

$$\Rightarrow n_{e_0} = 2n_v + n_{v_0} + n_{v_b} - 2n_{v_b} - 3$$

$$\Rightarrow n_{e_0} = 2n_v + n_{v_0} - n_{v_b} - 3,$$

so the total number of equation is

$$2n_v + n_{v_0} - n_{v_b} - 3 + n_{v_b} - 1 = 2n_v - 4 + n_{v_0}$$

Thus we have n_{v_0} more equations than the survey triangulation which is equal to the number of added variables because we parameterized the conductance in each triangle as the average value of conductances in each interior node in the triangulation mesh.

6.4 Jacobian of the system

We need to show that the Jacobian of the system defined in Section (6.2) has full rank to show that the formally correctly determined system has a unique solution. We believe this system has full rank for general planar resistor networks associated with isotropic finite element models because two thirds of the equation were shown to be linearly independent in Section (5.6) and adding cotangent equations may not affect the linear independence. However, we consider the special case of layered triangulated mesh explained in detail in Section (6.6). We write the angles of triangle i as $\theta_i^j, j = 1, 2, 3$ and we assign conductivity values S_i^1, S_i^2, S_i^3 to the interior vertices of triangle i. If the variables in the Jacobian have the following order $\partial\theta_1^1, \partial\theta_1^2, \partial\theta_1^3, \partial\theta_2^1, \partial\theta_2^2\partial\theta_2^3, ..., \partial S_1^1, \partial S_1^2, \partial S_1^3, \partial S_2^1, \partial S_2^2, \partial S_2^3, ...$ then the Jacobian of this system has the following pattern

$$
J(F) = \left(\begin{array}{cccccccccccccccccc|ccccccccccccccc}
1 & 1 & 1 & \cdot & \cdot & \cdot & \cdot & \cdot & \cdot & \cdot & \cdot & \cdot & \cdot & \cdot & \cdot & \cdot & \cdot & \cdot & \cdot & \cdot & \cdot & \cdot & 0 & & & & & & & & & & \\
0 & 0 & 0 & 1 & 1 & 1 & 0 & \cdot & \cdot & \cdot & \cdot & \cdot & \cdot & \cdot & \cdot & \cdot & \cdot & \cdot & \cdot & \cdot & \cdot & \cdot & \cdot & & & & & & & & & & \\
0 & \cdot & \cdot & \cdot & \cdot & \cdot & 1 & 1 & 1 & 0 & \cdot & \cdot & \cdot & \cdot & \cdot & \cdot & \cdot & \cdot & \cdot & \cdot & \cdot & \cdot & \cdot & & & & & & & & & & \\
0 & \cdot & \cdot & \cdot & \cdot & \cdot & \cdot & \cdot & \cdot & 1 & 1 & 1 & 0 & \cdot & \cdot & \cdot & \cdot & \cdot & \cdot & \cdot & \cdot & \cdot & \cdot & & & & & & & & & & \\
\cdot & \cdot & \cdot & \cdot & \cdot & \cdot & \cdot\cdot & \cdot\cdot & \cdot\cdot & \cdot\cdot & \cdot\cdot & \cdot & 1 & 1 & 1 & \cdot\cdot & \cdot\cdot & \cdot\cdot & \cdot\cdot & \cdot\cdot & \cdot\cdot & \cdot\cdot & \cdot\cdot & \cdot & \cdot & \cdot & \cdot & \cdot & \cdot & \cdot & \cdot & \cdot & \cdot \\
\cdot & \cdot & \cdot & \cdot & \cdot & \cdot & \cdot & \cdot\cdot & \cdot\cdot & \cdot\cdot & \cdot\cdot & \cdot\cdot & \cdot\cdot & \cdot\cdot & \cdot & 1 & 1 & 1 & \cdot\cdot & \cdot\cdot & \cdot\cdot & \cdot\cdot & \cdot\cdot & \cdot & \cdot & \cdot & \cdot & \cdot & \cdot & \cdot & \cdot & \cdot & \cdot \\
\cdot & \cdot & \cdot & \cdot & \cdot & \cdot & \cdot & \cdot\cdot & \cdot\cdot & \cdot\cdot & \cdot\cdot & \cdot\cdot & \cdot\cdot & \cdot\cdot & \cdot\cdot & \cdot\cdot & \cdot & \cdot & \cdot & \cdot & \cdot\cdot & \cdot\cdot & \cdot\cdot & \cdot & \cdot & \cdot & \cdot & & \cdot & \cdot & \cdot & \cdot & \cdot \\
\cdot & \cdot & \cdot & \cdot & \cdot & \cdot & \cdot & \cdot & \cdot\cdot & \cdot\cdot & \cdot\cdot & \cdot\cdot & \cdot\cdot & \cdot\cdot & \cdot\cdot & \cdot\cdot & \cdot\cdot & \cdot\cdot & \cdot\cdot & \cdot\cdot & \cdot\cdot & \cdot\cdot & \cdot\cdot & \cdot & \cdot & \cdot & \cdot & \cdot & \cdot & \cdot & \cdot & \cdot & \cdot \\
\cdot & \cdot\cdot & \cdot\cdot & \cdot\cdot & \cdot\cdot & \cdot\cdot & \cdot\cdot & \cdot\cdot & \cdot\cdot & \cdot\cdot & \cdot\cdot & \cdot\cdot & \cdot\cdot & \cdot\cdot & \cdot\cdot & \cdot\cdot & \cdot\cdot & \cdot\cdot & \cdot\cdot & \cdot\cdot & \cdot\cdot & \cdot\cdot & \cdot & \cdot & \cdot & \cdot & \cdot & \cdot & \cdot & \cdot & \cdot & \cdot & \cdot \\
\cdot & \cdot\cdot & \cdot\cdot & \cdot\cdot & \cdot\cdot & \cdot\cdot & \cdot\cdot & \cdot\cdot & \cdot\cdot & \cdot\cdot & \cdot\cdot & \cdot\cdot & \cdot\cdot & \cdot\cdot & \cdot\cdot & \cdot\cdot & \cdot\cdot & \cdot\cdot & \cdot\cdot & \cdot\cdot & \cdot\cdot & \cdot\cdot & \cdot & \cdot & \cdot & \cdot & \cdot & \cdot & \cdot & \cdot & \cdot & \cdot & \\
\hline
1 & 0 & 0 & 0 & 1 & 0 & \cdot & 0 & 0 & 1 & 0 & 0 & 1 & 0 & 0 & 1 & 0 & \cdot\cdot & \cdot\cdot & \cdot\cdot & \cdot\cdot & \cdot\cdot & \cdot\cdot & \cdot & & \cdot & \cdot & \cdot & \cdot & \cdot & \cdot & \cdot & \cdot \\
0 & 1 & 0 & 0 & 0 & 1 & 0 & 1 & 0 & 0 & 0 & 0 & 1 & 0 & 0 & 1 & \cdot\cdot & \cdot\cdot & \cdot\cdot & \cdot\cdot & \cdot\cdot & \cdot\cdot & \cdot\cdot & \cdot & \cdot & \cdot & \cdot & \cdot & \cdot & \cdot & \cdot & \cdot & \cdot \\
0 & \cdot\cdot & \cdot\cdot & \cdot\cdot & \cdot\cdot & \cdot\cdot & 1 & 0 & 0 & 1 & 0 & \cdot\cdot & \cdot\cdot & \cdot\cdot & 0 & 1 & 0 & \cdot\cdot & \cdot & 0 & \cdot\cdot & \cdot\cdot & 0 & \cdot & \cdot & \cdot & \cdot & \cdot & \cdot & \cdot & \cdot & \cdot & \cdot \\
1 & 0 & 0 & 1 & 0 & 0 & 1 & 0 & 0 & 1 & 0 & 0 & 1 & 0 & 0 & 1 & 0 & 0 & \cdot & 0 & 0 & \cdot & 0 & \cdot & \cdot & \cdot & \cdot & \cdot & \cdot & \cdot & \cdot & \cdot & \cdot \\
\cdot & \cdot\cdot & \cdot\cdot & \cdot\cdot & \cdot\cdot & \cdot\cdot & \cdot\cdot & \cdot\cdot & \cdot\cdot & \cdot\cdot & \cdot\cdot & \cdot\cdot & \cdot\cdot & \cdot\cdot & \cdot\cdot & \cdot\cdot & \cdot\cdot & \cdot\cdot & \cdot\cdot & \cdot\cdot & \cdot\cdot & \cdot\cdot & \cdot\cdot & \cdot & \cdot & \cdot & \cdot & \cdot & \cdot & \cdot & \cdot & \cdot & \cdot \\
\cdot & \cdot\cdot & \cdot\cdot & \cdot\cdot & \cdot\cdot & \cdot\cdot & \cdot\cdot & \cdot\cdot & \cdot\cdot & \cdot\cdot & \cdot\cdot & \cdot\cdot & \cdot\cdot & \cdot\cdot & \cdot\cdot & \cdot\cdot & \cdot\cdot & \cdot\cdot & \cdot\cdot & \cdot\cdot & \cdot\cdot & \cdot\cdot & \cdot\cdot & \cdot & \cdot & \cdot & \cdot & \cdot & \cdot & \cdot & \cdot & \cdot & \cdot \\
\cdot & \cdot\cdot & \cdot\cdot & \cdot\cdot & \cdot\cdot & \cdot\cdot & \cdot\cdot & \cdot\cdot & \cdot\cdot & \cdot\cdot & \cdot\cdot & \cdot\cdot & \cdot\cdot & \cdot\cdot & \cdot\cdot & \cdot\cdot & \cdot\cdot & \cdot\cdot & \cdot\cdot & \cdot\cdot & \cdot\cdot & \cdot\cdot & \cdot\cdot & \cdot & \cdot & \cdot & \cdot & \cdot & \cdot & \cdot & \cdot & \cdot & \cdot \\
\cdot & \cdot\cdot & \cdot\cdot & \cdot\cdot & \cdot\cdot & \cdot\cdot & \cdot\cdot & \cdot\cdot & \cdot\cdot & \cdot\cdot & \cdot\cdot & \cdot\cdot & \cdot\cdot & \cdot\cdot & \cdot\cdot & \cdot\cdot & \cdot\cdot & \cdot\cdot & \cdot\cdot & \cdot\cdot & 0 & \cdot\cdot & \cdot\cdot & \cdot & \cdot & \cdot & \cdot & \cdot & \cdot & \cdot & \cdot & \cdot & \cdot \\
\hline
a_1 & b_1 & 0 & a_2 & b_2 & 0 & \cdot & \cdot & 0 & \cdot & \cdot & 0 & \cdot & \cdot & 0 & \cdot & \cdot & \cdot & \cdot & \cdot & \cdot & \cdot & \cdot & \cdot & \cdot & \cdot & \cdot & \cdot & \cdot & \cdot & \cdot & \cdot & \cdot \\
0 & \cdot & \cdot & \cdot & \cdot & 0 & \cdot & \cdot & \cdot & \cdot & a_6 & b_6 & 0 & a_7 & b_7 & 0 & \cdot & \cdot & 0 & 0 & \cdot & \cdot & \cdot & \cdot & \cdot & \cdot & \cdot & \cdot & \cdot & \cdot & \cdot & \cdot & \cdot \\
\cdot & \cdot & \cdot & \cdot & \cdot & \cdot & \cdot & \cdot & \cdot & \cdot & \cdot & \cdot & \cdot & \cdot & \cdot & \cdot & \cdot & \cdot & \cdot & \cdot & \cdot & \cdot & \cdot & \cdot & \cdot & \cdot & \cdot & \cdot & \cdot & \cdot & \cdot & \cdot & \cdot \\
\cdot & \cdot & \cdot & \cdot & \cdot & \cdot & \cdot & \cdot & \cdot & \cdot & \cdot & \cdot & \cdot & \cdot & \cdot & \cdot & \cdot & \cdot & \cdot & \cdot & \cdot & \cdot & \cdot & \cdot & \cdot & \cdot & \cdot & \cdot & \cdot & \cdot & \cdot & \cdot & \cdot \\
\hline
0 & c_1 & \cdot & \cdot & \cdot & d_1 & \cdot & \cdot & \cdot & \cdot & \cdot & \cdot & \cdot\cdot & \cdot & \cdot & \cdot & \cdot & \cdot & k_1 & k_1 & k_1 & \cdot & \cdot & \cdot & \cdot & \cdot & \cdot & \cdot & \cdot & \cdot & k_8 & k_8 & k_8 \\
c_2 & 0 & 0 & 0 & d_2 & 0 & \cdot\cdot & \cdot\cdot & \cdot\cdot & \cdot\cdot & \cdot & \cdot & \cdot & \cdot & \cdot & & 0 & \cdot\cdot & \cdot & \cdot & \cdot & k_2 & k_2 & k_2 & k_3 & k_3 & \cdot & \cdot & \cdot & \cdot & \cdot & \cdot & \cdot \\
0 & \cdot\cdot & c_3 & \cdot\cdot & \cdot & d_3 & 0 & \cdot\cdot & \cdot\cdot & \cdot\cdot & \cdot\cdot & \cdot\cdot & \cdot & \cdot & \cdot & \cdot & \cdot & \cdot & 0 & \cdot\cdot & \cdot\cdot & \cdot\cdot & \cdot\cdot & \cdot & \cdot & \cdot & k_4 & k_4 & k_5 & \cdot\cdot & \cdot & \cdot & \cdot \\
0 & \cdot\cdot & \cdot\cdot & \cdot\cdot & \cdot\cdot & \cdot\cdot & \cdot\cdot & \cdot\cdot & \cdot\cdot & \cdot\cdot & \cdot\cdot & \cdot\cdot & \cdot\cdot & \cdot\cdot & \cdot\cdot & \cdot\cdot & \cdot\cdot & \cdot\cdot & \cdot\cdot & \cdot\cdot & \cdot\cdot & \cdot\cdot & \cdot\cdot & \cdot & \cdot & \cdot & \cdot & \cdot & \cdot & \cdot & \cdot & \cdot & \cdot \\
0 & \cdot\cdot & \cdot\cdot & \cdot\cdot & \cdot\cdot & \cdot\cdot & \cdot\cdot & \cdot & \cdot & \cdot\cdot & \cdot & \cdot\cdot & \cdot\cdot & \cdot & \cdot\cdot & \cdot & \cdot\cdot & \cdot\cdot & \cdot & \cdot & \cdot\cdot & \cdot & \cdot\cdot & \cdot & \cdot & \cdot & \cdot & \cdot & \cdot & \cdot & \cdot & \cdot & \cdot \\
0 & \cdot\cdot & \cdot & \cdot\cdot & \cdot & \cdot\cdot & \cdot & \cdot\cdot & \cdot & \cdot\cdot & \cdot & \cdot\cdot & \cdot & \cdot & \cdot\cdot & \cdot & \cdot\cdot & \cdot\cdot & \cdot & \cdot\cdot & \cdot & \cdot\cdot & \cdot & \cdot & \cdot & \cdot & \cdot & \cdot & \cdot & \cdot & \cdot & \cdot & \cdot
\end{array}\right)
$$

A careful look at the Jacobian shows it consists of four blocks. The first block comes from the π condition in each triangle which gives a row with entry 1 and the rest are zeros. The second block has 1 in different places because it is produced from the 2π condition around each interior node. Another block has rows with random entry $a_i = -\cot \alpha_i^1$ and $b_i = -\cot \alpha_i^2$ produced from the sine rule consistency condition around each interior vertex. The last block introduced by the cotangent equations where we have in each row few entries in random places. These entries are $c_i = -\sum \frac{S_i}{3} \csc^2 \alpha_i^1$, $d_i = -\sum \frac{S_i}{3} \csc^2 \alpha_i^2$ and $k_i = \cot \alpha_i^j$ where $j = 1, 2, 3$.

6.5 Labelling method

To show the Jacobian of the system of equations discussed in the previous section has full rank, we identify pivots in Gaussian elimination. We use a labelling system to determine the equation in which each variable is used as a pivot. The constraints of the labelling method need to be specified. The sum of angles in each triangle is π therefore we have one pivoting equation per triangle. Let $(+)$ be the label used to indicate this pivoting element. So the first constraint we need to satisfy is to have one $(+)$ in each triangle. Also, the sum of angles around each vertex is 2π. Assume the pivoting element of this equation is indicated by $(\times)$. The second constraint in our labelling method is one $(\times)$ per vertex. For each interior vertex the edges incident to the vertex in the triangles that enclose this vertex must satisfy one sine rule. Labelling the pivoting equation produced by $(\circ)$ imposes a constraint $(\circ)$ on one of the corner angles of the triangles enclosing each interior vertex. We also have one cotangent equation relating the conductances of the triangular faces and the conductance in the shared edge. Therefore, one pivoting equation corresponds to each interior edge which will be labelled by (Δ). Labelling each angle to indicate the equation will be used as a pivot to eliminate each variable in the following equations. This is a colouring approach to write the Jacobian in Gaussian elimination form, i.e. full rank. The labelling is summarized in the Table (6.1).

Label	Equation	Constraint
$+$	Sum of angle equal π	One per triangle
$\times$	Sum of angle equal 2π	one per vertex
$\circ$	Sine rule consistency condition	one corner of triangles centred at interior node
Δ	cotangent	one per interior edge

Table 6.1: Summary of the labelling system

6.6 Layered triangulated mesh

We now describe a special class of circular planar network of resistors called layered triangulated mesh.

Definition 6.6.1. A wheel is the set of triangles incident on an interior vertex.

Definition 6.6.2. A layered triangulated mesh is a set of triangles joined together and described as follows: The zero layer consists of a set of triangles joined together centred at the origin forming a wheel. This wheel has spoke edges joining the central node with the nodes in the first layer. The base of the triangles in the wheel joining two nodes in the first layer are called radial edges. In general, any edge joining two layers is a spoke edge and any edge which is a base of triangle is a radial edge. A spoke triangle is a triangle whose base is positioned on a radial edge. Any two spoke triangles are joined by at least two non spoke triangles between them.

Our next result is useful to show that the Jacobian discussed in Section (6.4) has full rank for the layered triangular mesh.

Lemma 6.6.1. Any layered triangulated mesh admits an ordered labelling such that each triangle has exactly one ($+$), each node has exactly one ($\times$), there is one ($\circ$) on a corner of one of the triangles around each interior node, for each two consecutive triangles the angle opposite to the edge between them in the first triangle is labelled by (Δ) and one angle opposite to each radial edge is labelled by (Δ). The variables in this labelled ordering guarantees that later pivots are not removed.

Proof. Number the triangles in the mesh counterclockwise starting from the central node.

Then we start labelling the zero layer using the following steps:

1. Label the angle with a vertex as the central node in the last triangle of this layer by ($\times$), and another angle by ($\circ$) and the last by ($+$).

2. Label the angle with a vertex as the central node in the first triangle by ($+$).

3. Label the remainder of the angles around the central node of the wheel by (Δ).

4. For each two consecutive triangles, the angle opposite to the shared edge in the triangle with minimum numerate is labelled by (Δ).

5. Label the remaining angle of each triangle by ($+$).

Then we move to label the first layer as follows:

1. Label the angle opposite to each radial edge by ($+$) if the angle opposite to this edge in the zero layer is marked by (Δ) otherwise by (Δ)

2. For each two consecutive triangles, the angle opposite to the shared edge in the triangle with minimum numerate is labelled by (Δ).

3. (a) If the angle of the vertex opposite to the base of a spoke triangle has (Δ) then mark the remaining angle by ($+$)

   (b) If the angle of the vertex opposite to the base of the spoke triangle is labelled by ($+$) then mark the remaining angle by ($\times$)

4. Mark the remaining angle in the first triangle of this layer by ($+$).

5. Mark the angle with a vertex in the first radial edges in the last triangle of this layer by ($\times$), one angle by ($\circ$) and the last by ($+$).

6. Mark one angle opposite to the base of the two non-spoke triangles by ($\times$) if the shared vertex has no ($\times$), otherwise mark both by ($+$).

7. Label the remaining angle in the triangle following each spoke triangle ($\circ$).
8. If the angle opposite to the base of the second non-spoke triangle is ($+$) then the left angle is labelled by ($\times$), otherwise mark it ($+$).

Let us suppose, by induction, that we label up to layer k then we obtain the labels in the next layer as follows:

1. Label the angle opposite to each radial edge by ($+$) if the angle opposite to this edge in the k^{th} layer is marked by (Δ), otherwise by (Δ).
2. For each two consecutive triangles, the angle opposite to the shared edge in the triangle with minimum numerate is labelled by (Δ).
3. (a) If the angle of the vertex opposite to the base of a spoke triangle has (Δ) then mark the remaining angle by ($+$).
   (b) If the angle of the vertex opposite to the base of the spoke triangle is labelled by ($+$) then mark the remaining angle by ($\times$).
4. Mark the remaining angle in the first triangle of this layer by ($+$).
5. Mark the angle with a vertex in the kth radial edges in the last triangle of the this layer by ($\times$),one angle by ($\circ$) and the last by ($+$).
6. Mark one angle opposite to the base of the two non-spoke triangles by ($\times$), if the shared vertex has no ($\times$), otherwise mark both by ($+$).
7. Label the remaining angle in the triangle following each spoke triangle ($\circ$).
8. If the angle opposite to the base of the second non spoke triangle is ($+$) the the left angle is labelled by ($\times$), otherwise mark it ($+$).

$\square$

Figure (6.1) Illustrates the labelling procedure.

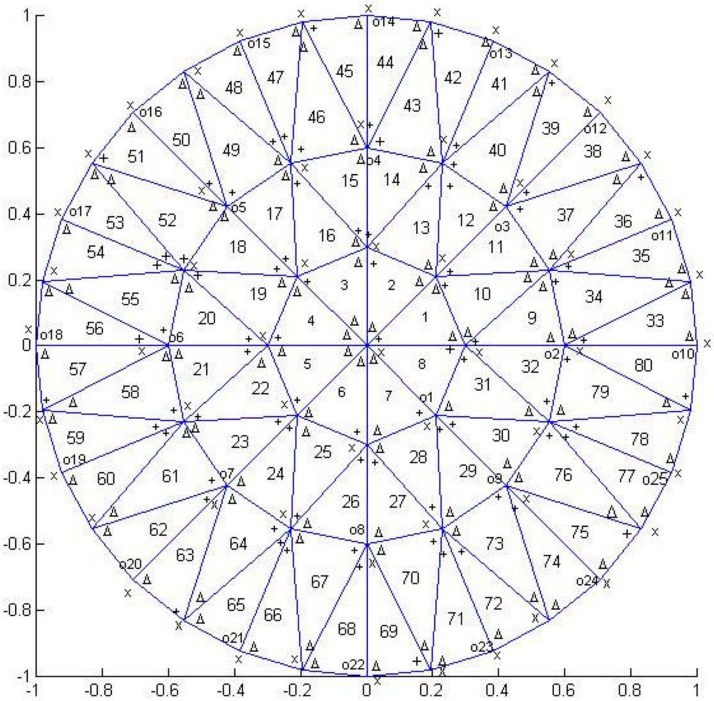

Figure 6.1: Illustration of labelling in layered triangulated mesh

6.7 Limitations of labelling method

The Jacobian of the system discussed in Section (6.4) has full rank for a more general planar resistor network associated with FEM. The labelling method discussed in Section (6.6) shows the Jacobian has full rank for the special class layered triangulated mesh. However, the resistor network in Figure (6.2) shows the limitation of the labelling method. This is an example of a resistor network associated with a finite element mesh for which the Jacobian is shown numerically to have a full rank and the solution of the system of equations converges in six iterations. This Jacobian can not be shown to have full rank using labelling method. The triangles 44 and 67 indicate the corner marked by $(\circ, +)$ at the same time, which violates the constraints of labelling method.

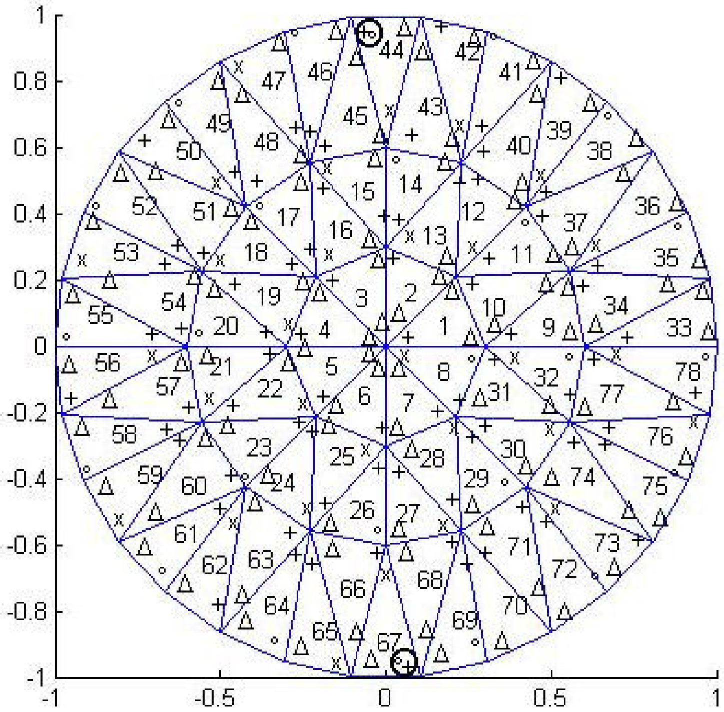

Figure 6.2: An example of limitation of labelling method

6.8 Embedding of a finite element model

Finite element models (FEM) with piece-wise linear basis functions and piece-wise constant conductivity give rise to a system matrix equivalent to the Ohm-Kirchhoff matrix for a resistor network with the same topology. For the planar two dimensional case we show how a resistor network close to those associated with an isotropic FEM can be embedded.

Definition 6.8.1. An isotropic conductivity on a finite element mesh is said to be parameterized by values at interior nodes (PVIN) if there is an $s \in \mathbb{R}^{n_v}$, where n_v is the number of interior nodes, such that for each triangle t, $\sigma(t)$ is the mean of $s(v)$ for each interior node $v \in t$.

We will use the well known Inverse Function Theorem.

Theorem 6.8.1. Let $F : \mathbb{R}^n \to \mathbb{R}^n$ be a C^1 and $F(x_0) = y_0$. Suppose $DF(x_0) \neq 0$ is invertible, then for any neighborhood of y_0 there is a unique neighborhood of x_0 such that $F(x_0) = y_0$.

Theorem 6.8.2. Given a layered finite element mesh F_0 with a conductivity $\sigma_0 \in \mathbb{R}^q$, where q is the number of triangles in the mesh and edge conductance $K_0 \in \mathbb{R}^e$, where e is the number of edges, then there is an $\epsilon > 0$ such that for all k with $|k - k_0| < \epsilon$ there is a finite element mesh F with the same topology as F_0 and a PVIN conductivity σ such that F has edge conductance k. Moreover, F is uniquely determined by the condition that $n_{v_b} - 1$ exterior angles in F and two vertices in a specific edge are the same as F_0 and orientation.

Proof. Lemma (6.6.1) implies the Jacobian of the system has full rank. Therefore the proof is immediate from Inverse Function Theorem (6.8.1) and theorem (5.12.1). □

6.9 Numerical results

We tested this method using both the optimization toolbox function fsolve (refer to MATLAB documentation) and our own implementation of Newton's method. Starting with a mesh generated by rmesh we assigned conductivities to vertices using uniform pseudo random numbers (rand in MATLAB). We then calculated edge conductances using the cot formula Eq.(4.8). These edge conductances are perturbed by a vector generated by calling rand again, scaled by some positive ϵ. In all meshes we tested, the Jacobian matrix was found to be non-singular as expected from Theorem (6.8.2). The singular values for one example are shown in Figure (6.9). In all cases we tested, a solution was found with edge conductances agreeing to specified tolerance (we used 10^{-7}) for some value of ϵ. While for large enough values of ϵ a solution was not found. Tables (6.2),(6.3) and (6.4) summarize some tested meshes also some of the figures are drawn. Refer to appendix for MATLAB codes.

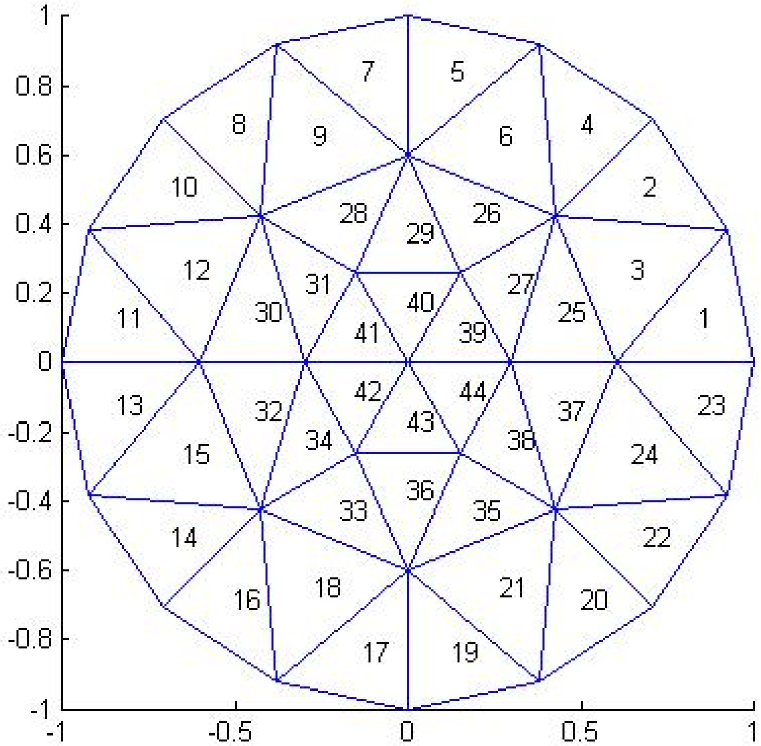

Figure 6.3: Original mesh 1 (16,8,6,1)

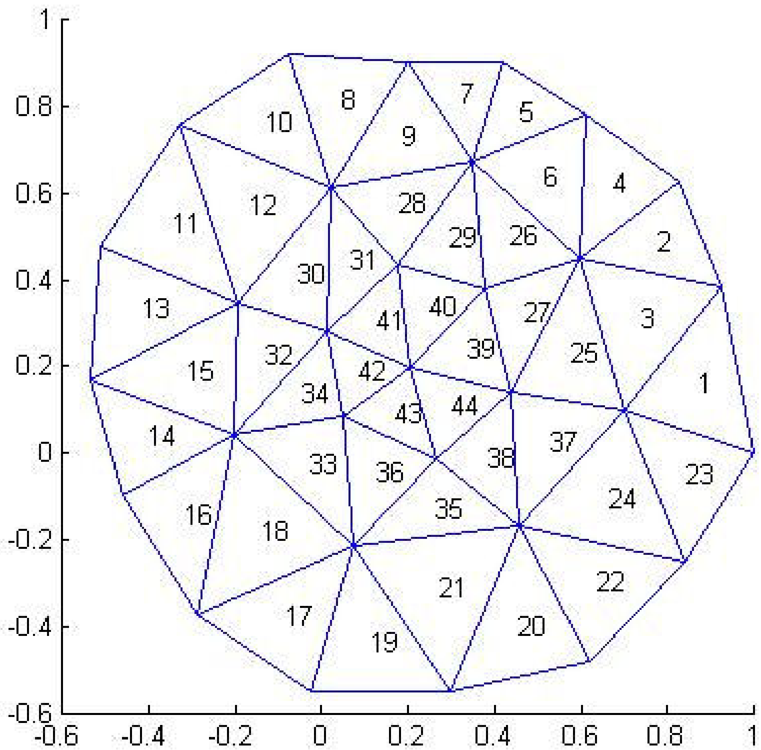

Figure 6.4: New mesh 1 ($\epsilon = 0.02$)(16,8,6,1)

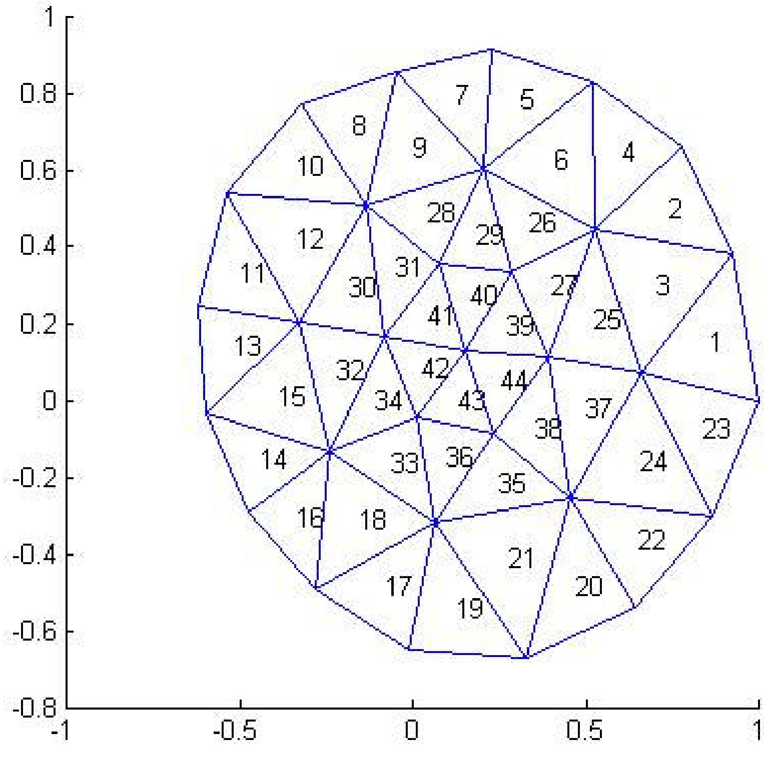

Figure 6.5: New mesh 1 ($\epsilon = 0.2$)(16,8,6,1)

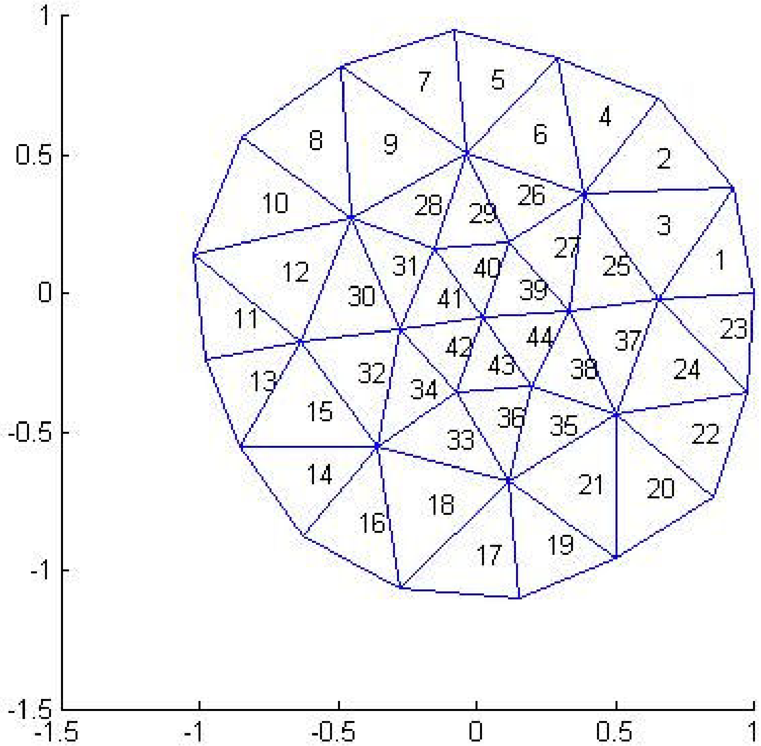

Figure 6.6: New mesh 1 ($\epsilon = 0.3$)(16,8,6,1)

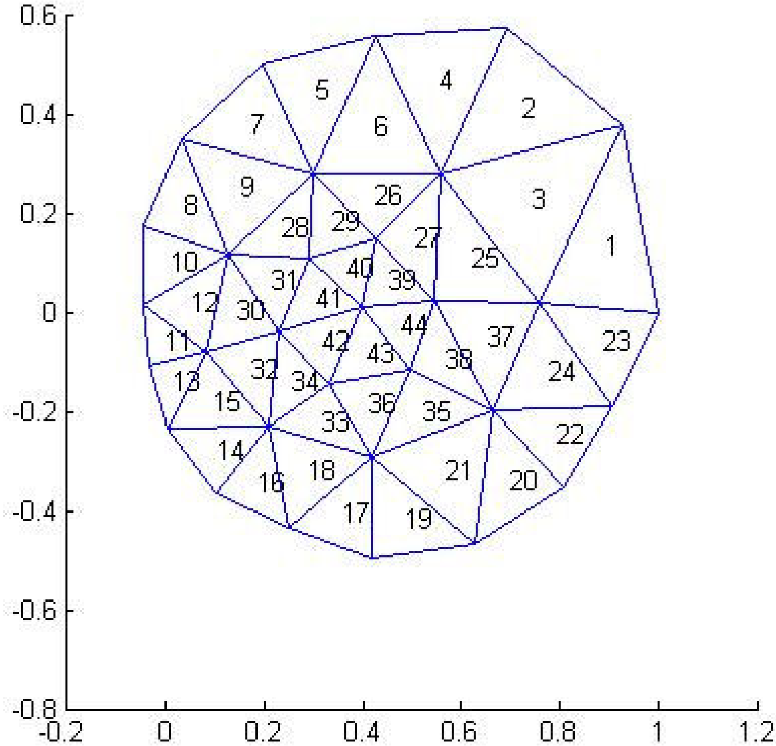

Figure 6.7: New mesh 1 ($\epsilon = 0.5$)(16,8,6,1)

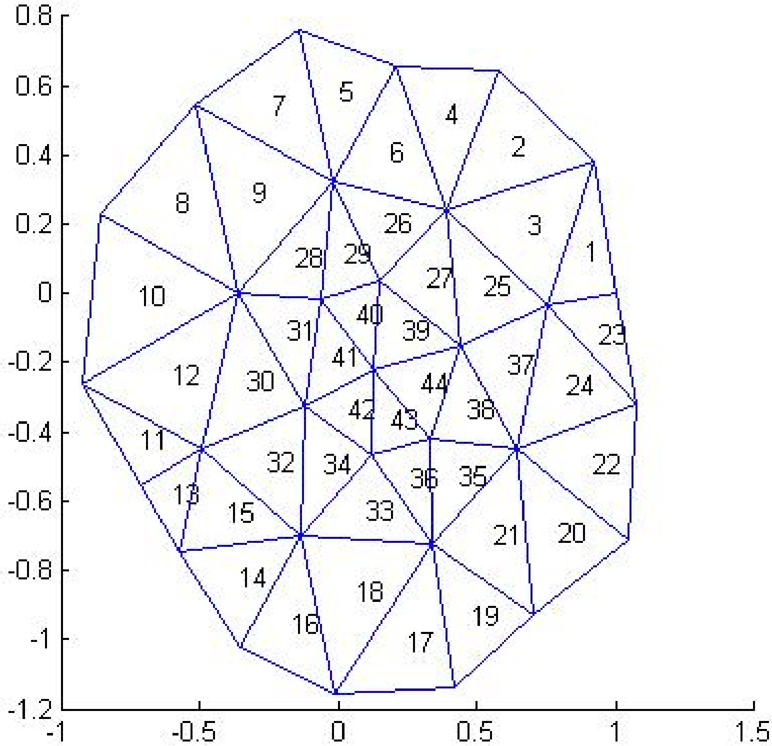

Figure 6.8: New mesh 1 ($\epsilon = 0.9$)(16,8,6,1)

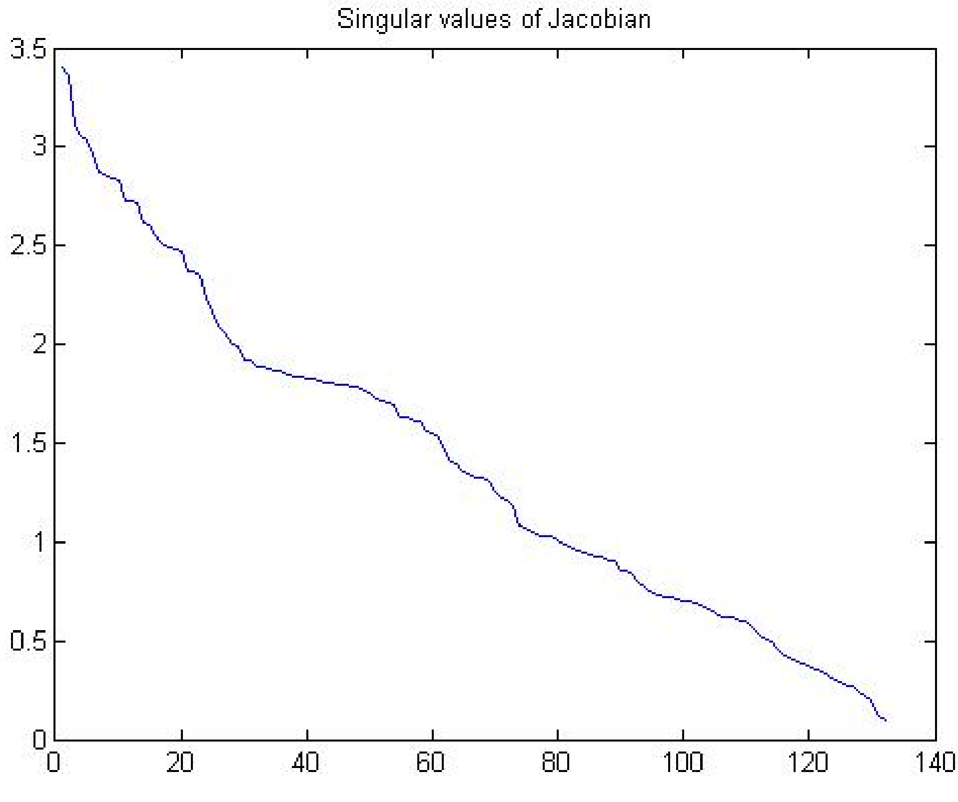

Figure 6.9: New mesh 1 singular values (16,8,6,1)

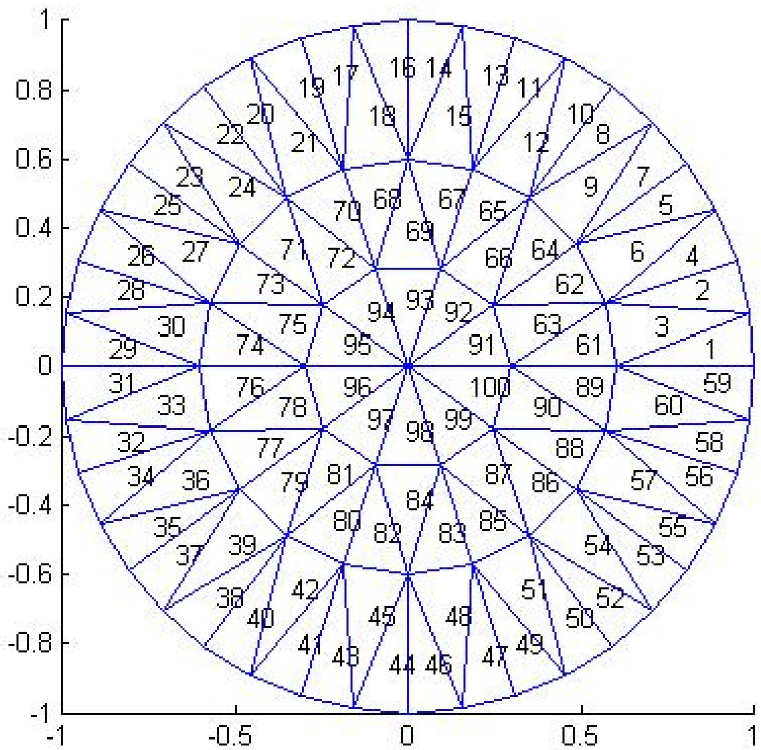

Figure 6.10: Original mesh 2 (40,20,10,1)

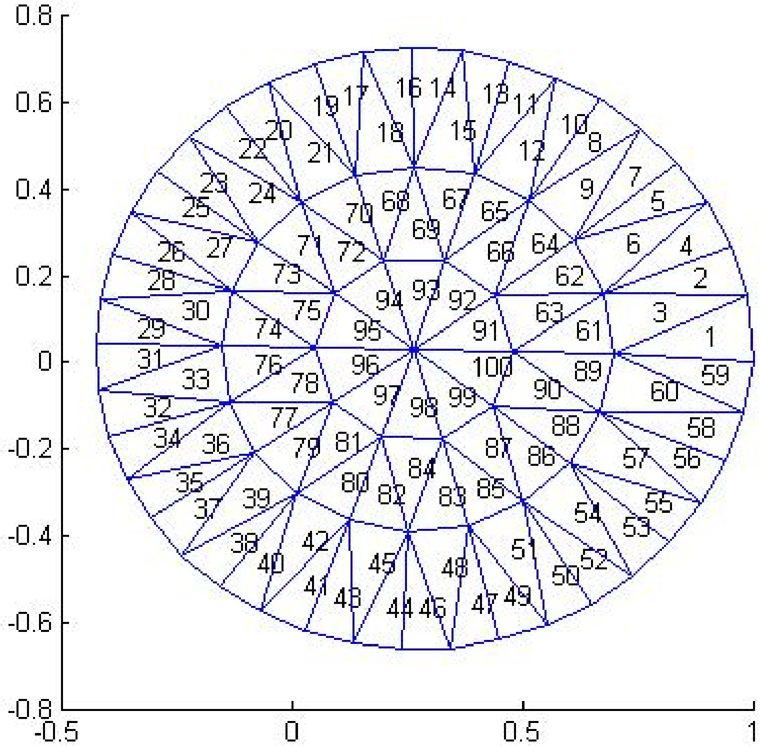

Figure 6.11: New mesh 2 ($\epsilon = 0.02$)(40,20,10,1)

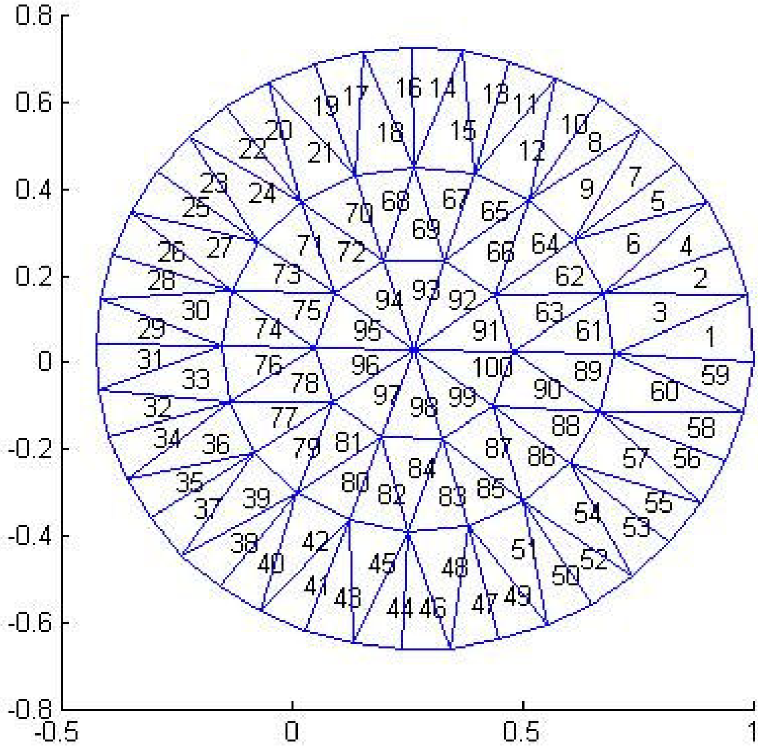

Figure 6.12: New mesh 2 ($\epsilon = 0.1$)(40,20,10,1)

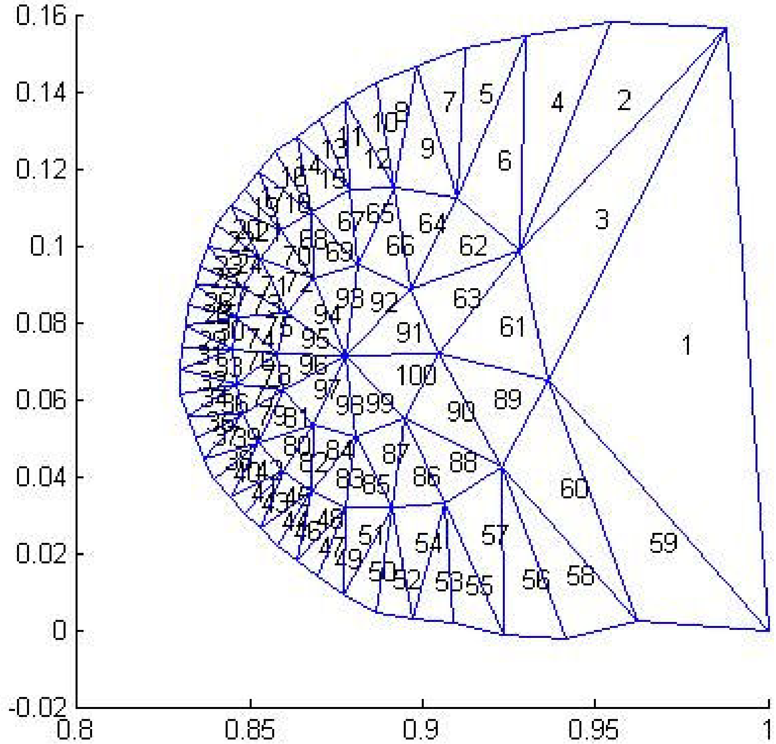

Figure 6.13: New mesh 2 ($\epsilon = 0.2$)(40,20,10,1)

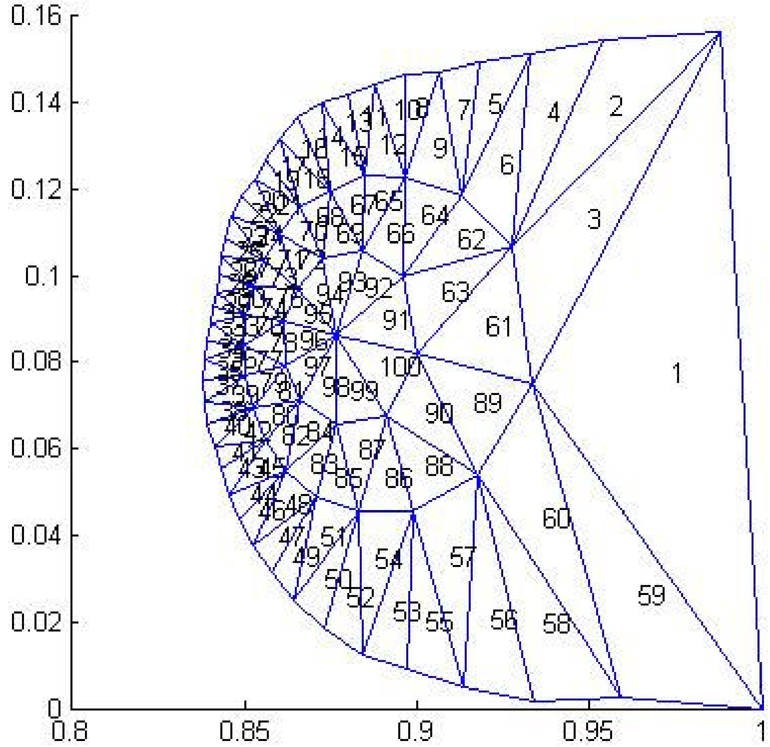

Figure 6.14: New mesh 2 ($\epsilon = 0.2$)(40,20,10,1)

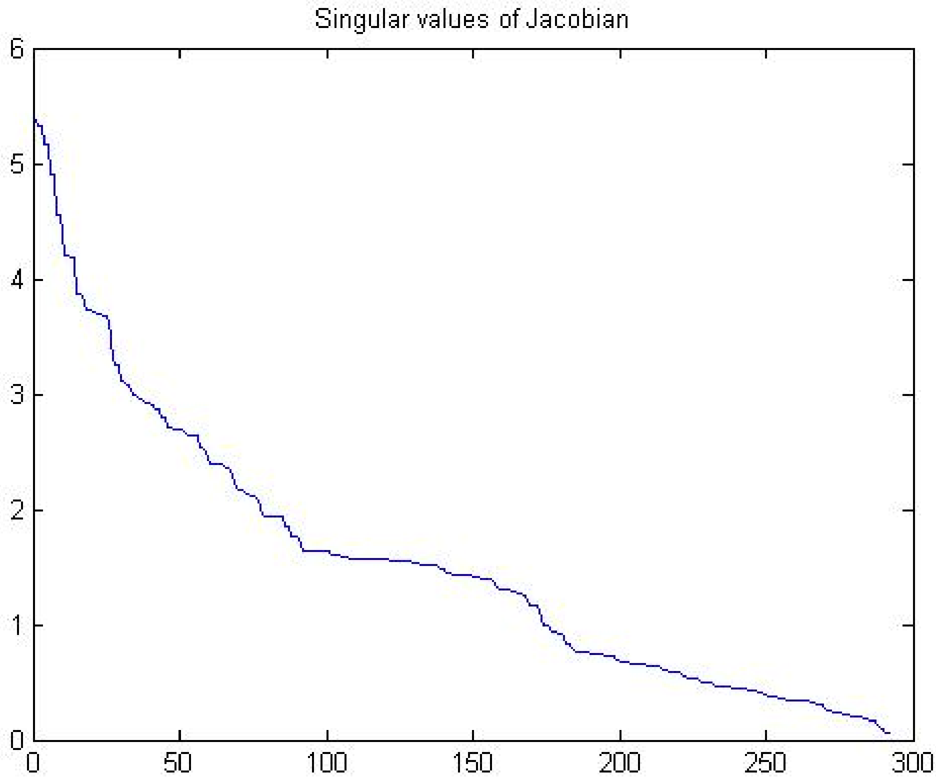

Figure 6.15: Singular values (40,20,10,1)

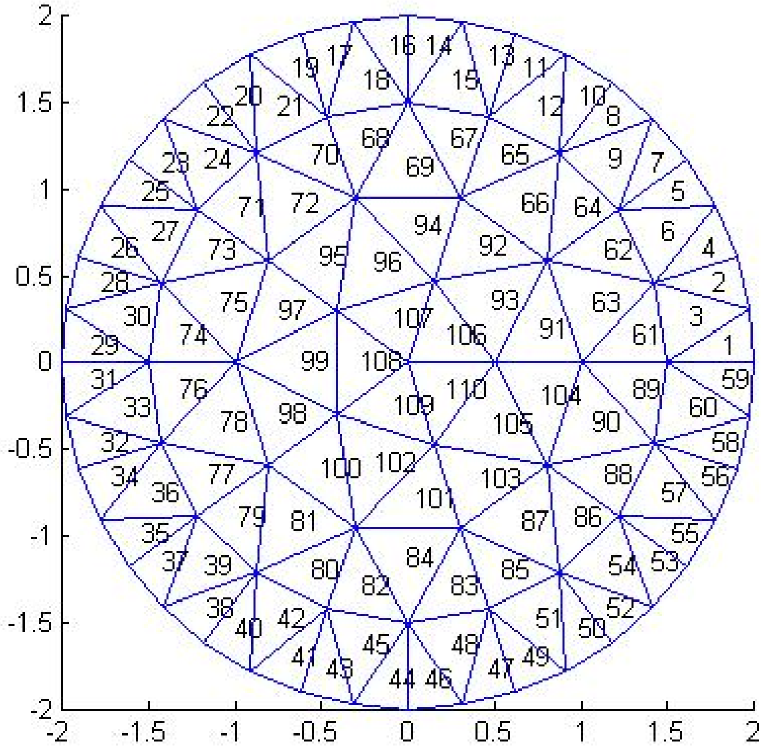

Figure 6.16: Original mesh 3 (40,20,10,5,1)

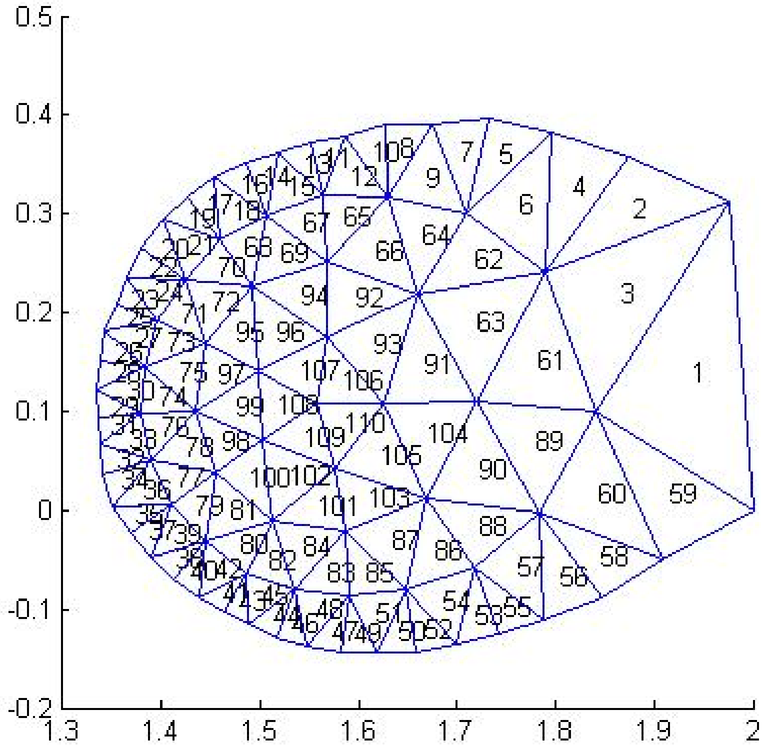

Figure 6.17: ew mesh3 ($\epsilon = 0.02$)(40,20,10,5,1)

ϵ	Convergence	Iterations a	Smallest Singular Values	Residual
0.02	Yes	4	0.0935	$9.98338e^{-012}$
0.2	Yes	5	0.0935	$1.81544e^{-011}$
0.5	Yes	6	0.0935	$8.09155e^{-010}$
0.3	Yes	5	0.0935	$4.9508e^{-010}$
0.9	Yes	8	0.0935	$2.55176e^{-008}$

Table 6.2: Mesh 1 (16,8,6,1)

ϵ	Convergence	Iterations a	Singular Values	Residual
0.02	Yes	4	0.0592	$4.58981e^{-010}$
0.1	Yes	5	0.0592	$9.17411e^{-08}$
0.2	Yes	7	0.0592	$1.35819e^{-008}$
0.25	Yes	8	0.0592	$5.9740e^{-008}$
0.3	No			

Table 6.3: Mesh 2 (40,20,10,1)

ϵ	Convergence	Iterations a	Singular Values	Residual
0.02	Yes	4	0.0539	$9.8510e^{-010}$
0.1	Yes	5	0.0539	$1.85653e^{-08}$
0.2	Yes	6	0.0539	$3.81123e^{-011}$
0.25	No			

Table 6.4: Mesh 3 (40,20,10,5,1)

Chapter 7

Conclusions and Future Work

7.1 Conclusion

Studying the link between finite element models and resistor networks opens several points and questions that need to be answered.Which resistor networks corresponds to a finite element model and what are the possible assignments of conductance to a resistor mesh with the same topology as a finite element mesh corresponds to a choice of vertex positions and conductivities? Moreover, one may think about the conditions needed to obtain a unique embedding for a general resistor network associated with finite element models. Another question we could ask "Is there a canonical form for special cases of triangular resistor networks"? Note that the planar resistor networks associated with the mesh we study is over-determined which means that one may use the least squares method to find the best fit data. Moreover, we can have a special class of triangular meshes that is well-connected and can be determined.

We also showed that angles need to satisfy the sine rule as a consistency condition for every closed basic cycle enclosing interior nodes in two dimensions. Analogous consistency conditions need to be developed for three dimensions. The extension of the work done in this thesis to three dimensions remains an open problem.

In two dimensions an improvement of the result for a more general class of meshes needs to be studied.

7.2 Future work

The Jacobian of the system of equation obtained in the embedding of the layered triangulated mesh can be reduced by Gaussian elimination method. We are very close to finding a constructive proof for this special case. Given that the survey solve problem has a constructive solution using a spanning tree of the dual graph we hope to find a systematic solution to the nonlinear isotropic embedding problem in a similar way. Furthermore, as we noted, the isotropic embedding is a discrete version of the problem of isothermal coordinates [12]. Another approach might be to discretize the nonlinear partial differential equations for isothermal coordinates (for example as a FEM approximation) and show the existence of a solution for this. So far we have not been able to interpret the system of equations that we have solved in this way. Another possibility for future work is to consider other discrete approximation to the inverse conductivity equation. For example [10] use the finite volume method and show that this is equivalent to a resistor mesh in the isotropic case. Other possibilities include the finite integral method and higher order finite element methods. Also we believe that our result is true for more general meshes. The difficulty is to obtain proof of full rank for the Jacobian. The extension of the problem to three dimensions requires an analogues consistency condition similar to the sine rule in two dimensions. Discrete analogous of the differential forms in three dimensions also needs to be obtained. There are no isothermal coordinates in three dimensions only orthogonal coordinates [21]. This suggests that we find conditions on resistor networks derived from three dimensional anisotropic finite element models which guarantees the existence of orthogonal coordinates, that is an embedding in which conductivity is diagonal. The existence of such an embedding was assumed implicitly in the paper of [1] but not proven. Finally, as in the continuum problem, the existence of isothermal coordinates (in two dimensions) and orthogonal coordinates (in three dimensions) is known. One would expect to be able to prove that in the limit as the mesh size tends to zero, the discrete isothermal (orthogonal) coordinates converge to the isothermal (orthogonal) coordinates of the limiting continuum conductivity problem. The implication for practical EIT includes the design of resistor networks to test EIT system [26]. It is important to know if resistor networks are constant with some isotropic conductivity, if the EIT system is to be applied to isotropic objects.

Appendix A

MATLAB Codes

A.1 Test mesh MATLAB code

```
% Some test code for circular grids
% Bill Lionheart, Abdul-Aziz al Humaidi 2010
addpath ../graph' theory'/
% Global variables passed to the optimization function
global H vtoe twinelts bdryverts g edges nedges  btris C
global x_to_corner corner_to_x angs xlastang
nvint Xtocond EdgeCond intverts
global firstcall
%global H  g centroids
% Radii of each ring
r=[2,1.5,1,0.5,0];
% Numbers of vertices in each ring
N=[40,20,10,5,1];
eI=[1,0];
% Make a mesh
[g,gp,H,E]=cirgrid_eit (r,N,eI);
H=orientH(H,g);
```

```
% Here g is the x and y coordinates of vertices and
% H is the element topolgy ie a list of vertices
%in each traingel Plot the mesh
figure,plcigrid(g,H);
bdryverts = 1:N(1);
centroid=[];
for el=1:size(H,1)
    els=H(el,:);
   xs=g(els,1);
    %xs=vtx(els,1);
    ys=g(els,2);
    %ys=vtx(els,2);
 Mx=mean(xs);
   My=mean(ys);
   centroids(els,1)=Mx;
   centroids(els,2)=My;
  centroids=(g(H(:,1),:)+g(H(:,2),:)+g(H(:,3),:))/3;
end
nvint = size(g,1)-length(bdryverts);
[th,r]=cart2pol(centroids(:,1),centroids(:,2));
intverts=setdiff(1:size(g,1),bdryverts)
% Now our conductivites are one per interior vertex
%and are in
% X(xlastang+1) to X(xlastang+nintv);
% We need a matrix to multiply the conductivities
%at each int vertex to give us a conductivity
% on each element (ie the average)
Xtocond=sparse(size(H,1),nvint);
for ie=1:size (H,1)
 for iv =1:nvint; % non boundary verts
```

```
   if ismember(intverts(iv),H(ie,:))
      Xtocond(ie,iv)=1;
   end
  end;
end;
sums= sum(Xtocond'); % row sum
for ie=1:size (H,1)
    if(sums(ie)~=0)
       Xtocond(ie,:)= Xtocond(ie,:)./sums(ie);
    end;
end;
% Make a PIV conductivity
vcond=ones(size(intverts))+0.1*rand(size(intverts));
Conductivity = Xtocond*vcond';
K= zeros (size (g,1),size (g,1));
z=size(g,1);
vtoe = cell ([ z,1]);
for ie=1:size (H,1)
     for k=1:3
      b=H (ie,k);
         vtoe{H(ie,k)}=[vtoe{b},ie];
       side1 = g(H(ie,mod(k,3)+1),:)-g(H(ie,k),:);
       side2 = g(H(ie,mod(k-2,3)+1),:)-g(H(ie,k),:);
       angles(ie,k)=
       acos( side1*side2'/( norm(side1)*norm(side2)));
     end


        K(H (ie,1), H(ie,2))=K(H (ie,1), H(ie,2))+
         Conductivity(ie)*cot(angles(ie,3))/2;
        K(H (ie,2), H(ie,3))=K(H (ie,2), H(ie,3))+
```

```
        Conductivity(ie)*cot(angles(ie,1))/2;
       K(H (ie,3), H(ie,1))=K(H (ie,3), H(ie,1))+
       Conductivity(ie)*cot(angles(ie,2))/2;
end
K= K+K';
rowsums = sum (K,1);
Ksu = sparse (triu (K)-diag (diag (K)));
Ks=sparse (K);
[ied,jed,s]=find (Ksu);
edges=[ied,jed];
nedges=size (edges,1);
for ie = 1:nedges
    EdgeCond(ie) =K(edges(ie,1),edges(ie,2));


end;
% Now to perturb EdgeCond
EdgeCond= EdgeCond + 0.1*rand(size(EdgeCond));
% we need to know the indices of the two angles in each edge
btris=[]; % outward facing triangles with no partner
for ied=1:nedges
  [r1,c]=find (H==edges (ied,1));
  [r2,c]=find (H==edges (ied,2));
  twinelt=intersect (r1,r2);
  if length (twinelt)==1
      btris=[btris,twinelt]; % it is only one!
  else
      twinelts (ied,:)=twinelt;
  end;
end
btris=unique (btris);
```

```
% Assemble indexing arrays for x variables
%   Find the triangles on the boundaryand
%the angle which is outward
corner_to_x=ones(size(H));
nbtris=length (btris);
for ibt=2:nbtris %miss off the first
        insideone=setdiff (H (btris (ibt),:)

        ,bdryverts);
    ind=find (H (btris (ibt),:)==insideone);
    % Now triangle btris(ibt) has angle ind facing outwards
    corner_to_x(btris(ibt),ind)=0;
end
count_angles=0;
for ie=1:size (H,1)
    for k=1:3
        if corner_to_x(ie,k)==1
            count_angles=count_angles+1;
            corner_to_x(ie,k)=count_angles;
        end
    end
end
% now construct theinverse of this index array
x_to_corner=zeros(3*size(H,1)-nbtris,2);
xcount=0;
for ie=1:size (H,1)
    for k=1:3
        if corner_to_x(ie,k)~=0
            xcount=xcount+1;
            x_to_corner(xcount,:)=[ie,k]';
```

```
        end
    end
end
xlastang=xcount;
% we need to know the indices of the two angles in each edge
btris=[]; % outward facing triangles with no partner
for ied=1:nedges
    [r1,c]=find (H==edges (ied,1));
    [r2,c]=find (H==edges (ied,2));
    twinelt=intersect (r1,r2);
    if length (twinelt)==1
        btris=[btris,twinelt]; % it is only one!
    else
        twinelts (ied,:)=twinelt;
    end;
end
btris=unique (btris);

% Now we attempt to find a distribution of angles
%that give us the \same system
% matrix K but with homogeneous conductivity
% global variable angs is used to pass the fixedangles
angs=angles;
% Initalize X
if xlastang ~= 3*size(H,1)-nbtris +1
    error('xlastang = %d, but  3*size(H,1)-nbtris+1= %d'
    , xlastang,
    1+3*size(H,1)-nbtris);
end
X=zeros(xlastang + nvint,1);
```

```
X((xlastang+1):(xlastang + nvint))=1; % initial conductivity
count_angles=0;
for ie=1:size (H,1)
    for k=1:3
        if corner_to_x(ie,k)~=0
            count_angles=count_angles+1;
            X(count_angles)=angs(ie,k);
        end
    end
end
options = optimset('Jacobian','on');
options = optimset('DerivativeCheck','on');
options = optimset('FunValCheck','on');
options = optimset('Display','final');
options = optimset('MaxFunEvals',1000);
firstcall=1;
[F,J]=myfunc5(X);
figure,s=svd(J);plot(s);title('Singular values of Jacobian');
%if exist('fsolve')
% Xnew=fsolve(@myfunc5,X,options);
%else
 Xnew=myfsolve(@myfunc5,X);
%end
angsnew=zeros(size(H,1),3);
count_angles=0;
for ie=1:size (H,1)
    for k=1:3
        if corner_to_x(ie,k)~=0
            count_angles=count_angles+1;
            angsnew(ie,k)=Xnew(count_angles);
```

```
        else
            angsnew(ie,k)=angs(ie,k);
        end
    end
end
C=centroids;
% The old centroids just for plotting in survey solve
Vnew =surveysolve(H,angsnew,[1,2],g([1,2],:),'disp');
figure,plcigrid(Vnew,H);
```

A.2 Survey solve MATLAB code

```
function V =surveysolve(H,angles,e1,v,op)
% V =surveysolve(H,angles,e1,v,op)
% given an "element topology" matrix H, that is
% a list of vertex numbers for the traingles
%in a triangulation of a % polygon, the angles
%in each triangle angles and and edge
%e1 (that is a pair of vertices) and the
% cooridinates of % the two vertices of that edge,
% this function calculates the vertex  coordiantes V.
%g Cjust for plotting for the moment
global newV plothandle g C
[E,D]=meshtograph(H);
if op=='disp'
    figure,grPlot(g,E);
end
s=grMinSpanTree(D);
if op=='disp'
    plothandle=figure;
```

```
    mygrplot(C,D(s,:),plothandle);
    figure(plothandle);
    hold on
    axis auto
end
% Edges of min spanning tree of dual graph
Dm=D(s,:);
% The root of the tree is edge e1, find this in edge in E
[r1,c]=find(E==e1(1));
[r2,c]=find(E==e1(2));
r = intersect(r1,r2);
if length(r)~=1
    error(sprintf('Not found edge [%d, %d]',e1));
else
    e1n=r;
end
%Which triangle is this edge in?
[r1,c]=find(H==e1(1));
[r2,c]=find(H==e1(2));
r = intersect(r1,r2);
roottri=r;
Dm=treesort(Dm,roottri);
nv = max(max(H));% number of vertices
newV= zeros(nv,2);
newV(e1(1),:)=v(1,:);
newV(e1(2),:)=v(2,:);
traversetriangles(H,Dm,angles,roottri,e1,v,op);
V=newV;
```

A.3 f solve MATLAB code

```
function xn=myfsolve (fun,x0)
nmax=10000;
err = 1e-6;
xn=x0;
for n=1:nmax
    [F,J]=fun (xn);
    jsize=size (J);
    if jsize (1) ~= jsize (2)
        size (J)
        error ('Jacobian is not square')
    end
 %   if jsize (1) ~= size (F,1)
 %       size (J)
 %       size (F)
 %       error ('Jacobian size does not match F')
 %   end
    if norm (F)<err
        fprintf('Converged after
%d iterations with a residual of %10.5e\n',n,norm(F));
        return
    end
    xn=xn-(J'*J+0.000001*eye(size(J,2)))\J'*F';
end
fprintf('Quit after)
%d iterations with a rsidual of %10.5e',nmax,norm(F));
end
```

A.4 Myfunction MATLAB Code

```
function [F,J]=myfunc (X)
global H vtoe  g bdryverts edges nedges twinelts nbtris
global x_to_corner corner_to_x
angs xlastang nvint Xtocond EdgeCond intverts
% F function values
% J jacobian
%angs is a global used to pass the  FIXED angles
%angs=  zeros(size (H,1),3);
%angs=zeros(1+3*size(H,1)-nbtris,2);
%cond_homog=X(1); % Homogeneous conductivity
fnum=1; % number of equations
% Conductivity here is local, calculated from X
Conductivity = Xtocond*X((xlastang+1):end);
angs1=angs; % includes those that do not vary!
for ie=1:size (H,1)
    for k=1:3
        if corner_to_x(ie,k)~=0
          angs1(ie,k) =X(corner_to_x(ie,k));
        end
    end
end
% First sum of angles in each triangle
for el = 1:size (H,1)
     F (fnum) = angs1 (el,1)+angs1 (el,2)+angs1 (el,3)-pi;
     for k=1:3
       if corner_to_x(el,k)~=0
        J (fnum,corner_to_x(el,k))=1;
       end
```

```
      end
        fnum=fnum+1;
end
% now sum of angles around interior verices
for iv=intverts(1:end-1);
% We need just the interior vertices
    vinele=vtoe {iv};
% List of elements around this vertex
    angsum=0;
    for el=vinele
% all the elements that include this vertex
% Within this element which of the three vertices is iv?
        thisone=find (H (el,:)==iv);
        angsum=angsum+ angs1 (el,thisone);
        if corner_to_x(el,thisone)~=0
          J (fnum,corner_to_x(el,thisone))=1;
        end
    end
    F(fnum)=angsum - 2*pi;
    fnum=fnum+1;
end
%Now the sine rule formulae around interior vertices.
for iv=intverts; % We need just the interior vertices
    vinele=vtoe {iv};
% List of elements around this vertex
    logsinsum=0;
    for el=vinele
% all the elements that include this vertex
% Within this element which two vertices are not iv?
        outsideverts=find (H (el,:)~=iv);
```

```
        % so outside verts is eg [1,3], or [1,2] [2,3]
        if outsideverts(1)==1 & outsideverts(2)==3
            outsideverts=outsideverts([2,1]);
% to keep cyclic ordering
        end
        logsinsum = logsinsum +
        log(sin(angs1(el,outsideverts(2))))...
            - log(sin(angs1(el,outsideverts(1))));
% as the cyclic order of the vertices in each triangel is
% anticlockwise the first is plus and the second is minus
        if corner_to_x(el,outsideverts(1))~=0
%the ones that are not fixed
         J (fnum,corner_to_x(el,outsideverts(1)))=...
            cot(angs1(el,outsideverts(1)));
% deriv of log sin is cot
        end
        if corner_to_x(el,outsideverts(2))~=0
        J (fnum,corner_to_x(el,outsideverts(2)))=...
            -cot(angs1(el,outsideverts(2)));
        end
    end
    F(fnum)=logsinsum; % should be zero
    fnum=fnum+1;
end

% Now the cot formulae
% We have to loop over edges that share two triangles
for ied= 1:nedges
  if twinelts (ied,1)~=0 && twinelts (ied,2)~=0
      t1=twinelts (ied,1);
```

```
        t2=twinelts (ied,2);
        tl1=H (t1,:);
        tl2=H (t2,:);
        ti1=find (setdiff (tl1,edges (ied,:))==H (t1,:));
        ti2=find (setdiff (tl2,edges (ied,:))==H (t2,:));
        a1 = angs1 (t1,ti1);
        a2 = angs1 (t2,ti2);
        F (fnum)= Conductivity(t1)*cot(a1)/2 +
        Conductivity(t2)*cot(a2)/2  -EdgeCond(ied) ;
        J (fnum,corner_to_x(t1,ti1))=
        -Conductivity(t1)/(2*(sin (a1))^2);
        J (fnum,corner_to_x(t2,ti2))=
        -Conductivity(t2)/(2*(sin (a2))^2);
        J(fnum,1) = (cot (a1)+cot (a2) )/2;
        fnum=fnum+1;
    end
end
```

A.5 Meshtograph MATLAB code

```
function [E,D,C]=meshtograph(H,V);
% [E,D,C]=meshtograph(H,V)
% From the matrix H listing vertices
%for each triange produce
% the list of edges and the dual graph D
% the centroids of the triangles
%are returned in C and can be used
% for plotting the dual graph.
nt = size(H,1);
E=[];
% This will produce interior edges twice
for it=1:nt
    E=[E;H(it,[1,2])];
    E=[E;H(it,[2,3])];
    E=[E;H(it,[3,1])];
end
E=sort(E,2);
E=unique(E,'rows');
if nargout>1
ne=size(E,1);
D=[];
for ie=1:ne
    [ts1,j]=find(H==E(ie,1));
    [ts2,j]=find(H==E(ie,2));
    ts=intersect(ts1',ts2');
    if length(ts)==2
       D=[D;ts];
    end
end;
```

```
if nargout>2 & nargin==2
C=[];
for it=1:nt
  Hii=V(H(it,:),:);
  com = mean(Hii);
  C=[C;com];
end
end
end
```

A.6 Mygrplot MATLAB Code

```
function h1=mygrplot(V,E,h)
figure(h);
axis equal
hold on
for ie = 1:size(E,1)
    x= V(E(ie,:),1);
    y= V(E(ie,:),2);
    plot( x,y)
end
plot(V(:,1),V(:,2),'k.','MarkerSize',20)
h1=h;
```

A.7 OrientH MATLAB Code

```
function  H1= orientH(H,V)


nt=size(H,1);
nv=size(V,1);

for it = 1:nt
    v1 = V(H(it,1),:);
    v2 = V(H(it,2),:);
    v3 = V(H(it,3),:);
    s = det( [v2-v1;v3-v1]);
    if s<0
        H(it,:)=H(it,[2,1,3]);
    end
end
H1=H;
```

A.8 Plcigrid MATLAB code

```
function []=plcigrid (g,H)
% plcigrid Plots a 2D FEM mesh
% Function []=plcigrid (g,H,E);
% plots a given 2D FEM mesh.
%
% INPUT
%
% g = node coordinate matrix
% H = topology
% E = elements under the electrodes (can also be empty)
% co = colour of the mesh
% J. Kaipio, 11.4.1994.
% Modified by M. Vauhkonen 1999,
% University of Kuopio,
% Department of Applied Physics, PO Box 1627,
% FIN-70211 Kuopio, Finland, email: Marko.Vauhkonen@uku.fi
% Stripped down by Bill Lionheart 06/05/2010
nH=max (size (H));
axis ('xy'),axis ('square')
hold on
% loop
for ii=1:nH
  Hii=g (H (ii,:),:);
  com = mean(Hii);
  Hii=[Hii;Hii(1,:)];
  hHii=plot(Hii (:,1),Hii (:,2));
  text (com(1),com(2),sprintf ('%d',ii));
end
```

A.9 Isinorder MATLAB code

```
function isit=isinorder(a,b)
% checks if two element list b
% is in the same cyclic order as list a
aa=[a,a(1)];
[r,c]=find(aa==b(1));
if aa(c(1)+1)==b(2)
    isit=1;
else
    isit=0;
end
```

A.10 Trisolve MATLAB code

```
function v3=trisolve(v1,v2,a1,a2)
% Finds the third vertex given
%two vertices and two angles of a triangle
a3= pi - a1-a2;
d = v1-v2;
l3=norm(d);
p = [d(2),-d(1)]./l3; % unit vec perp to d c/w
l1 = sin(a1)*l3/sin(a3); %sin rule
s= l1*cos(a2);
h= l1*sin(a2);
v3 = v2 + s*d./l3 + h*p;
```

A.11 Treesort MATLAB code

```
function Ts=treesort(T,root);
% sortes the vertices in the edges
%of a rooted tree to make a directed
% tree (edges have diferent numbers)
Ts=[];
nr=size(T,1);
[r,c]=find(T==root); % edges containing root
r=r';
if length(r)>0
for ir=r
    if T(ir,2)==root
        nextroot(ir)=T(ir,1);
    else
        nextroot(ir)=T(ir,2);
    end
    Ts=[Ts;root,nextroot(ir)];
end
% call recursively on sub trees
setdiff(1:nr,r);
prunings= T(setdiff(1:nr,r),:);
for ir=r
    Ts=[Ts;treesort(prunings,nextroot(ir))];
end
end
```

A.12 Traverse triangles MATLAB code

```
function traversetriangles(H,Dm,angles,troot,edgein,v,op)
global newV plothandle
 troot and entered it from edgein
nextvertex = setdiff(H(troot,:),edgein);
if length(nextvertex)~=1
    error('Next vertex not unique!');
else
% if newV(nextvertex,:)==[0,0]

    r1=find(H(troot,:)==edgein(1));
    r2=find(H(troot,:)==edgein(2));
    r1;
    r2;
    troot ;
    angles(troot,r1);
    angles(troot,r2);
    newV(nextvertex,:) = trisolve(v(1,:),v(2,:),
    angles(troot,r1),...angles(troot,r2));
    if op=='disp'
        figure(plothandle)
        hold on
        plot(newV(nextvertex,1),newV(nextvertex,2),'ob')
        plot(newV(edgein,1),newV(edgein,2),'-b')
        pause(1)
    end
    [r,c]=find(Dm(:,1)==troot);
    for ir =r'
        nexttri=Dm(ir,2); %The next triangle
        nextedge=intersect(H(troot,:),H(nexttri, :));
```

```
        nextv(1,:)= newV(nextedge(1),:);
        nextv(2,:)= newV(nextedge(2),:);
%to be positively ordered wrt the ordering of nexttri
        if isinorder(H(nexttri,:),nextedge)==0
            nextedge=nextedge([2,1]);
            nextv=nextv([2,1],:);
        end
   traversetriangles(H,Dm,angles,nexttri,nextedge,nextv,op);
    end
 %end
end
```

A.13 Testssol MATLAB code

```
% Test harness for surveysolve
global H vtoe twinelts bdryverts
g edges nedges angles btris C
%Radii of each ring
r=[1,0.5,0.25,0];
%Numbers of vertices in each ring
N=[16,8,4,1];
eI=[1,0];
%Make a mesh
[g,gp,H,Ejunk]=cirgrid_eit(r,N,eI);
H=orientH(H,g);
% Here g is the x and y coordinates
%of vertices and H is the element
% topolgy
% ie a list of vertices in each traingel
%Plot the mesh
figure,plcigrid(g,H);
bdryverts = 1:N(1);
 %The vertices on the boundary  for a more general
 % mesh we will need to do this betetr
%Make a list (cellarray) of the elements meeting
% at each vertex and angles
vtoe = cell([size(g,1),1]);
% so vtoe{i} is going to be a list (of variable length)
% of the triangles (elements)
% that inclued the vertex numbered i. Cell arrays
%can have any type in them
angles = zeros(size(H,1),3);
% this will be the three angles  in each triangle
```

```
% in the same order as in H
% we will have to flatten it to a vector for the fsolve part
for ie=1:size(H,1)
    for k=1:3
      vtoe{H(ie,k)}=[vtoe{H(ie,k)},ie];
      side1 = g(H(ie,mod(k,3)+1),:)-g(H(ie,k),:);
      side2 = g(H(ie,mod(k-2,3)+1),:)-g(H(ie,k),:);
      angles(ie,k)=
       acos( side1*side2'/( norm(side1)*norm(side2)) );
    end
end
% centroids
C=zeros(size(H,1),2);
for ii=1:size(H,1);
  Hii=g(H(ii,:),:);
  C(ii,:) = mean(Hii);
end
angles=angles + 0.0003*randn(size(angles));
% errors for test
%bdryverts = 1:N(1);
 % The vertices on the boundary  for a more \general
 %mesh we will need to do this betetr
%centroid=[];
%for el=1:size(H,1)
   %els=H(el,:);
   %xs=g(els,1);
   %xs=vtx(els,1);
   %ys=g(els,2);
   %ys=vtx(els,2);
    %Mx=mean(xs);
```

```
    %My=mean(ys);
    %centroid(els,1)=Mx;
   %centroid(els,2)=My;
  %centroids=(g(H(:,1),:)+g(H(:,2),:)+g(H(:,3),:))/3;
%end
%[th,r]=cart2pol(centroid(:,1),centroid(:,2));
%Conductivity=ones(size(H,1),1);
%Conductivity (find(r<0.3))=1.5;
V =surveysolve(H,angles,[1,2],g([1,2],:),'disp');
figure,plcigrid(V,H);
```

Bibliography

[1] J. Abascal, W. Lionheart, S. Arridge, M. Schweiger, D. Atkinson, and D. Holder. Electrical impedance tomography in anisotropic media with known eigenvectors. *Inverse Problems*, 27:1–17, February 2011.

[2] A. Adler, R. Gaburro, and W. Lionheart. *Handbook of mathematical methods in imaging,EIT*. Springer Science and Business Media LLC, 2010.

[3] G. Alessandrini. Singular solutions of elliptic equations and the determination of conductivity by bounary measurements. *Journal of Differntial Equations*, 84(2):252–272, 1990.

[4] G. Alessandrini and R. Gaburro. Determining conductivity with special anisotropy by bounary measurements. *SIAM Journal on Mathematical Analysis*, 33:153–171, 2001.

[5] G. Alessandrini and R. Gaburro. The local Calderón problem and the determination at bounary of the conductivity. *Communications in Partial Differential Equations*, 34:918–936, 2009.

[6] K. Astala and L. Päivärinta. Calderón's inverse conductivity problem for anisotropic conductivity in the plane. *Communications in Partial Differential Equations*, 30(1-3):207–224, 2005.

[7] K. Astala and L. Päivärinta. Calderón's inverse conductivity problem in the plane. *Annals of Mathematics*, 163:265–299, 2006.

[8] C. Berge. *Graphs and hypergraphs*, volume 6. North-Holland Publishing Company Amsterdam, 1973.

[9] J.A. Bondy and U.S.R Murty. *Graph theory with applications*. The Machillan Press LTD, 1976.

[10] L. Borcea, V. Druskin, and A. Mamonov. Circular resistor networks for electrical impedance tomography with boundary mesaurements. *Inverse Problems*, 26:1–32, 2010.

[11] W. Breckon. *Image reconstruction in electrical impedance tomography*. PhD thesis, Oxford Polytechnic, 1990.

[12] R. Bryant, S. Chern, R. Garder, H. Goldschmidt, and P. Griffiths. Exterior differential systems. *Berlin: Springer*, 1991.

[13] A.P. Calderón. On an inverse boundary value problem. *In: Seminar on numerical analysis and its applications to continuum physics*, 283:65–73, 1980.

[14] E. Curtis, D. Ingerman, and J. Morrow. Circular planar graphs and resistors networks. *Linear Algebra and its Applications*, 283:115–150, 1998.

[15] E. Curtis, E. Mooers, and J. Morrow. Finding the conductors in circular networks from boundary measurements. *Mathematical Modelling in Numerical Analysis*, 28(7):781–813, 1994.

[16] E. Curtis and J. Morrow. Determining the resistors in a network. *SIAM Jounal on Applied Mathematics*, 50(3):918–930, June 1990.

[17] E. Curtis and J. Morrow. The Dirichlet to Neumann map for a resistor network. *SIAM Jounal on Applied Mathematics*, 51(4):1011–1029, August 1991.

[18] E. Curtis and J. Morrow. *Inverse problems for electrical networks*, volume 13. World Scientific Publishing Co. Pte. Ltd, 2000.

[19] J. de Munck, T. Faes, and R. Heethaar. The boundary element method in the forward and invrese problem of electrrical impedence tomography. *IEEE Transaction of Biomedical Engineering*, 47(6):792–800, 2000.

[20] Y.Colin de Verdière, I. Gitler, and D. Vertigan. Reseaux électriques planaires II. *Comment. Math. Helvetici*, 71(2010.35):144–167, 1996.

[21] D. DeTurck and D. Yang. Existence of elastic deformations with prescribed principal strains and triply orthogonal systems. *Duke Mathematical Journal*, 51(2):243–260, June 1984.

[22] G. Dong, H. Endo, S. Hayano, S. Gao, and Y. Saito. GVSPM for reconstruction in electrical impedence tomography. *IEEE Transaction on Magnetics*, 39(3):1630–1633, May 2003.

[23] M. Floater. Parametrization and smooth approximation of surface triangulations. *Computer Aided Geometric Design*, 14:231–250, 1997.

[24] G. Folland. *Introduction to partial differential equations.* University of Tokyo Press, Princeton University Press, 1976.

[25] R. Gaburro and W. Lionheart. Recovering riemannian metrics in monotone families from bounary data. *Inverse Problems*, 25(045004), 2009.

[26] H. Gagnon, A. Hartinger, M. Cousineau, A. Adler, and R. Guardo. A resistive mesh phantom for assesing the performance of EIT systems. *IEEE Biomedical Engineering*, 57:2257–2266, 2010.

[27] N.D. Haasbroek. *Gemma Frisius,Tycho Brahe and Snellius and their triangulations.* Publication of the Netherlands Geodetic Commission, 1968.

[28] D. Holder. *Clinical and physiological applications of electrical impedance tomography.* London: UCL Press, 1993.

[29] D. Holder. *Electrical impedance tomography.* Institute of Physics, Bristol, 2005.

[30] Sergii Iglin. *http://www.iglin.exponenta.ru*, Accessed on November 2010.

[31] R. Kohn and M. Vogelius. Identification of an unknown conductivity by measurements at the bounary. *SIAM-AMS Proceedings*, 14:113–123, 1984.

[32] R. Kohn and M. Vogelius. Determining conductivity by boundary measurements II.Interior results. *Communications on Pure and Applied Mathematics*, 38:643–667, 1985.

[33] J. Lee and G. Uhlmann. Determining anisotropic real-analytic conductivities by boundary measurements. *Communications on Pure and Applied Mathematics*, 42(8):1097–1112, 1989.

[34] W. Lionheart. Conformal uniqueness results in anisotropic electrical impedance imaging. *Inverse Problems*, 13:125–134, 1997.

[35] W. Lionheart and K. Paridis. Finite elements and anisotropic EIT reconstruction. *Journal of Physics: Conference Series*, 224(1):12–22, 2010.

[36] Loke. *MH(2010)Tutorial: 2-D and 3-D electrical imaging surveys, geotomo software*. www.geoelectrical.com, 2010.

[37] T. Murai and Y. Kagawa. Electrrical impedence computed tomography based on a finite element model. *IEEE Transactions on Biomedical Engineering*, BME-32:177–184, 1985.

[38] A. Myl'nikov and A. Prangishvili. Homological and cohomological invariants of electric circuts. *Automation and Remote Control*, 63(4):578–586, 2002.

[39] A. Nachman. Global uniqueness for two-dimensional inverse boundary value problem. *Annals of* M*athematics*, 142:71–96, 1995.

[40] K. Nakayama, W. Yagi, and S. Yagi. Fundamental study on electrical impedence plethsmography. *In Proceedings Vth International Conference on Electrical Bioimpedance, Tokyo, Japan*, pages 99–102, 1981.

[41] R. Patterson and J. Zhang. Evaluation of an EIT reconstruction algorithm using finite difference human thorax models as phantoms. *Physiological Measurements*, 24:467–475, 2003.

[42] A. Ramirez, W. Daily, A. Binley, D. LaBreque, and D. Roelant. Detection of leaks in underground storage tanks using electrical resistance methods. *Journal of Environmental and Engneering Geophysics*, 1(297-330), 1996.

[43] A. Sheffer and E. de Sturler. Parametrization of faceted surfaces for meshing using angle-based flattening. *Engineering with Computers*, 17:326–337, 2001.

[44] G. Strang and G. Fix. *An analysis of the finite element method.* Prentice-Hall, New york, 1973.

[45] Z. Sun and G. Uhlmann. Generic uniqueness for an inverse boundary value problem. *Duke Mathematical Journal*, 62:131–155, 1991.

[46] J. Sylvester. Remarks on an inverse boundary value problem. *Lecture Notes in Mathematics, Springer-Verlag*, 1256:430–441, 1986.

[47] J. Sylvester. An anisotropic inverse boundary value problem. *Communications on Pure and Applied Mathematics*, 43:201–232, 1990.

[48] J. Sylvester. A convergent layer stripping algorithm for the radially symmetric impedence tomography problem. *Communications in Partial Differential Equations*, 17:1955–1994, 1992.

[49] J. Sylvester and G. Uhlmann. A uniqueness theorem for an inverse boundary problem in electrical prospection. *Communications on Pure and Applied Mathematics*, 39:92–112, 1986.

[50] J. Sylvester and G. Uhlmann. A global uniqueness theorem for an inverse boundary value problem. *Annals of Mathematics*, 125:153–169, 1987.

[51] L. Tarassenko. *Electrical impedance techniques for the study of cerebral circulation and granial Imaging in the newborn.* PhD thesis, University of Oxford, 1985.

[52] G. Uhlmann. Topical review: electrical impedance tomography and Calderón's problem. *Invrse Problems*, 25(123011), 2009.

[53] M. Vauhkonen. *Electrical impedance tomography and prior information.* PhD thesis, Kuopio University, 1997.

[54] M. Vauhkonen, W. Lionheart, L. Heikkinen, P. Vauhkonen, and J.P. Kaipio. A MATLAB package for the EIDORS project to reconstruct two-dimensional EIT images. *Physiological Measurements*, 22(1):107–111, February 2001.

[55] T. Yorkey, J. Webster, and W. Tompkins. Comparing reconstruction algorithms for electrrical impedence tomography. *IEEE Transaction on Biomedical Engineering*, 34(11):843–851, November 1987.

[56] T.J. Yorkey. *Comparing reconstruction methods for electrical impedance tomography.* PhD thesis, Department of Electrical and Computer Engineering, University of Wisconsin, 1986.